Back-scatter measurements of certain targets at circular polarization

Allan, L. E.; Markell, R. C.; McCormick, G. C.

Report (National Research Council Canada. Radio and Electrical Engineering Division : ERB); no. ERB-672, 1964-05

ERB-672

CONFIDENTIAL

COPY NO. 77

NATIONAL RESEARCH COUNCIL OF CANADA

RADIO AND ELECTRICAL ENGINEERING DIVISION

BACK-SCATTER MEASUREMENTS OF CERTAIN TARGETS AT CIRCULAR POLARIZATION

L. E. ALLAN, R. C. MARKELL, AND G. C. McCORMICK

OTTAWA

MAY 1964 NRC # 35670

ABSTRACT

Back-scatter patterns at circular polarization of the following full-scale models are reproduced: 81-mm mortar shell, $4\frac{1}{2}$-inch Russian mortar shell, M30 mortar shell, 105-mm artillery shell, and 155-mm artillery shell. Measurements were made at 16.0 Gc/s. The corresponding patterns at linear polarization are shown for comparison. Several patterns showing the variation of cross section with frequency are presented.

CONTENTS

	Page
1. Introduction	1
2. Equipment and Measurement Technique	3
3. Patterns of Projectile Models	6
4. Other Patterns	7
5. Conclusions	8
References	8

BACK-SCATTER MEASUREMENTS OF CERTAIN TARGETS AT CIRCULAR POLARIZATION

- L.E. Allan, R.C. Markell, and G.C. McCormick -

1. INTRODUCTION

The use of circular polarization for anti-clutter purposes is a well-established technique. The development of a polarizer as an auxiliary device for the AN/MPQ-501 counter mortar radar has been described previously [1]. When early operational tests with the polarizer proved disappointing, it became of interest to see whether the performance was consistent with the parameters of the system, and especially with the radar cross section of the targets. Information on the reduction of the cross section of targets of interest in changing from linear to circular polarization was mainly speculative. A limited measurement program was therefore undertaken to obtain some typical data.

It was realized that in establishing a scattering range a considerable amount of specialized equipment is normally needed, and that a lengthy period of time is required in order to assure proper operation of a rather complicated setup. Our requirements did not include the measurement of low cross section targets; furthermore, we had some equipment immediately adaptable to the purpose, viz., a scanner antenna, several polarizers, a rotator, a 1-watt TWT amplifier, and the superheterodyne receiver from the counter mortar radar. It was felt, therefore, that there was a chance of obtaining a few patterns quickly from a typical target, so that the order of magnitude of the cross section at circular polarization could be determined.

The transmitting antenna used throughout the work was the McGill-NRC Foster scanner which produces a beam of approximately 1° width in both azimuth and elevation. The receiving antenna was designed to provide directivity in elevation and to minimize coupling between the two antennas. These antennas were placed on the ground at a separation of 8 feet, and were directed toward the roof of the buildi of the Radio and Electrical Engineering Division at a distance of 400 feet and an elevation angle of 12°. A photograph of the antennas and a block diagram of the transmitter-receiver equipment are shown in Plate I and Fig. 1.

In the initial phase of the work the mortar shell was supported by means of a short steel spindle threaded into the body of the shell and the spindle was attached to the top of an 8-foot steel pipe. The whole assembly was mounted in a vertical position on a rotator, with rotation about the axis of the pipe. The long metal pipe was therefore at 12° to line-of-sight; consequently, the back-scatter intensity from it was small. However, the fitting at the end for attaching to the target, even when covered with the best quality absorber available, produced a comparatively high background, namely -25 db m^2 (-34.54 db m^2 = 0 db χ^2) using linear polarization and -33 db m^2 using circular polarization. The finned mortar, of diameter $4\frac{1}{2}$ inches, which was available for measurement has a comparatively high cross section, and the measured values of the patterns taken would possibly have an error of several decibels at the level of interest. However, the order of magnitude of the cross section, and, in particular, the relative magnitude of the level at circular polarization compared with that at linear polarization was clearly established. It was evident also that the lobe structure of the cross sections was basically as shown in the measured patterns although it may have been inaccurate in detail. It could therefore be said that the initial objective of the measurement program was achieved.

The range, and the transmitting and receiving antennas, seemed to be well suited to back-scatter measurements. Difficulties encountered in the initial phase of the work were due to instrumentation and to the means for mounting the target. A reduction in the difficulties appeared straightforward; and to this end, a new mount was designed and made in our Model Shops, and a commercial polar pattern recorder and superheterodyne receiver were procured. Using the modified apparatus, back-scatter patterns were obtained on models of three mortar shells and two artillery shells. The uncancelled background from the supporting structure was reduced to -45 db m^2 at linear polarization and to less than -50 db m^2 at circular polarization.

Details of the support and of a cancellation technique are given below. Certain features of the arrangement are apparently novel. It is not claimed that they represent a significant advance in the state of the art in back-scatter measurements. They were, however, suited to the facilities available and to the range of cross sections which were of interest to us.

Patterns shown below were all taken using the improved facilities. Targets actually used were full-scale wooden models of the projectiles spray-painted with aluminum. If the projectile had a finned tail, it was simulated in sheet aluminum and made rotatable. Patterns

at various orientations of the fins were recorded. Nose cones were simulated on the model with rotational symmetry whereas, in fact, they have certain asymmetrical features. Patterns of one target using an actual nose cone at various orientations were obtained.

Finally, patterns of a single target at three frequencies separated by 0.5% were recorded at the request of the Northern Electric Company.

2. EQUIPMENT AND MEASUREMENT TECHNIQUE

Plate I shows the antennas used at the transmitter-receiver site [2]. The McGill-NRC model of the AN/MPQ-501 scanner was used for transmission. It was operated on lower beam near the center of scan because previous patterns had shown that side lobes below the beam were low for this scan position. The receiving antenna consisted of an enclosed section of a parabolic cylinder with an active width of 12" and a focal length of 90". It was fed by a horn of aperture 3" × 5", and radiated through an aperture 12" × 44½". The structure was made of sheet metal and angle iron, and over half of the interior surface was lined with microwave absorber. The design was intended to provide elevation directivity for the reduction of spurious background scattering, and to reduce coupling between the transmitting and receiving antennas. The coupling was, in fact, not measurable. The antennas were at a separation of 8 feet, and were directed to peak on the target which was at a distance of 400 feet and elevated 12° above the horizontal.

A plastic strip polarizer was available, and was placed in front of the receiver feed horn, as desired, to produce a circularly polarized antenna. The position of the polarizer was adjusted to optimize the polarization pattern at the target site. The interior of the antenna with the polarizer is shown in Plate II. The orientation of the polarizer could be changed through 90°, thereby changing the antenna polarization from right-hand circular to left-hand circular. For transmission, one of the early production units of the polarizer for the AN/MPQ-501 was available for use with the scanner.

The supporting mount for the targets was attached to the top of a 7-foot platform which was on the roof of the building of the Radio and Electrical Engineering Division. The mount proper extended to a total height of 8 feet, thereby placing the centers of the antenna beams at a height of 15 feet above the roof. Therefore, scattering from the building was reduced because of the directivity of the antennas, and apparently was not a significant factor. The platform was sheltered by means of a large screen of microwave absorber. The basis upon which the final model of the mount was designed was that as much of it as possible should be fixed.

No part upon which radiation from the transmitter was incident rotated, except a small spindle or Styrofoam column projecting from the top. This rotating part was connected by a steel rod and two universal joints to the rotator which was behind the microwave screen. The rod and joints were enclosed within the 3-inch steel tubing.

The resulting mount was, therefore, one in which the rotating part of the support produced, or was intended to produce, a very low background. The back-scatter from the fixed part of the structure was reduced as much as possible by inclining large scattering areas at an angle to line-of-sight in order to eliminate specular reflections, and by using microwave absorber where it seem appropriate. Nevertheless, the residual was quite high — in the order of $-25\,\mathrm{db\,m^2}$. This was cancelled by means of a small horn mounted on the 3-inch tubing, directed toward the antennas and connected by waveguide to an attenuator and phase shifter. The background, with the rotating Styrofoam column removed, could thereby be cancelled to a level better than $-50\,\mathrm{db\,m^2}$ for a period long enough to take a series of patterns. Under very favourable conditions a cancellation of $-60\,\mathrm{db\,m^2}$ could be maintained for a useful period. The complete mount and cancellation horn are shown in Plate III.

Supporting columns for targets were turned from 2 $\mathrm{lb/ft^3}$ Styrofoam of such diameter that reflections from the exterior and interior interfaces cancelled. The condition for cancellation is that

$$d = \frac{\lambda}{4\sqrt{\varepsilon}}\left(2n + \tfrac{1}{2}\right)$$

where d is the diameter, ε the dielectric constant of the Styrofoam, and n an integer. Smaller targets were supported by columns of diameter 3.70" (n = 10) or 3.33" (n = 9). The largest target, viz., the model of the 155-mm artillery shell, was supported on a column of diameter 6.58" (n = 18). Patterns at non-zero tilt were taken by placing the target in a hemispherical Styrofoam bowl fitted to the top of the larger column (Plate IV).

The block diagram of the transmitter-receiver assembly is shown in Fig. 1. A 1-watt TWT amplifier was used for transmission at 16 Gc/s with an X-12 klystron. It was necessary that the latter be maintained to about 0.2 Mc/s. This was a tedious procedure without special stabilization techniques requiring frequent manual adjustment, and could only be justified by the limited and temporary nature of the

measurement program. The Scientific Atlanta receiver did not have adequate sensitivity in its normal mode of operation. Therefore, it was used with an X-12 klystron as an external local oscillator and a conventional mixer. The equipment could then operate usefully to the -110 dbm level which is estimated to correspond to a cross section of -65 db m^2. In addition to the signal from the receiving antenna, an alternative signal was provided from the transmitter line by means of a directional coupler and several attenuators, including a precision rotary-vane attenuator. The mixer was connected to a hybrid tee, one arm of which was connected to a waveguide switch that could be turned either to the receiving antenna or a flat load. The other arm of the tee was connected to the attenuator — directional coupler — transmitter line. This arm was used for level-setting, for calibration, and for determining the sensitivity of the system; or, it could be effectively switched out during the taking of patterns by turning the precision attenuator to maximum.

The standard for the calibration of the system was a sphere of 5.225" diameter which was obtained on loan from the Defence Research Board. The theoretical cross section of the sphere at 16.0 Gc/s was -18.75 db m^2 at linear polarization, and zero for circular polarization. The level-set attenuators in the reference line were set so that, with the precision attenuator reading -18.75 db, the recorder level, using the reference line, equalled that scattered from the standard sphere. All subsequent measurements could then be referred to the precision attenuator, the level corresponding to 0 db on the attenuator being 1 $(meter)^2$. The adjustment of the receiver and recorder gain controls then made it possible to have the top of the recorder chart correspond to any desired level of back-scattered signal.

A number of test patterns are reproduced in Figs. 2 to 5. Fig. 2 shows polarization patterns of the transmitting antenna with the scanner polarizer in place, and of the receiving antenna after the polarizer had been adjusted to its optimum position. Patterns of the sphere at vertical polarization and at circular polarization are shown in Fig. 3. A cancellation of 29 db will be noted on comparison of these two patterns. The background levels were -47 db m^2 with the smaller Styrofoam column, -45 db m^2 with the larger Styrofoam column, and -41 db m^2 with the hemispherical bowl.

It was anticipated that a significant source of error at lower scattering levels might be the mutual coupling between the target and the fixed supporting structure, an effect not capable of elimination by the cancellation procedure described above. It was estimated that this effect might in certain aspects be in the order of 30 db below the

peak of the scattered radiation. Fig. 4 shows patterns of a target taken at separations between target and fixed support which differ by one-half wavelength (3/8"). Certainly no gross error is apparent at the level of these patterns. As a final check patterns of a low cross-section target, viz., a 75° ogive of length 2.04" were recorded. There were significant asymmetries in the patterns at the -40 db m^2 level due to background from the Styrofoam column and possibly to field distortion by the column. Patterns of the ogive in the hemispherical bowl showed clear evidence of effects due to the proximity of the Styrofoam dielectric. Ogive patterns are shown in Fig. 5.

Targets were held in place, in order of preference, by (a) a friction fit; (b) wedging with small pieces of Styrofoam; (c) a small piece of cellulose tape; (d) a minimum length of nylon thread so placed as to have as little as possible parallel to the electric vector. The use of string and thread was generally disappointing owing, presumably, to the relatively high frequency at which measurements were taken.

3. PATTERNS OF PROJECTILE MODELS

Models were made of the 81-mm mortar shell, and a Russian mortar shell of approximate diameter $4\frac{1}{2}$"; also, of the 105-mm artillery shell and the 155-mm artillery shell. The five models are shown in Plate V. Patterns of the models are shown in Figs. 6 to 35. Patterns were recorded in polar form because it was believed that these were easier to interpret physically.

The polarizations of the transmitting and receiving antennas could be changed independently. Vertical (V) and right-hand circular (RHC) polarization were available with the transmitter, and vertical (V), right-hand circular (RHC) and left-hand circular (LHC) polarization with the receiver. Polarizations are identified on the individual patterns. A considerable number were taken with the transmitter having right-hand circular polarization and the receiver left-hand circular polarization. These patterns are almost identical with those for vertical-vertical polarization over considerable portions of the patterns, particularly at broadside aspects.

The main purpose of the investigation was to obtain data at circular polarization. Patterns at other polarizations were obtained for direct comparison. It follows from considerations of symmetry that all the information with respect to the back-scatter cross section at circular polarization of a target with rotational symmetry is obtainable from one pattern at zero tilt angle. Hence all RHC-RHC patterns for symmetrical targets can be used to synthesize other patterns for non-zero tilt. A set of RHC-RHC patterns at non-zero tilt for the

81-mm model with tail fins removed was, in fact, taken using the Styrofoam bowl. While a point-by-point comparison was not made between these patterns and the one at zero tilt, they appeared to be consistent with each other. The same considerations apply to RHC-LHC patterns; that is, patterns for a symmetrical target at non-zero tilt may be obtained from the pattern at zero tilt.

Targets with a finned tail had fin orientation (θ_F) identified by number, beginning with No. 1 in which a fin was vertical. Most targets were positioned with the target axis perpendicular to the axis of rotation. However, a set of patterns (Figs. 36 to 44) was taken of the 81-mm mortar-shell model at various angles of tilt (θ_T). The target was placed in the Styrofoam hemisphere for this set of patterns. While some pattern distortion due to the hemisphere undoubtedly occurred, it is believed, nevertheless, that these patterns are useful because they provide a direct indication of what occurs outside the principal plane in the form which is most directly applicable to an operational situation. Similar patterns (not shown) were obtained for the 81-mm model with the tail fins removed, at both linear and circular polarizations.

Patterns of the 105-mm model, with an actual nose cone at several orientations instead of the model nose cone, are shown in Figs. 45 and 46. Certain nose-cone asymmetries produce significant pattern alterations at 16 Gc/s, and these patterns were taken to provide an example of the extent of the alteration.

Patterns of the 81-mm model with tail fins removed were taken at 15.92 Gc/s, 16.00 Gc/s, and 16.08 Gc/s, and one of each is reproduced in Figs. 47-49. The marked frequency dependence of the front-to-back ratio is presumably characteristic of a target with rotational symmetry. A shift of the lobe structure with frequency can also be established by careful measurement of the patterns.

4. OTHER PATTERNS

Patterns of a corner reflector for use with the counter mortar radar are shown in Fig. 50. Patterns of a 1/36 model of the "Alouette" satellite are shown in Fig. 51. The model of the satellite proper was a spherical ball of 1" diameter, and the antennas were simulated by steel rods of lengths $24\frac{1}{2}$" and $12\frac{1}{4}$". Note that the pattern of the ball is much decreased at circular polarization, and that travelling-wave lobes are quite prominent at circular polarization.

5. CONCLUSIONS

It is not the purpose of this report to analyse or interpret the projectile patterns or to devise a means by which they may be used operationally to the best advantage. However, attention will be drawn to certain results which are clearly evident. Firstly, finned targets must be considered as a class apart from targets with rotational asymmetry. Typically, a target with rotational symmetry has a cross section at linear polarization in the order of 1 (meter)^2 at broadside, and wide aspects, possibly as much as 150° out of 360°, at which the cross section drops to -25 db m^2 to -35 db m^2. Much less variation with aspect occurs at circular polarization, typical values being -20 db m^2 to -35 db m^2. If the system design is based on the minimum back-scatter response of a target, there is little, if any, difference between linear and circular polarization. But, if it is necessary, as is generally the case, to depend on a cross section considerably in excess of the minimum, then the scattered response available will be reduced at circular polarization by a factor varying up to 20 db for the strong broadside responses.

The response from a target with rotational symmetry depends only on the angle between the target axis and line-of-sight when the polarization is circular. Hence the patterns as shown in the figures, with both target axis and line-of-sight perpendicular to the axis of rotation, are basic patterns from which all others at non-zero tilt angles can be obtained. The same consideration applies to the RHC-LHC patterns; they are reproduced because they can be converted to all aspects and because they provide a useful comparison with V-V patterns from which they generally do not differ significantly.

The cross sections of finned targets at linear polarization have similar broadside peaks (in the order of 1 (meter)^2), but null regions which are neither as deep or as broad as for targets without fins. Patterns at circular polarization (RHC-RHC) depend markedly on fin orientation. Pronounced lobes may be generated at unexpected aspects. The average level may be 5 db - 10 db higher than for a comparable symmetrical target, and null regions may be less extensive.

REFERENCES

1. G.C. McCormick and J.C. Barnes, "A Polarizer for AN/MPQ-501" National Research Council Report ERB-636, January 1963

2. An extensive bibliography of scattering measurement techniques is contained in "Techniques for Measurement of Reduced Radar Cross Sections" by C.G. Bachman, H.E. King, and R.C. Hansen. Microwave Journal, VI No. 2, p. 67, February 1963

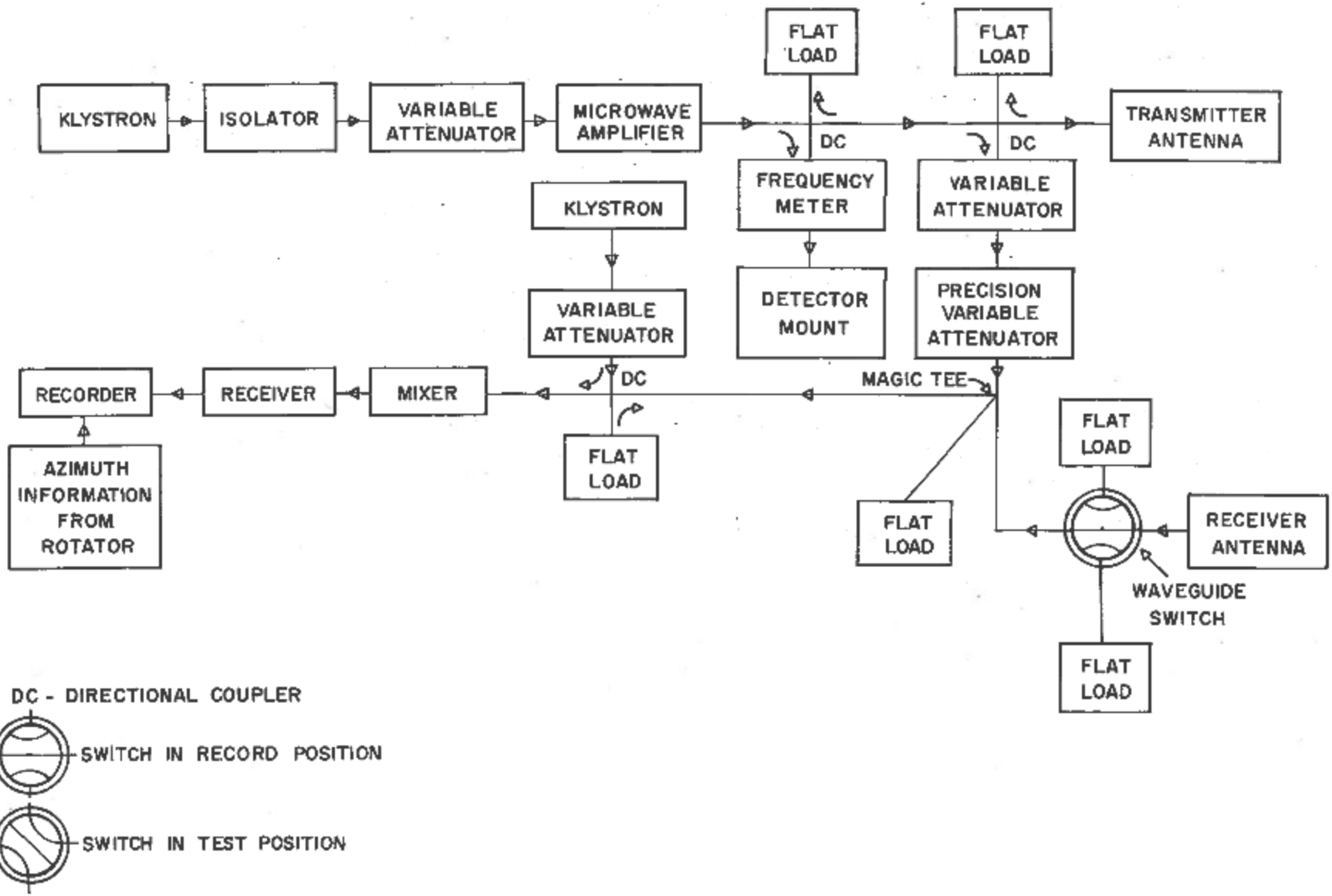

Fig. 1 Block diagram of the transmitter-receiver equipment

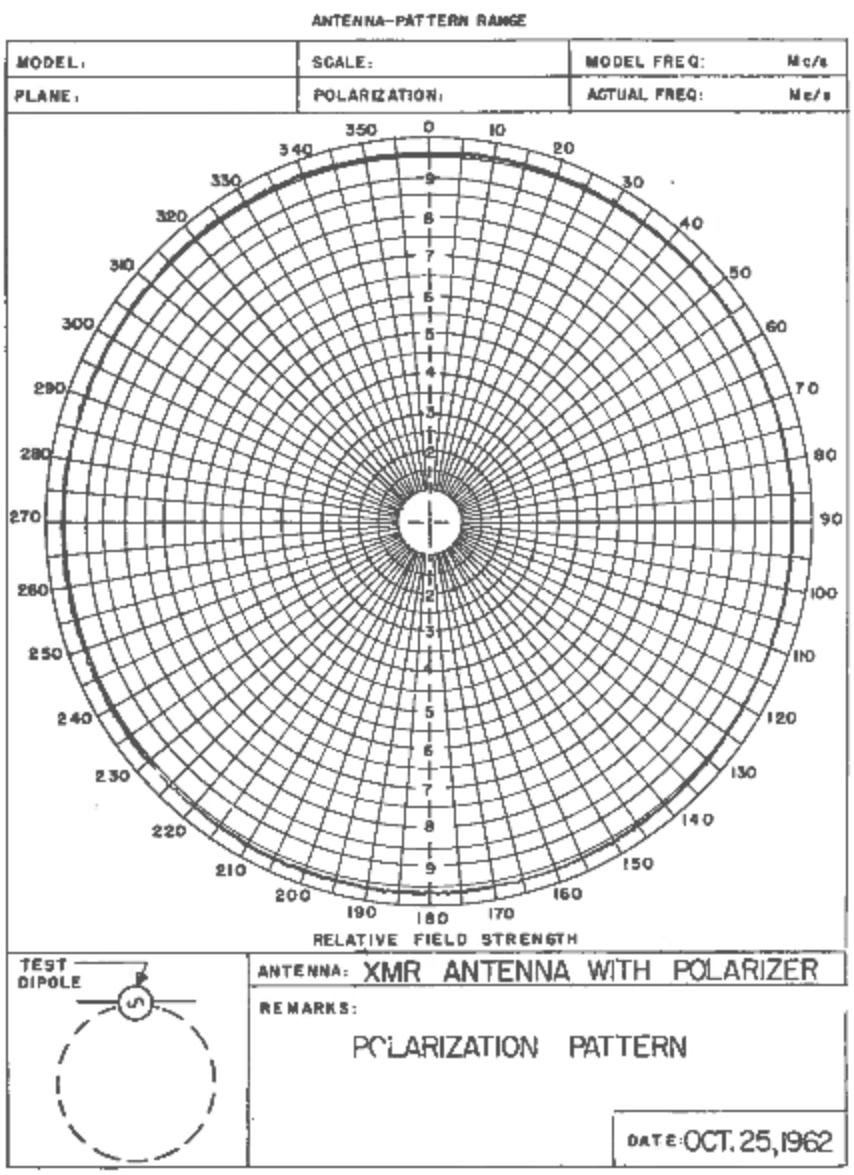

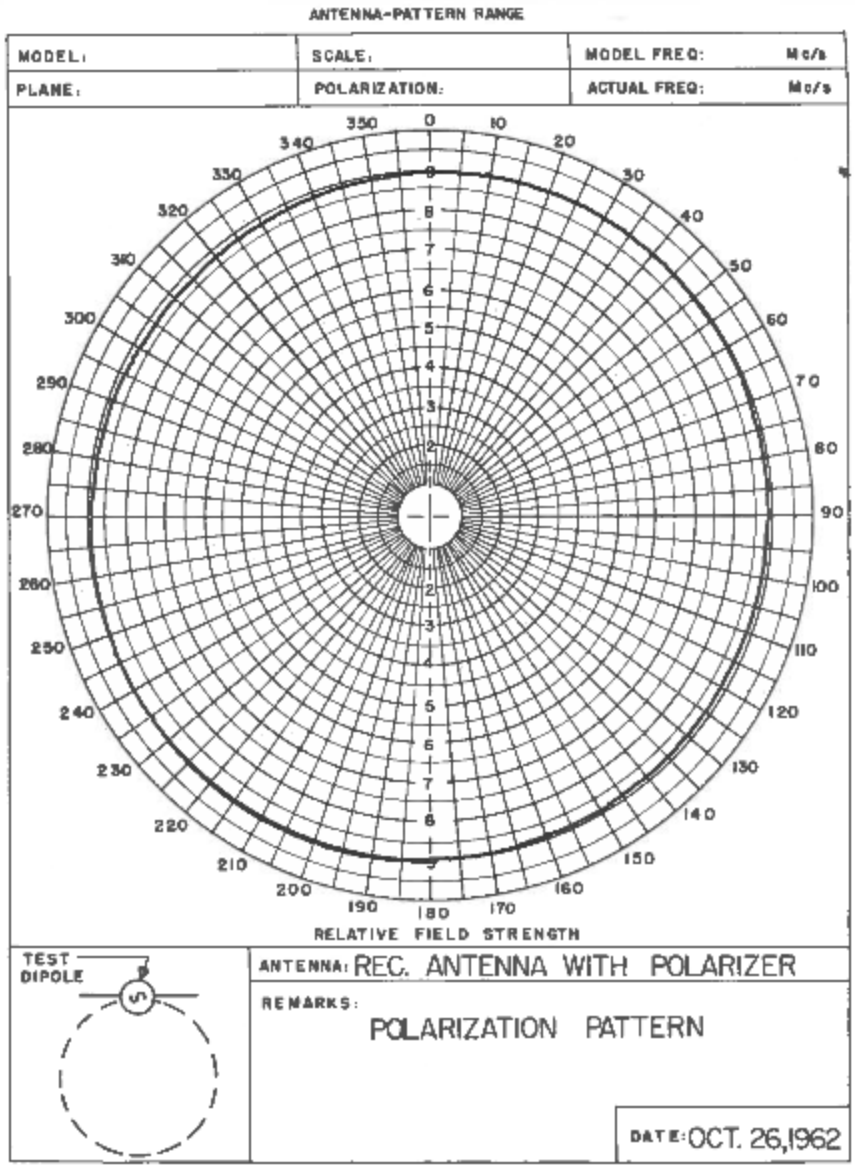

Fig. 2 Polarization pattern of the transmitting antenna with polarizer (left), and of the receiving antenna with polarizer (right)

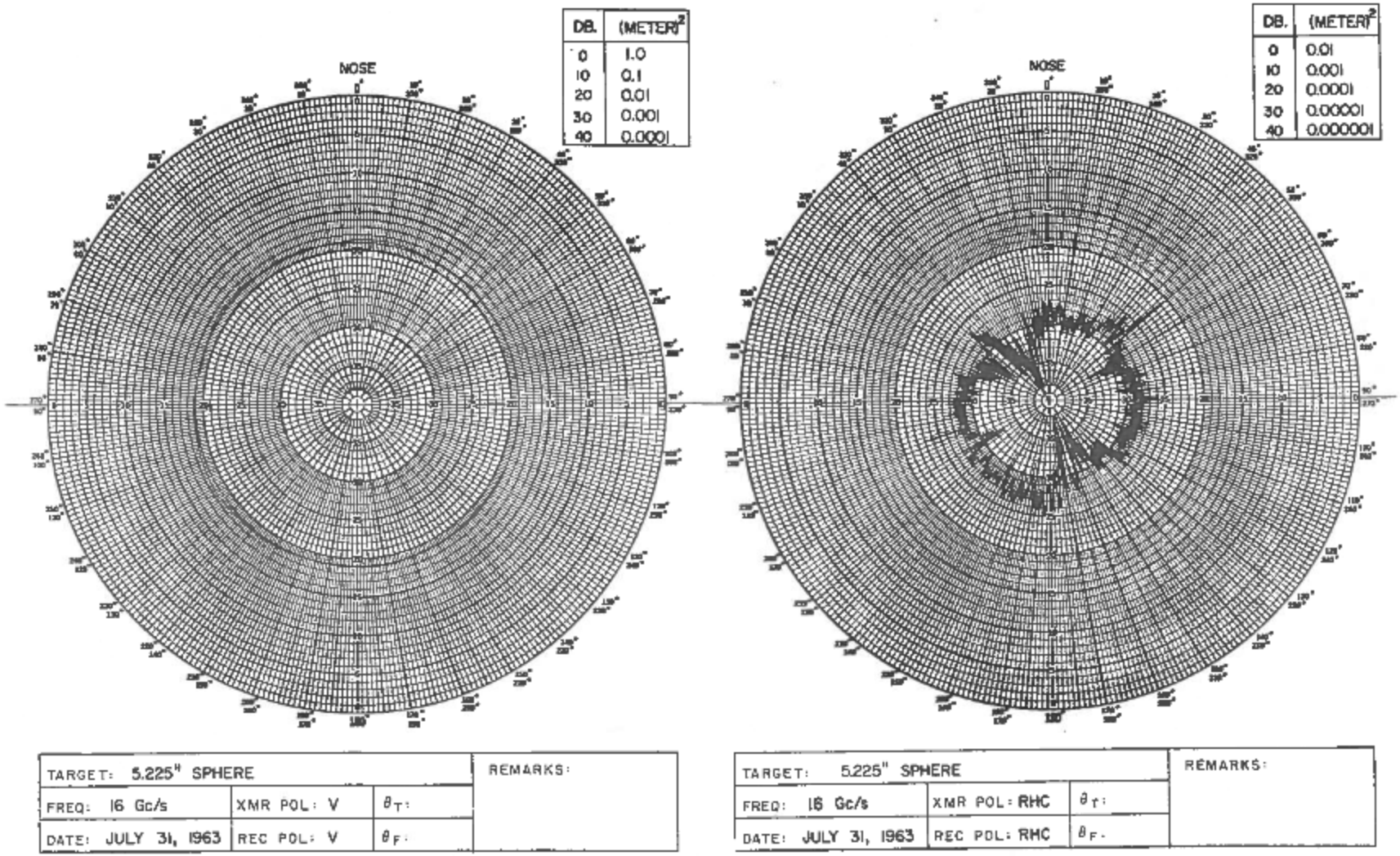

Fig. 3 Test patterns of a 5.225" sphere (ka = 22.26) at vertical polarization and at circular polarization

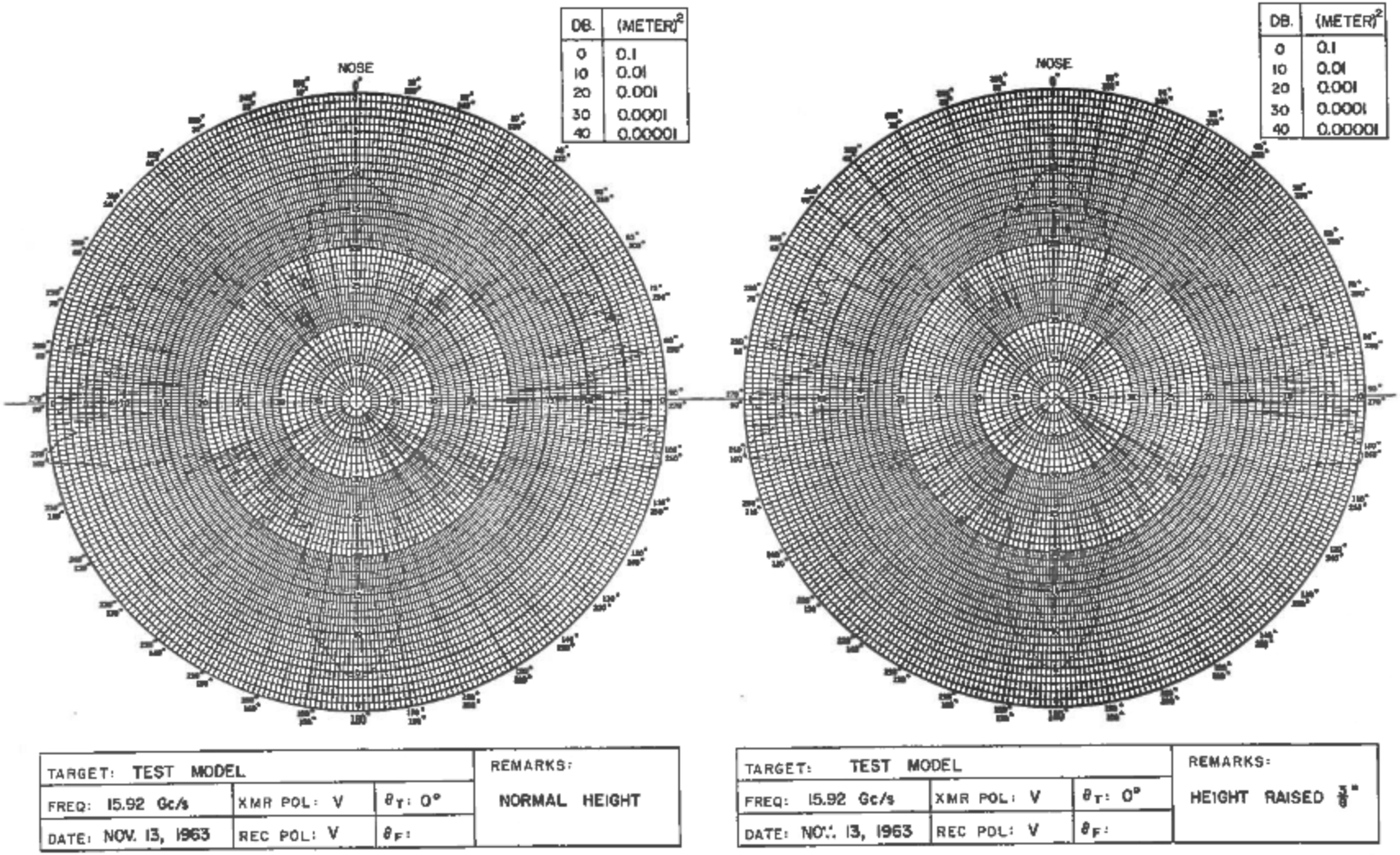

Fig. 4 Patterns of a modified mortar shell model taken at separations between target and support which differ by one-half wavelength

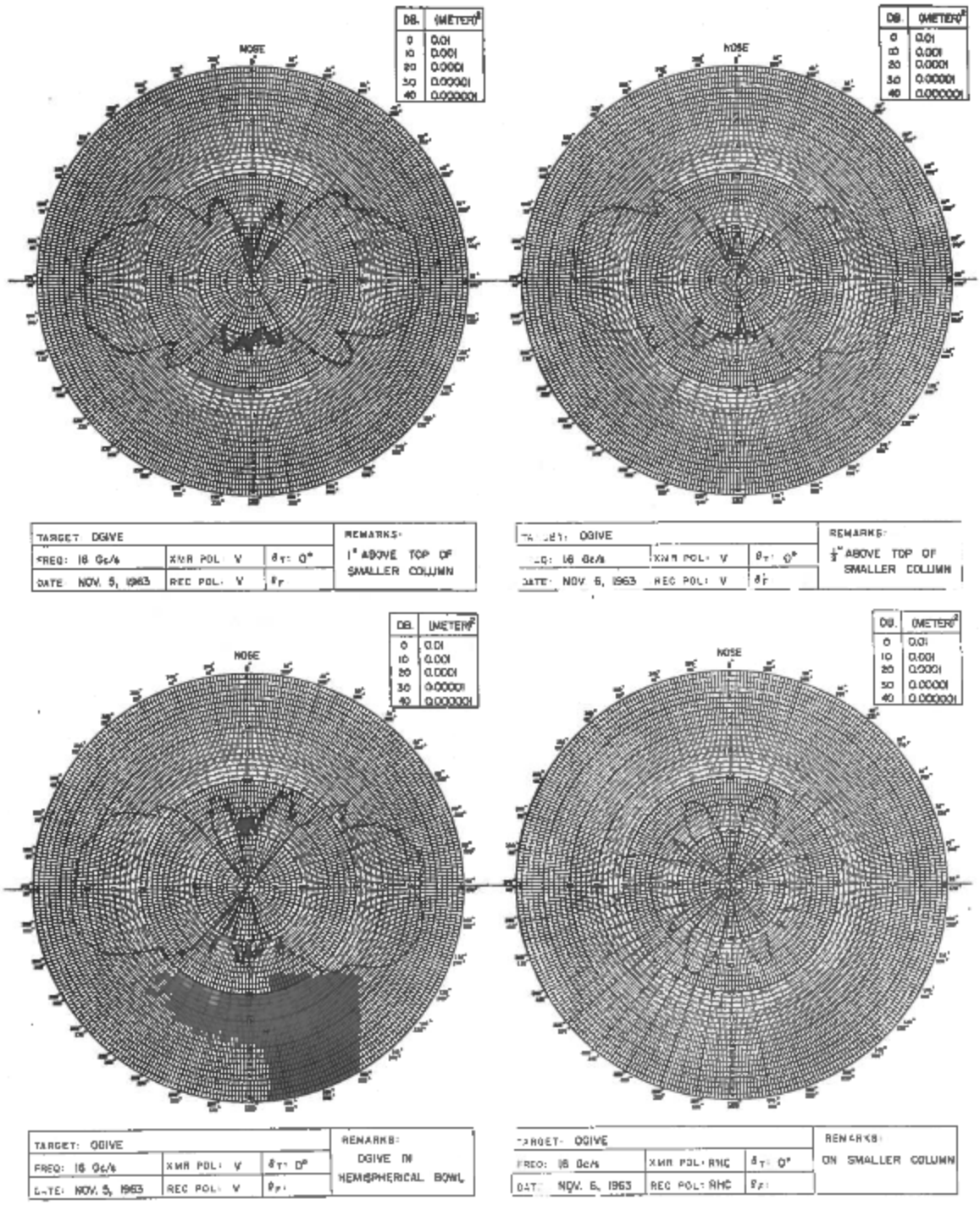

Fig. 5 Test patterns of a 75° ogive of length 2.04" (upper left) ogive 1" above small column (upper right) ogive ½" above small column (lower left) ogive in Styrofoam bowl (lower right) ogive on small column, circular polarization

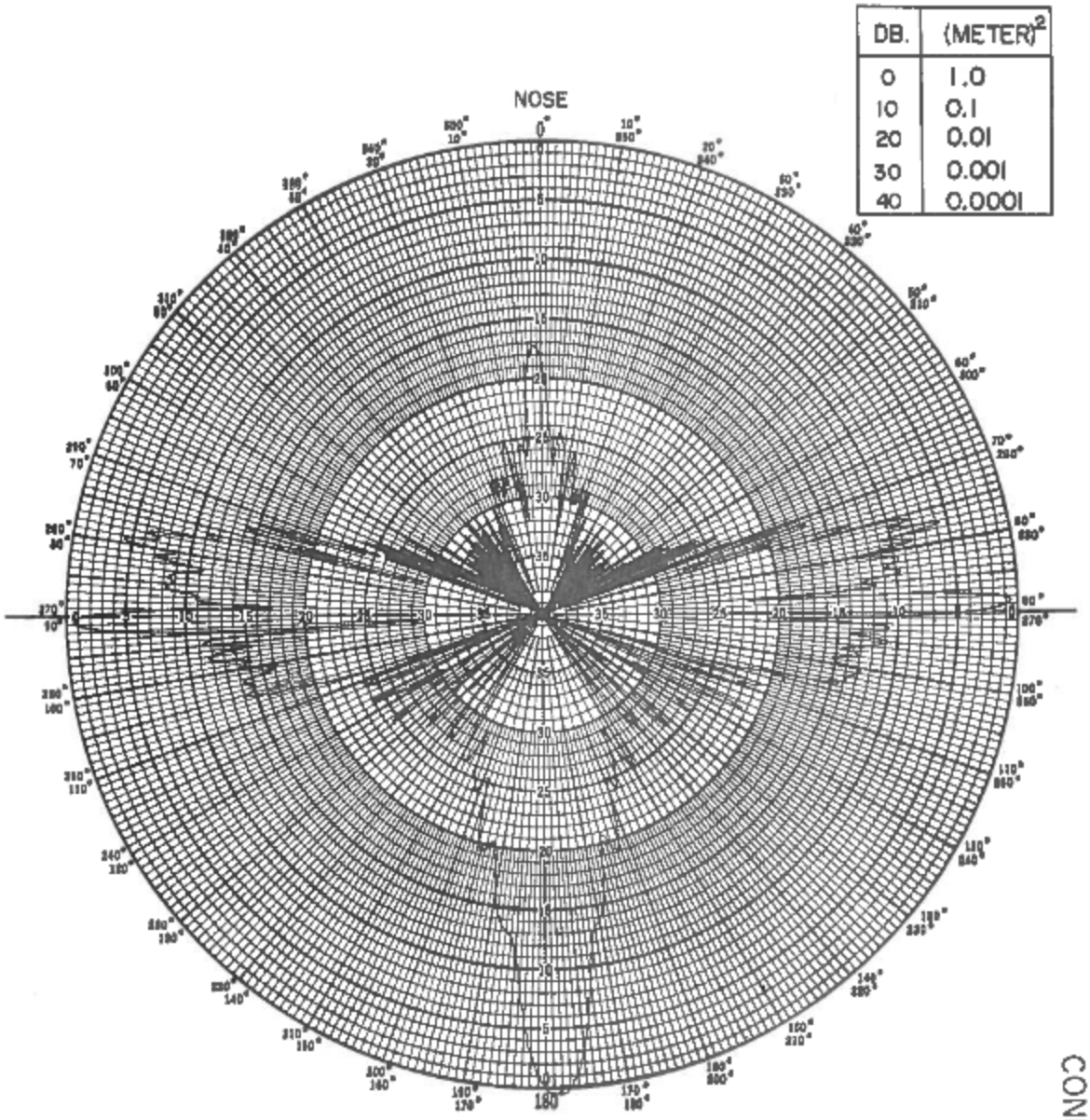

TARGET: MODEL OF 105 mm. SHELL			REMARKS:
FREQ: 16 Gc/s	XMR POL: V	θ_T: 0°	
DATE: JULY 19, 1963	REC POL: V	θ_F:	

CONFIDENTIAL

Fig. 6 Back-scatter pattern of model of 105-mm artillery shell V-V polarization, 0 db = 1.0 (meter)^2

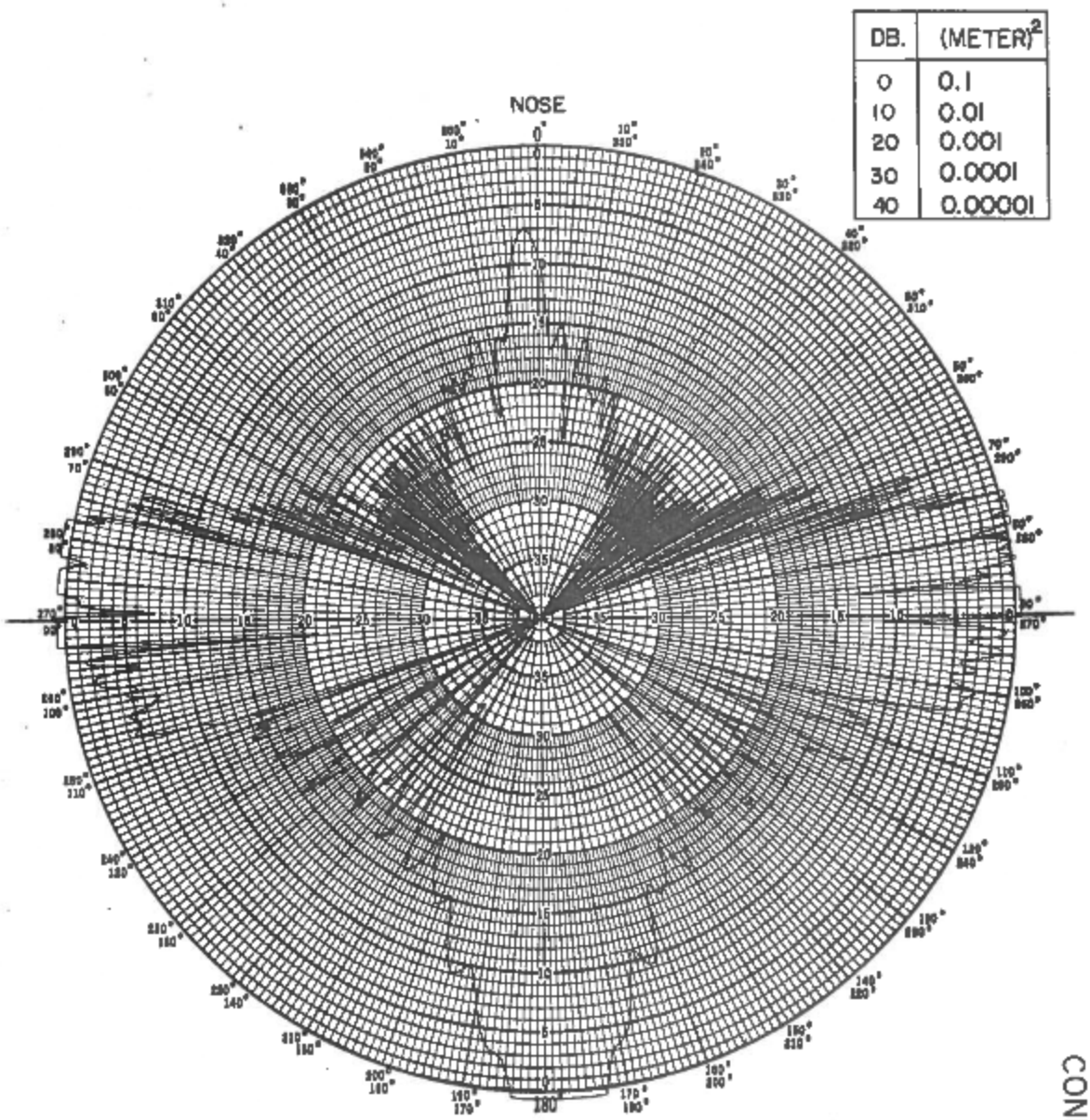

TARGET: MODEL OF 105 mm. SHELL			REMARKS:
FREQ: 16 Gc/s	XMR POL: V	θ_T: 0°	
DATE: JULY 19, 1963	REC POL: V	θ_F:	

CONFIDENTIAL

Fig. 7 Back-scatter pattern of model of 105-mm artillery shell V-V polarization, 0 db = 0.1 (meter)^2

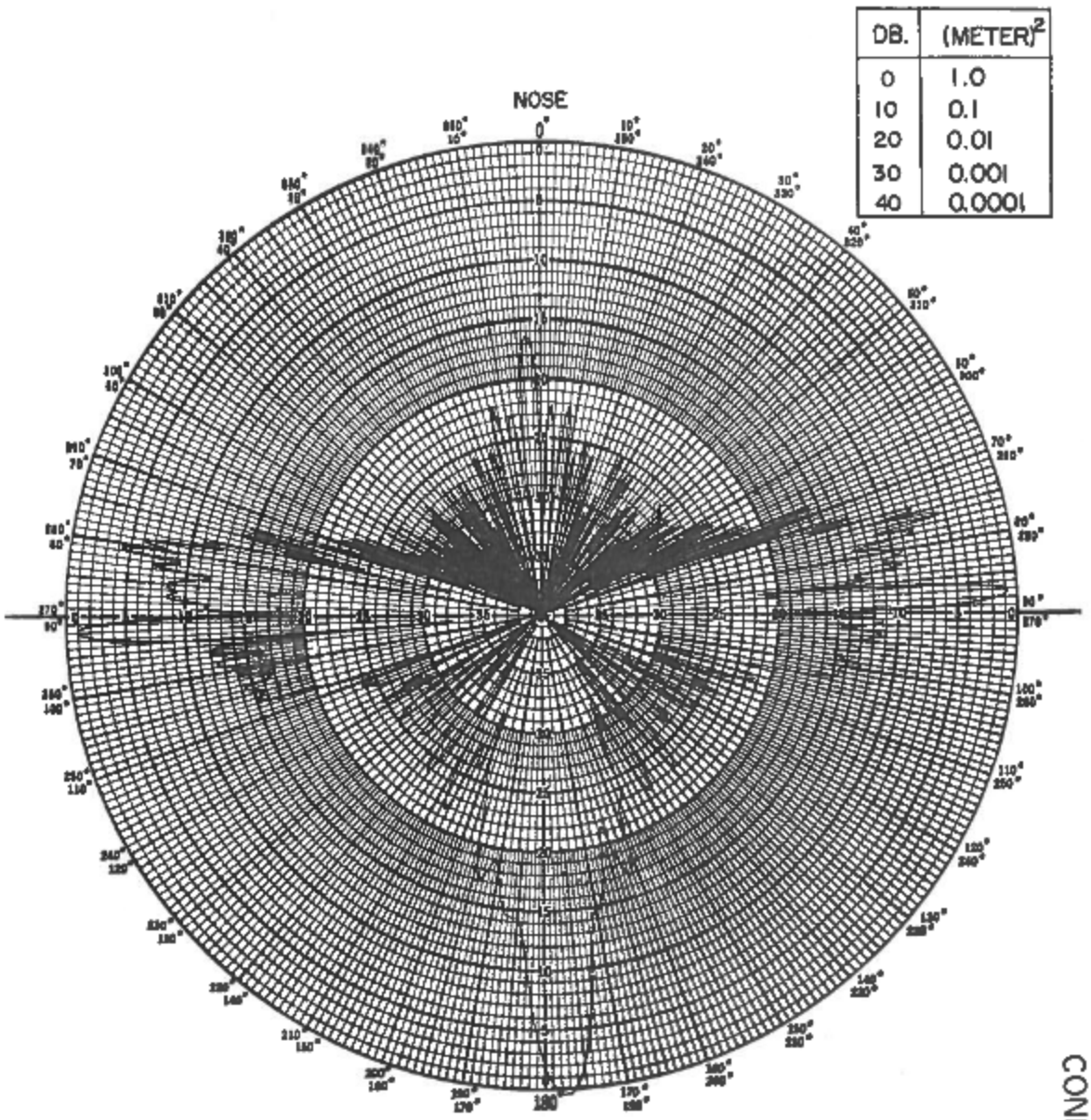

TARGET: MODEL OF 105 mm. SHELL			REMARKS:
FREQ: 16 Gc/s	XMR POL: RHC	θ_T: 0°	
DATE: JULY 19, 1963	REC POL: LHC	θ_F:	

CONFIDENTIAL

Fig. 8 Back-scatter pattern of model of 105-mm artillery shell R-L polarization, 0 db = 1.0 (meter)^2

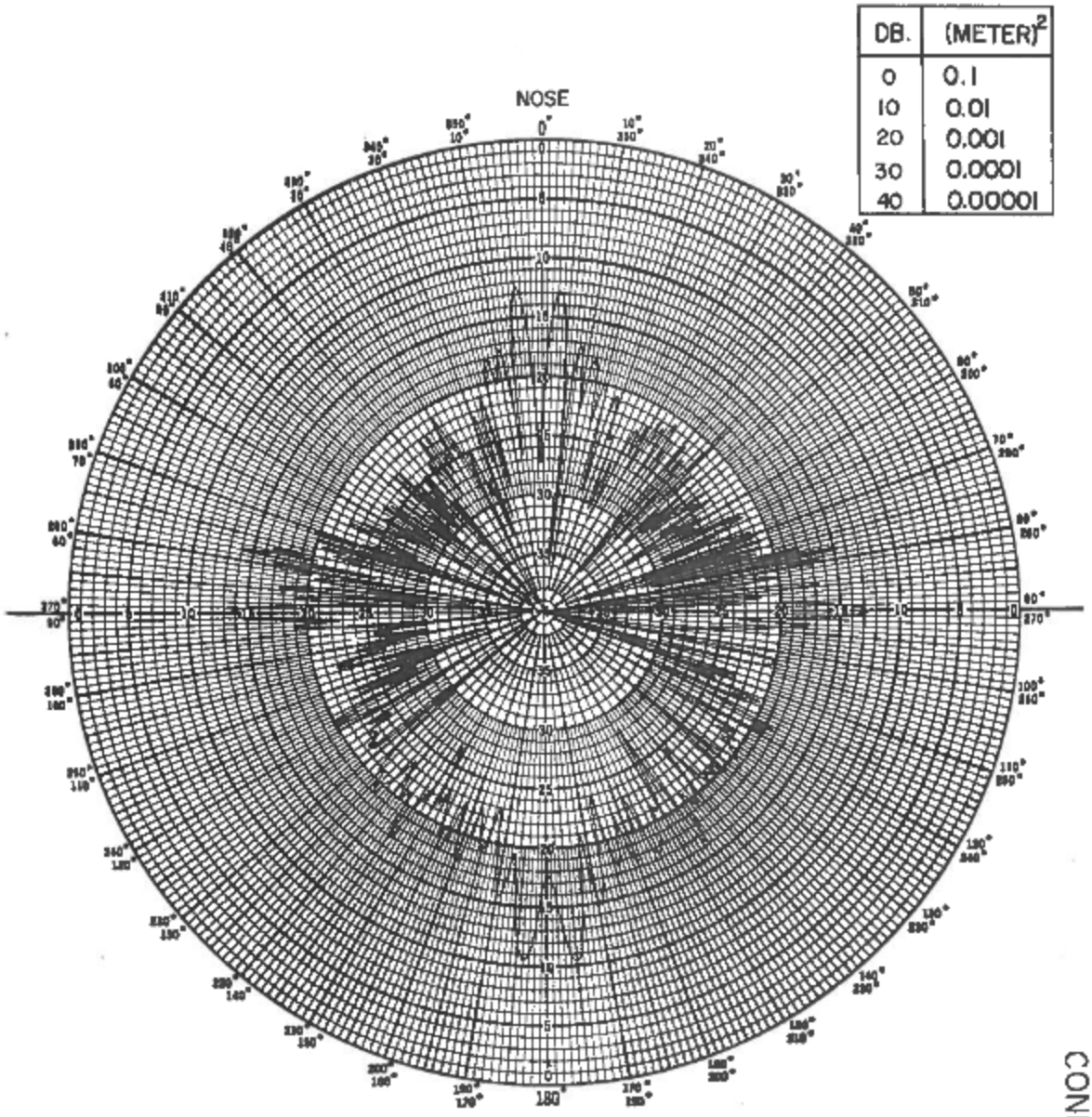

CONFIDENTIAL

Fig. 9 Back-scatter pattern of model of 105-mm artillery shell R-R polarization, 0 db = 0.1 (meter)^2

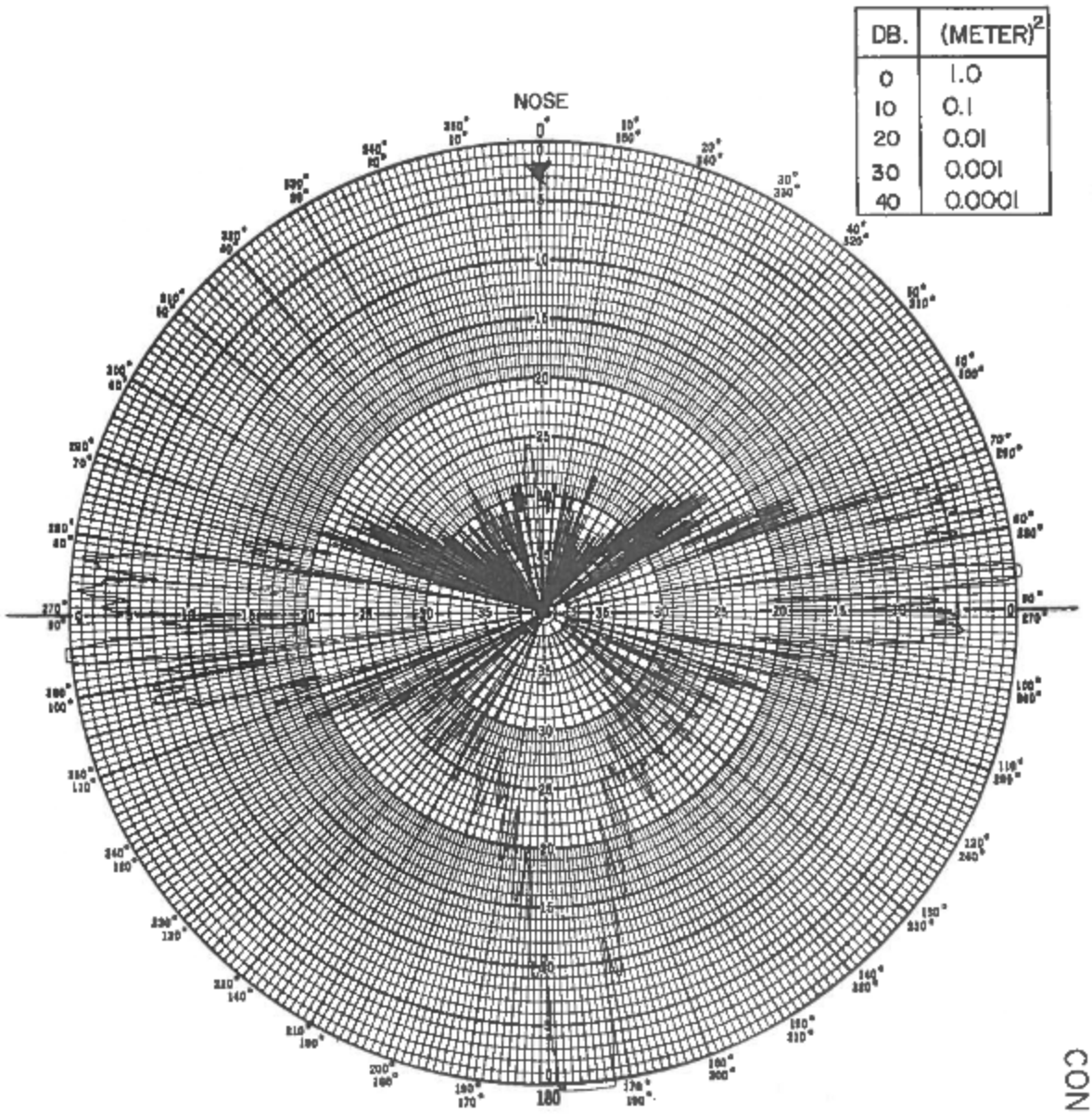

TARGET: MODEL OF 155 mm. SHELL			REMARKS:
FREQ: 16 Gc/s	XMR POL: V	θ_T: 0°	
DATE: AUG. 7, 1963	REC POL: V	θ_T:	

CONFIDENTIAL

Fig. 10 Back-scatter pattern of model of 155-mm artillery shell V-V polarization, 0 db = 1.0 (meter)^2

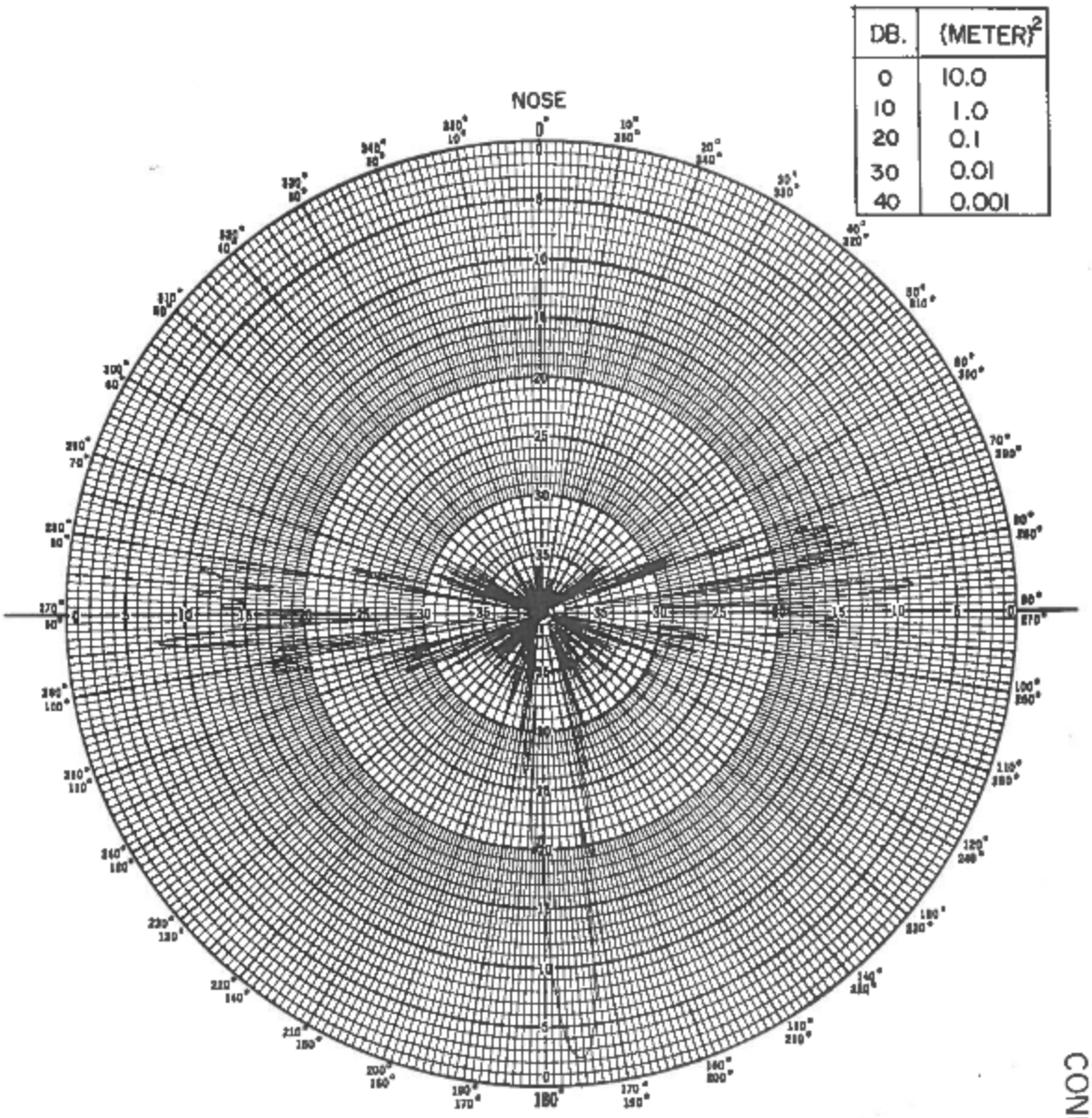

TARGET: MODEL OF 155 mm. SHELL			REMARKS:
FREQ: 16 Gc/s	XMR POL: V	ϑ: 0°	
DATE: AUG. 7, 1963	REC POL: V	θ_F:	

CONFIDENTIAL

Fig. 11 Back-scatter pattern of model of 155-mm artillery shell V-V polarization, 0 db = 10 (meters)^2

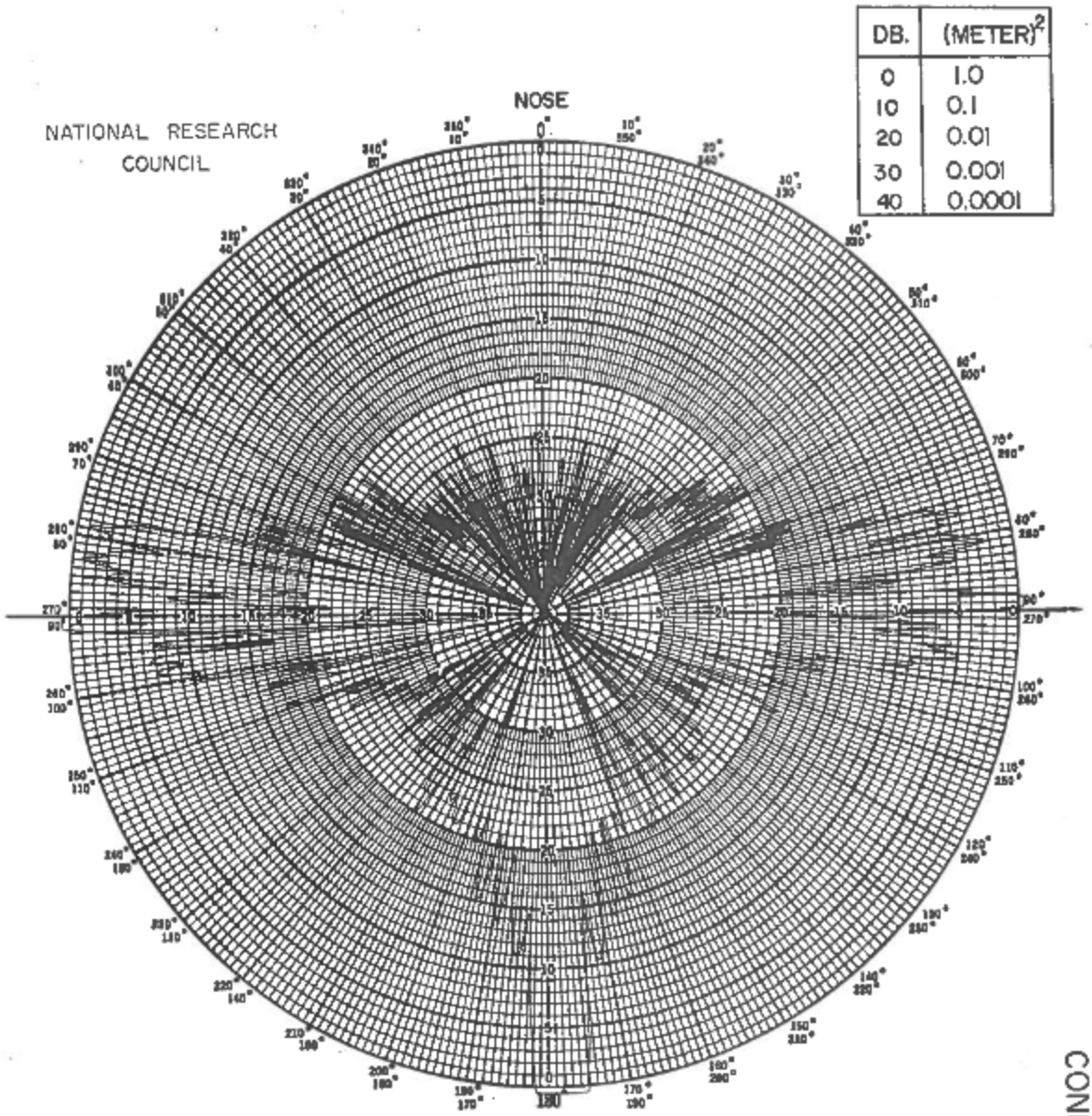

TARGET: MODEL OF 155 mm. SHELL			REMARKS:
FREQ: 16 Gc/s	XMR POL: RHC	θ_T: 0°	
DATE: AUG. 7, 1963	REC POL: LHC	θ_T:	

CONFIDENTIAL

Fig. 12 Back-scatter pattern of model of 155-mm artillery shell R-L polarization, 0 db = 1.0 (meter)^2

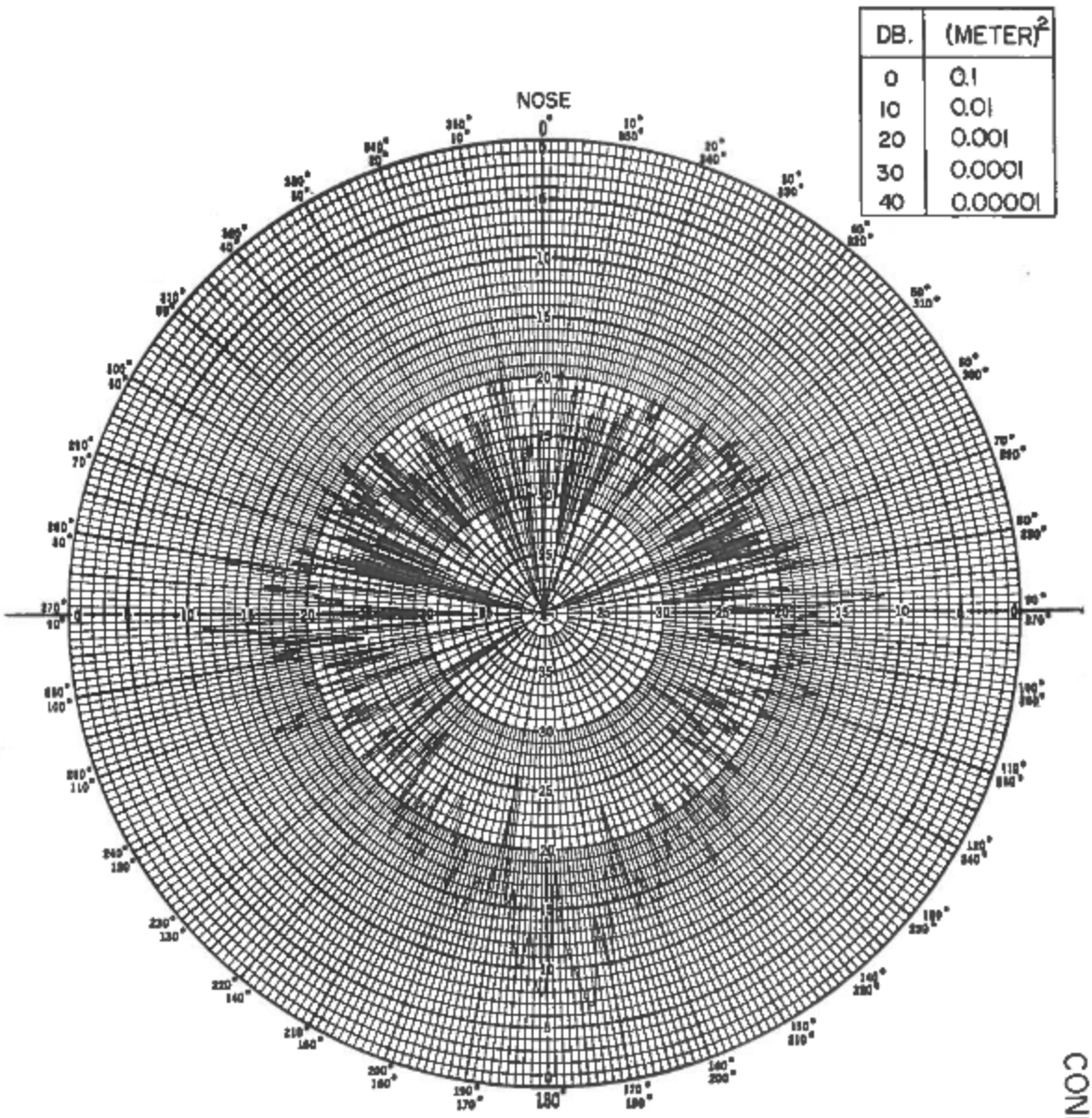

TARGET: MODEL OF 155 mm. SHELL			REMARKS:
FREQ: 16 Gc/s	XMR POL: RHC	θ_T: 0°	
DATE: AUG. 7, 1963	REC POL: RHC	θ_F:	

CONFIDENTIAL

Fig. 13 Back-scatter pattern of model of 155-mm artillery shell R-R polarization, 0 db = 0.1 (meter)^2

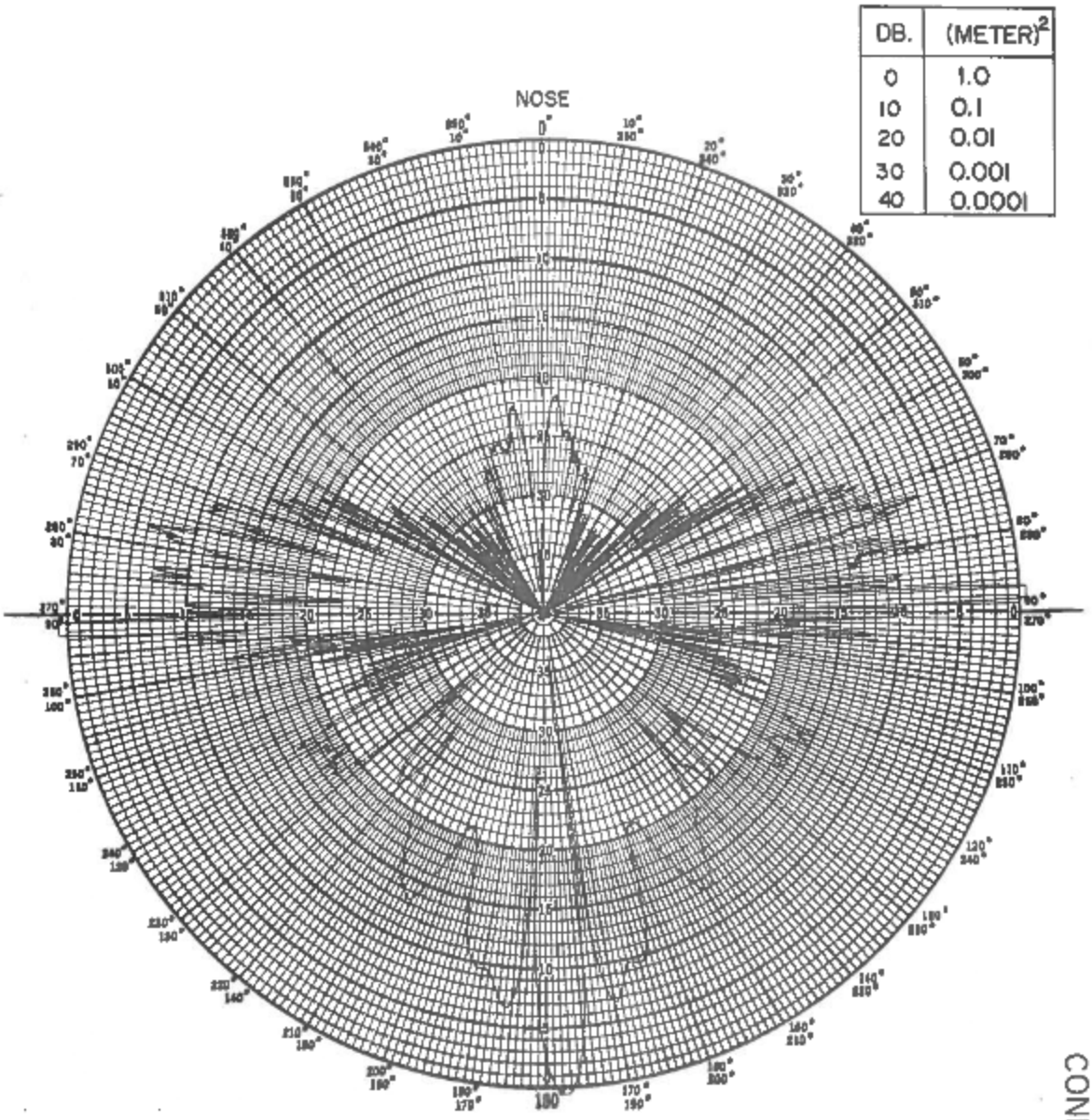

TARGET: MODEL OF M30 MORTAR SHELL			REMARKS:
FREQ: 16 Gc/s	XMR POL: V	θ_T: 0°	
DATE: JULY 19, 1963	REC POL: V	θ_F:	

CONFIDENTIAL

Fig. 14 Back-scatter pattern of model of M30 mortar shell V-V polarization, 0 db = 1.0 (meter)^2

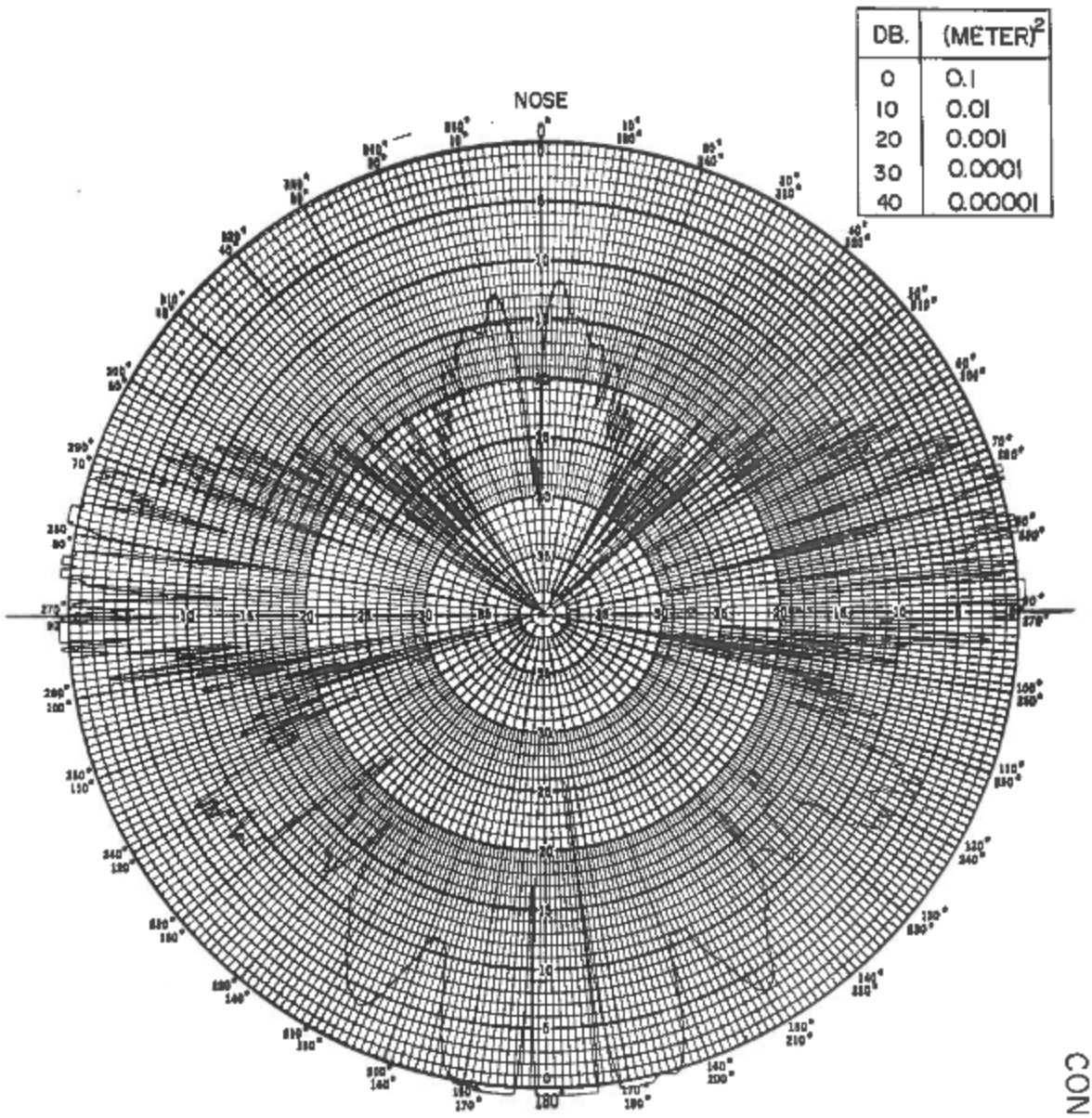

TARGET: MODEL OF M30 MORTAR SHELL			REMARKS:
FREQ: 16 Gc/s	XMR POL: V	θ_T: 0°	
DATE: JULY 19, 1963	REC POL: V	θ_F:	

CONFIDENTIAL

Fig. 15 Back-scatter pattern of model of M30 mortar shell V-V polarization, 0 db = 0.1 (meter)^2

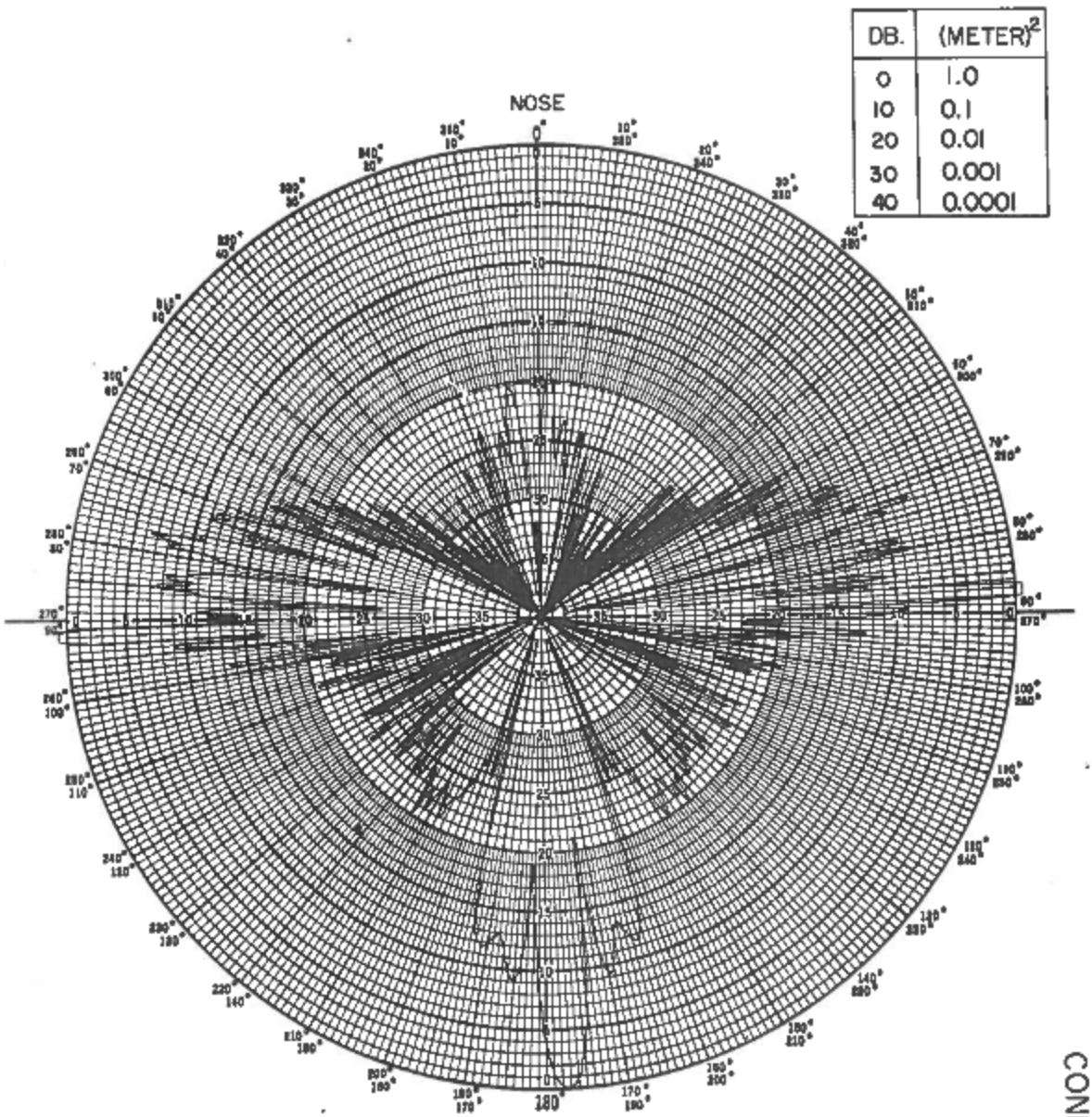

TARGET: MODEL OF M30 MORTAR SHELL			REMARKS:
FREQ: 16 Gc/s	XMR POL: RHC	θ_T: 0°	
DATE: JULY 19, 1963	REC POL: LHC	θ_F:	

CONFIDENTIAL

Fig. 16 Back-scatter pattern of model of M30 mortar shell R-L polarization, 0 db = 1.0 (meter)^2

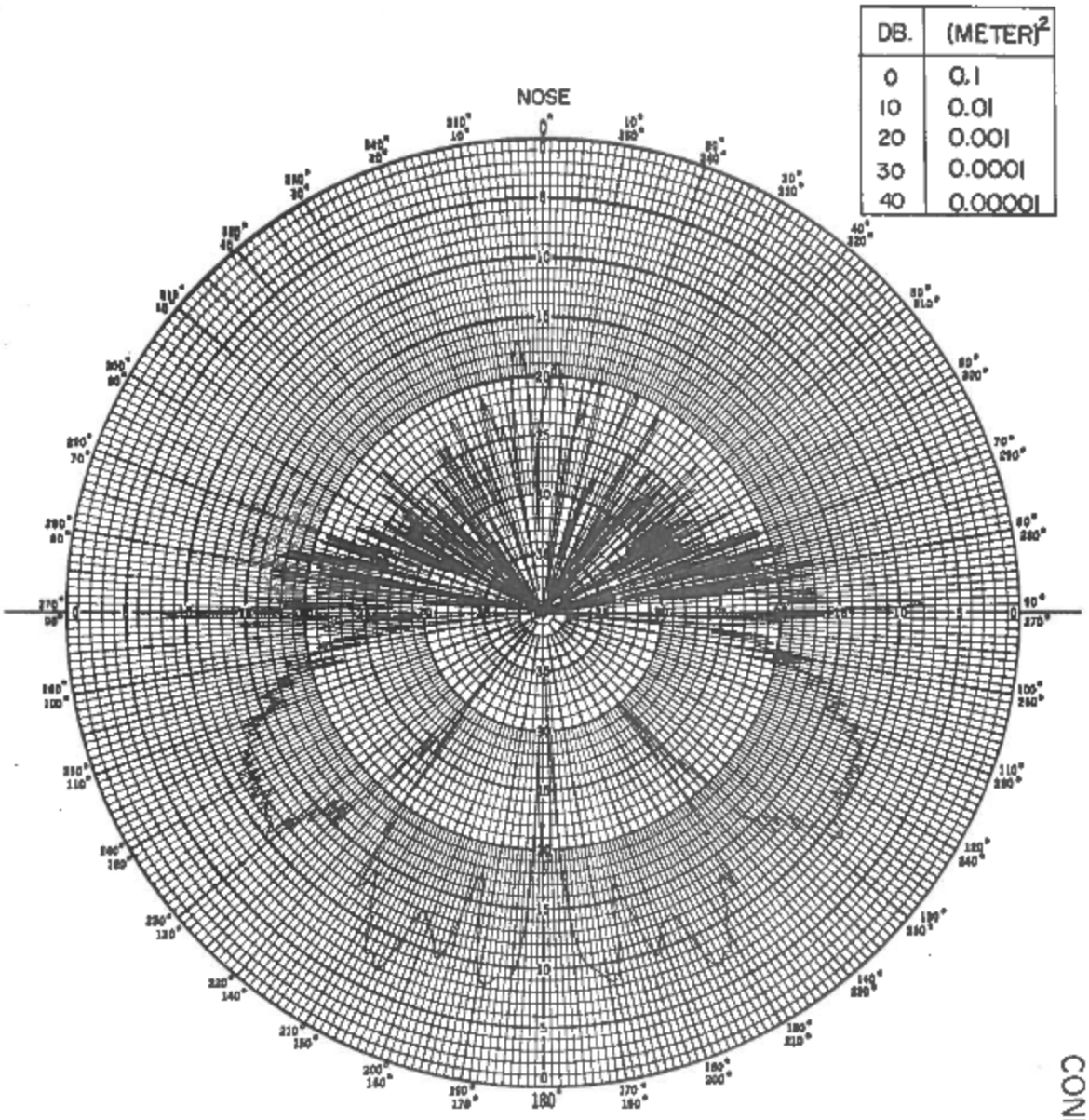

TARGET: MODEL OF M30 MORTAR SHELL			REMARKS:
FREQ: 16 Gc/s	XMR POL: RHC	θ_T: 0°	
DATE: JULY 19, 1963	REC POL: RHC	θ_F:	

CONFIDENTIAL

Fig. 17 Back-scatter pattern of model of M30 mortar shell R-R polarization, 0 db = 0.1 (meter)^2

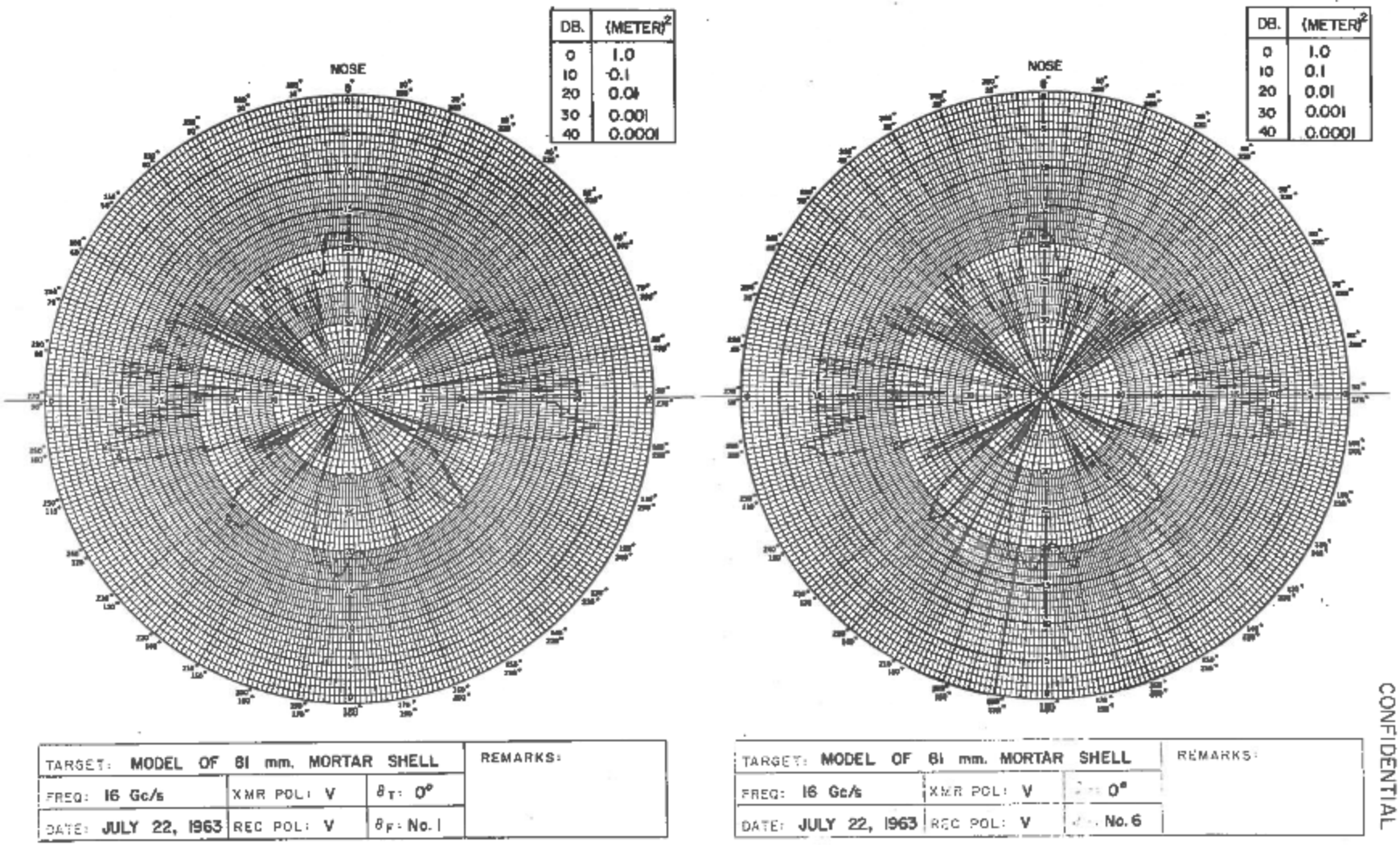

CONFIDENTIAL

Fig. 18 Back-scatter patterns of model of 81-mm mortar shell, V-V polarization, 0 db = 1.0 (meter)^2
Fin positions vertical (No. 1 and No. 6)

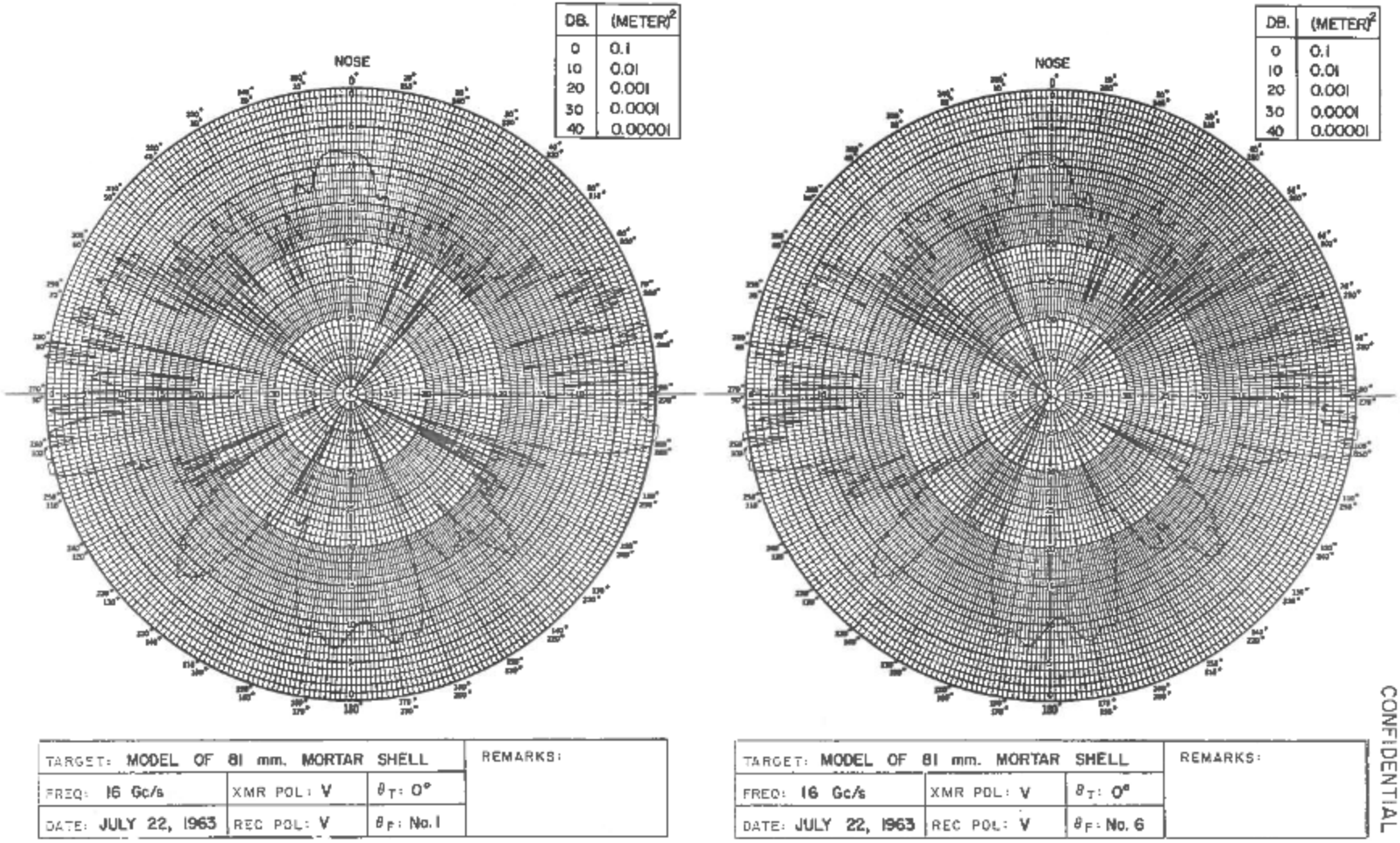

CONFIDENTIAL

Fig. 19 Back-scatter patterns of model of 81-mm mortar shell, V-V polarization, 0 db = 0.1 (meter)^2. Fin positions vertical (No. 1 and No. 6)

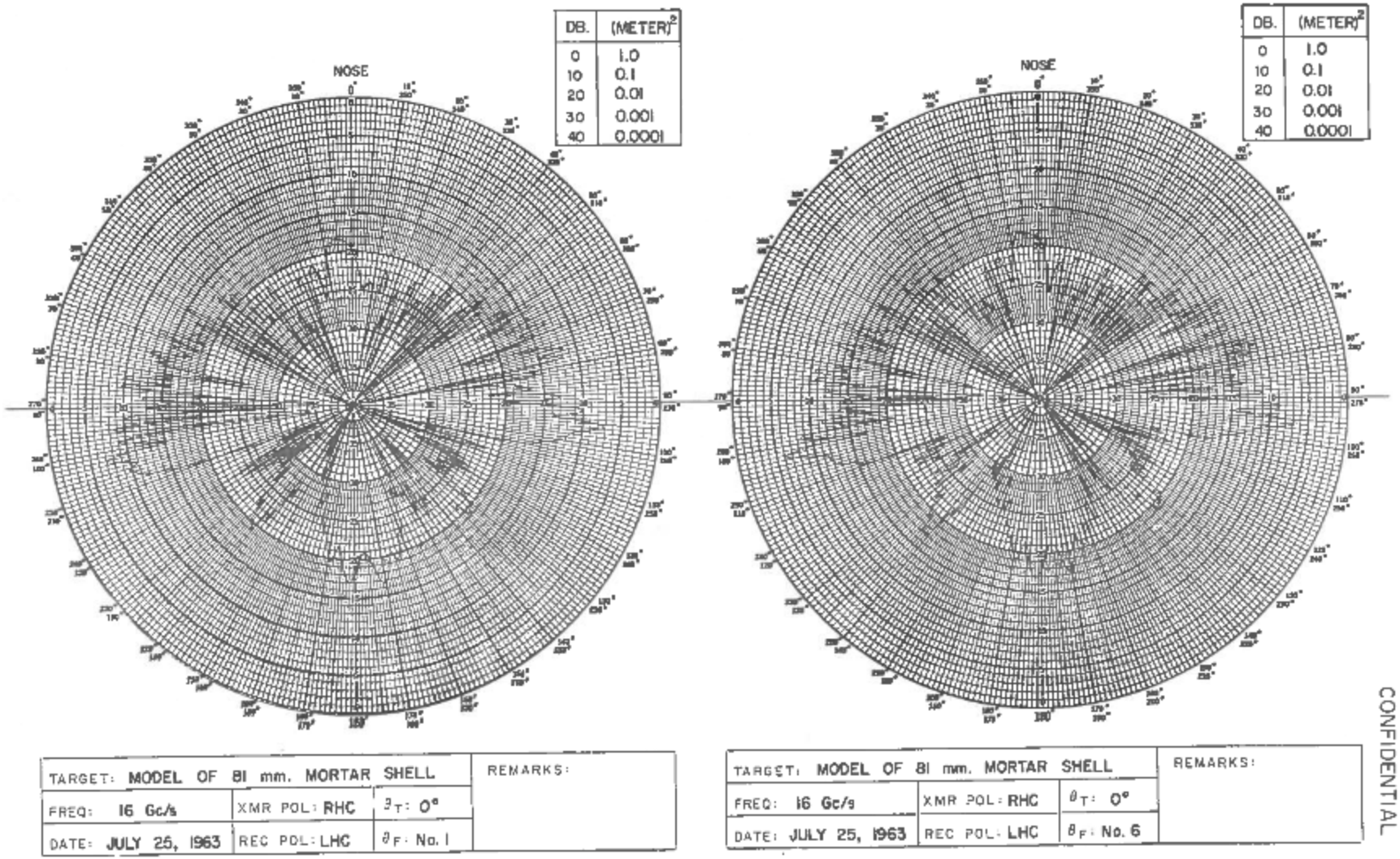

Fig. 20 Back-scatter patterns of model of 81-mm mortar shell, R-L polarization, 0 db = 1.0 (meter)^2. Fin positions vertical (No. 1 and No. 6)

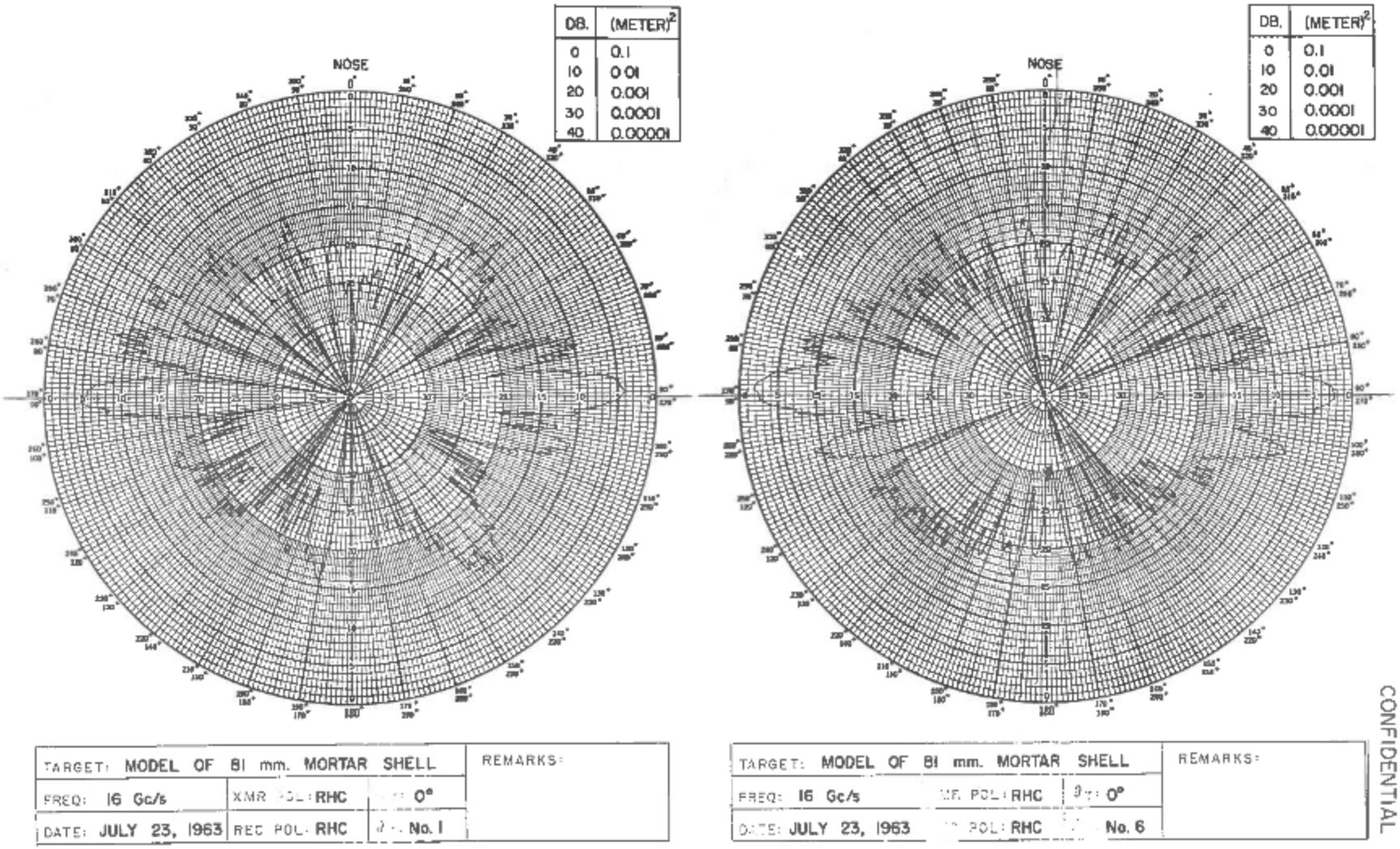

CONFIDENTIAL

Fig. 21 Back-scatter patterns of model of 81-mm mortar shell, R-R polarization, 0 db = 0.1 (meter)^2. Fin positions vertical (No. 1 and No. 6)

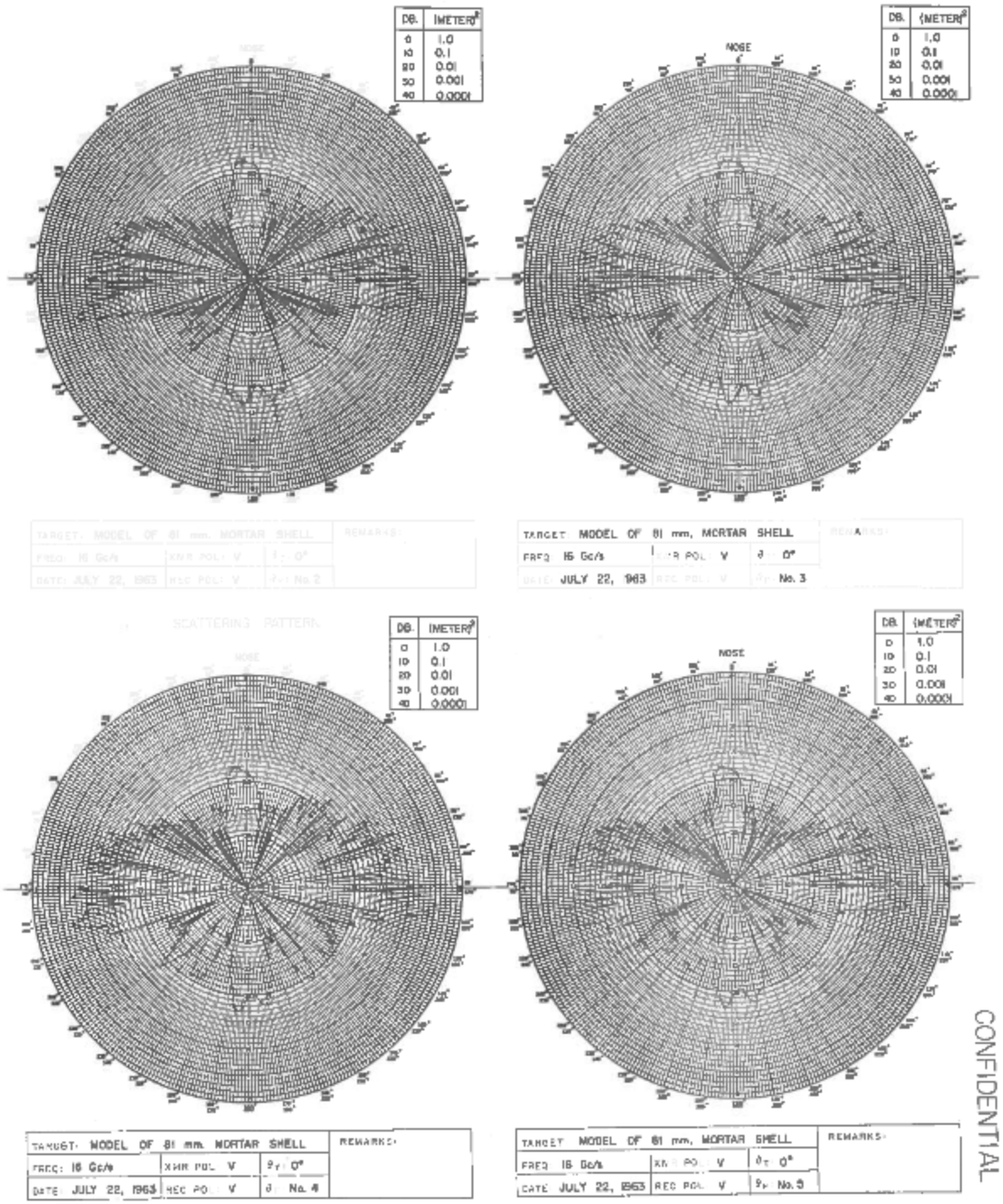

CONFIDENTIAL

Fig. 22 Back-scatter patterns of model of 81-mm mortar shell, V-V polarization, 0 db = 1.0 (meter)^2. Fin positions Nos. 2, 3, 4 and 5

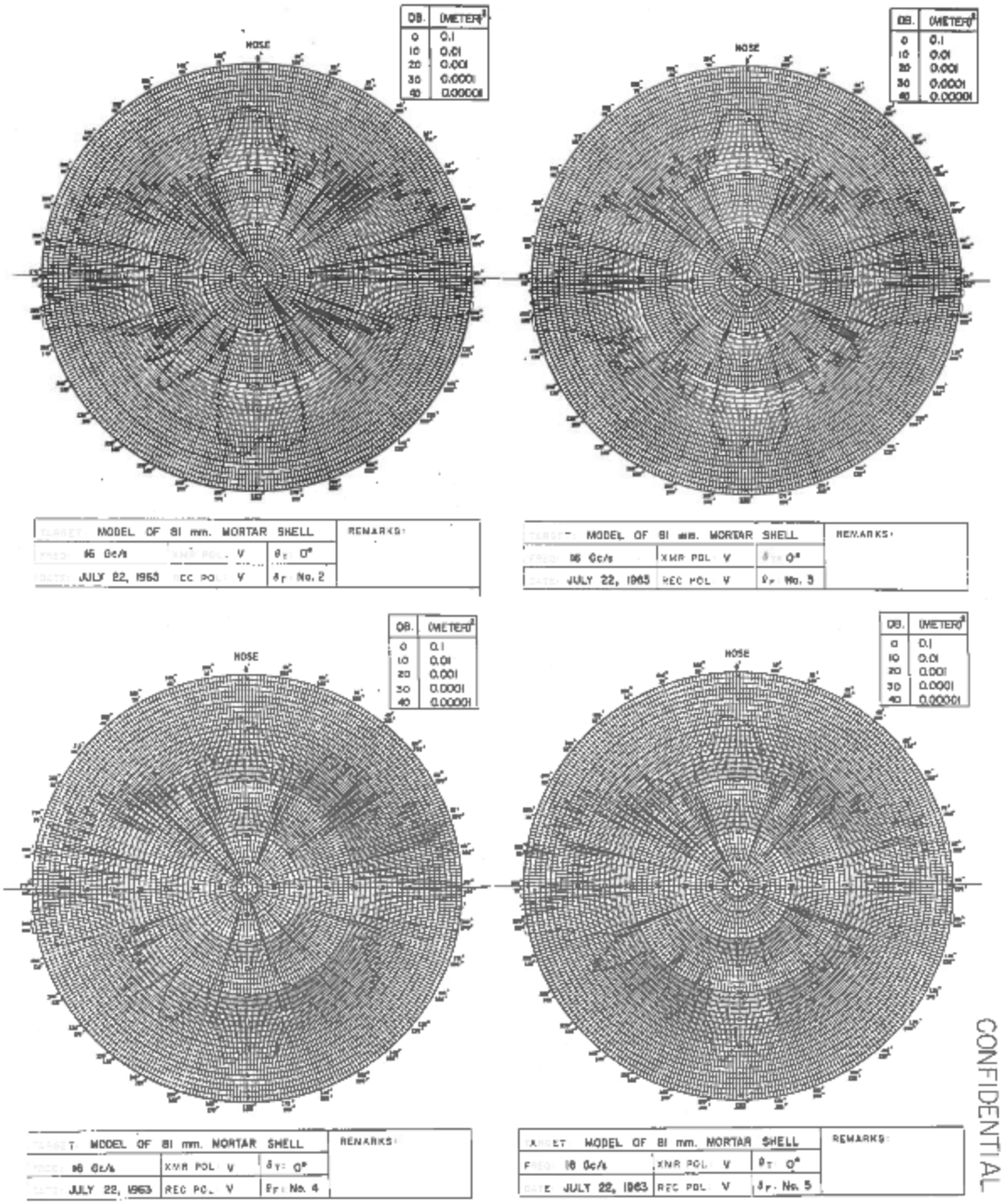

CONFIDENTIAL

Fig. 23 Back-scatter patterns of model of 81-mm mortar shell V-V polarization, 0 db = 0.1 (meter)^2. Fin positions Nos. 2, 3, 4 and 5

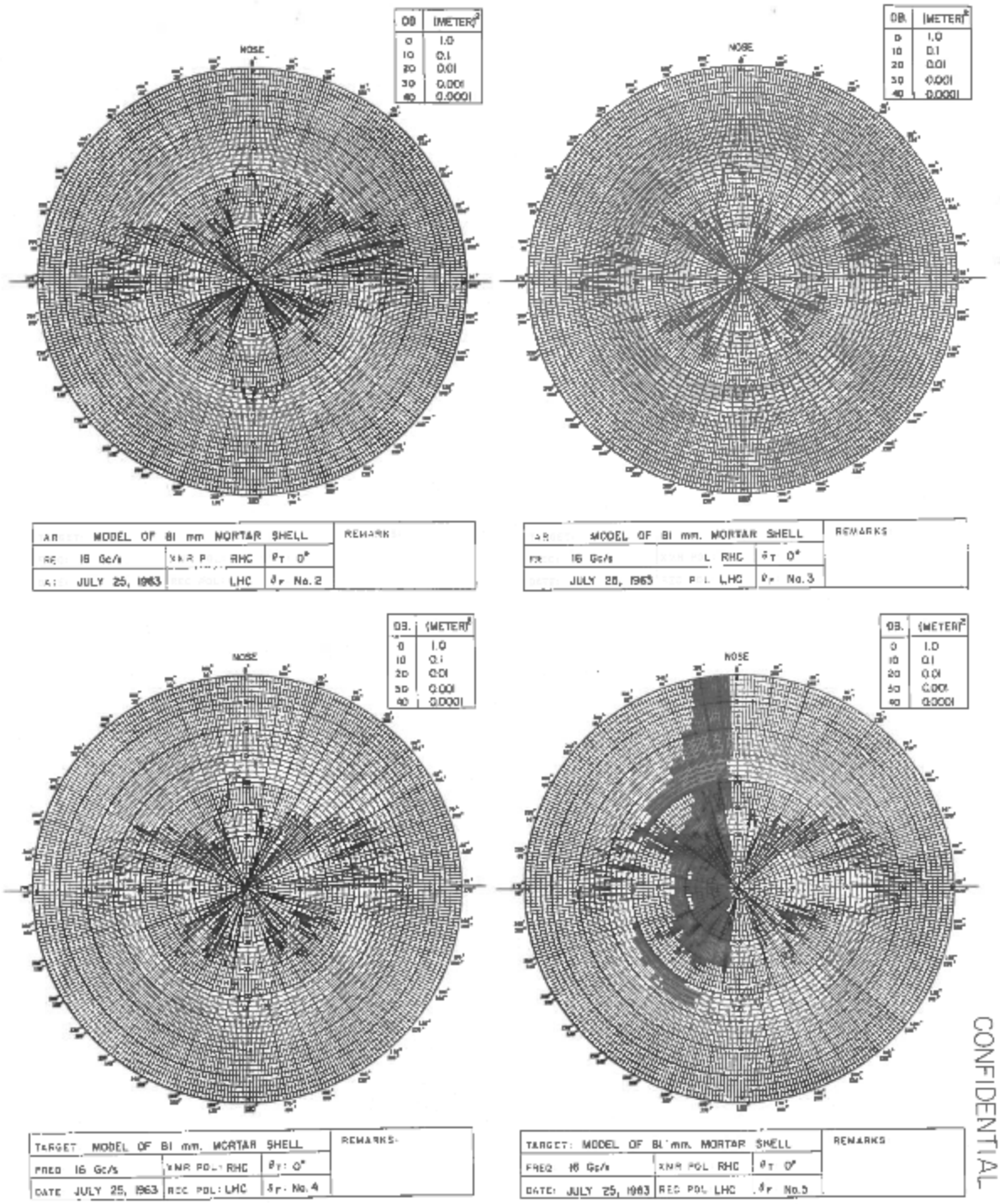

CONFIDENTIAL

Fig. 24 Back-scatter patterns of model of 81-mm mortar shell R-L polarization, 0 db = 1.0 (meter)^2. Fin positions Nos. 2, 3, 4 and 5

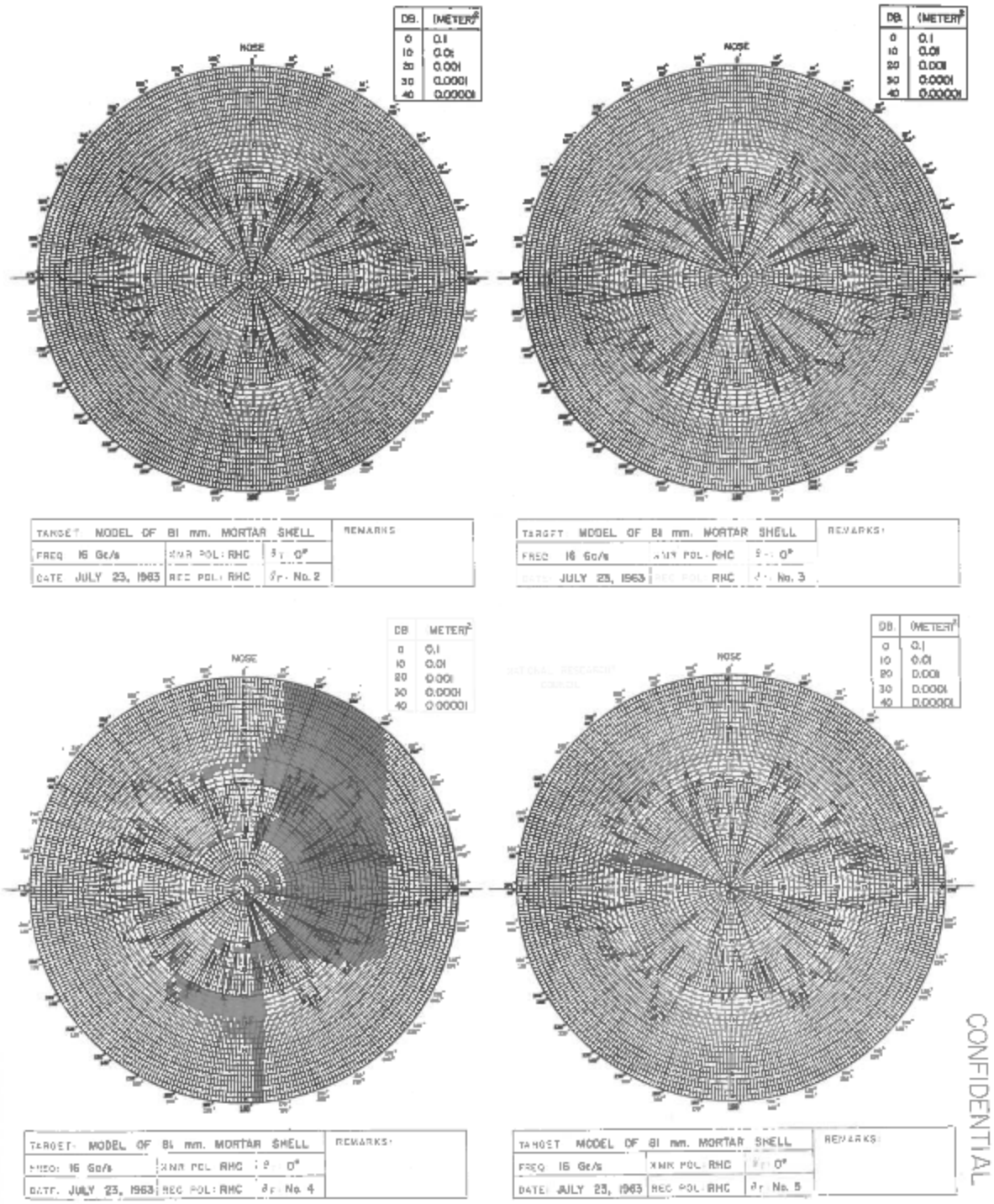

CONFIDENTIAL

Fig. 25 Back-scatter patterns of model of 81-mm mortar shell R-R polarization, 0 db = 0.1 (meter)^2. Fin positions Nos. 2, 3, 4 and 5

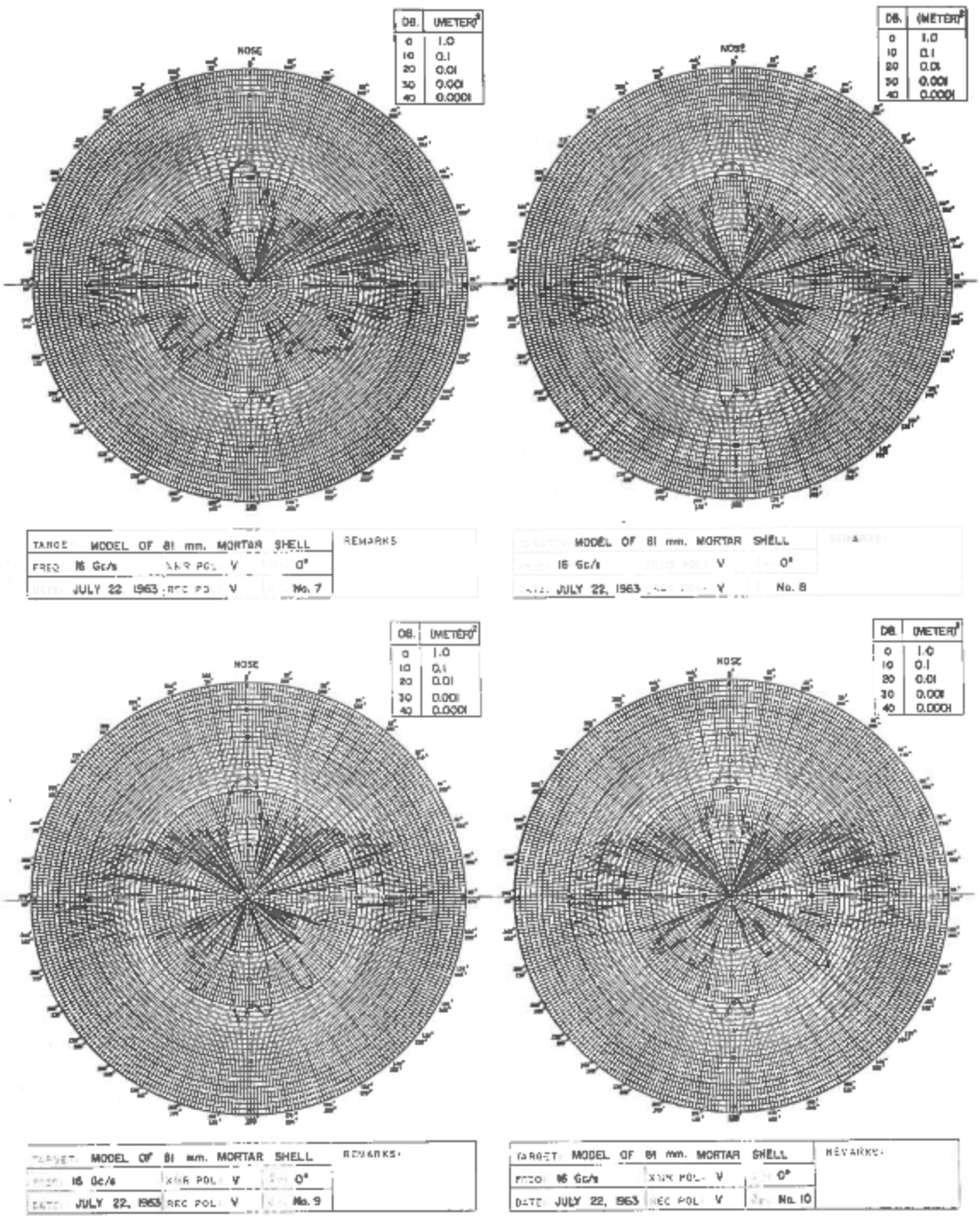

CONFIDENTIAL

Fig. 26 Back-scatter patterns of model of 81-mm mortar shell V-V polarization, 0 db = 1.0 (meter)^2. Fin positions Nos. 7, 8, 9 and 10

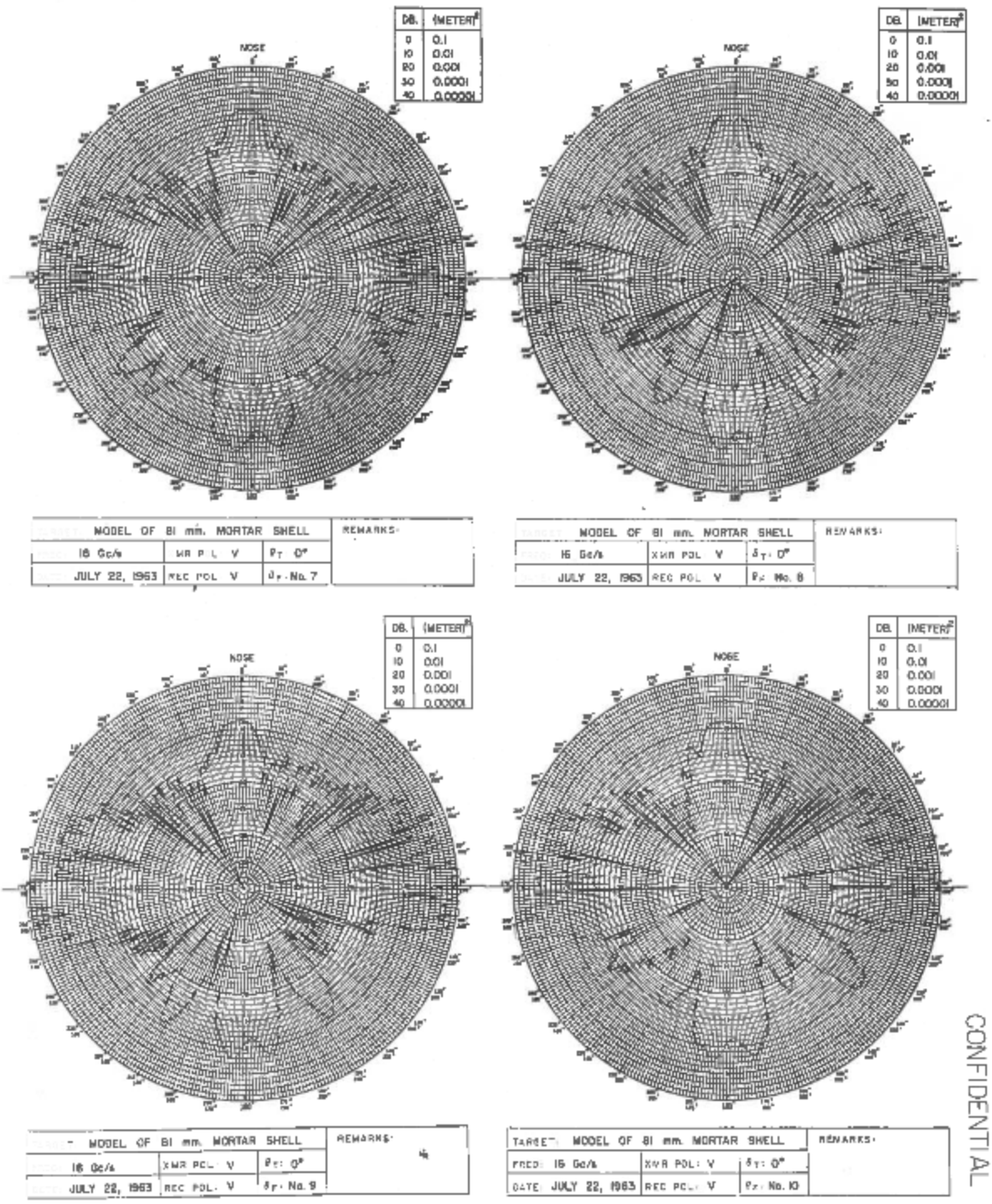

Fig. 27 Back-scatter patterns of model of 81-mm mortar shell V-V polarization, 0 db = 0.1 (meter)^2. Fin positions Nos. 7, 8, 9 and 10

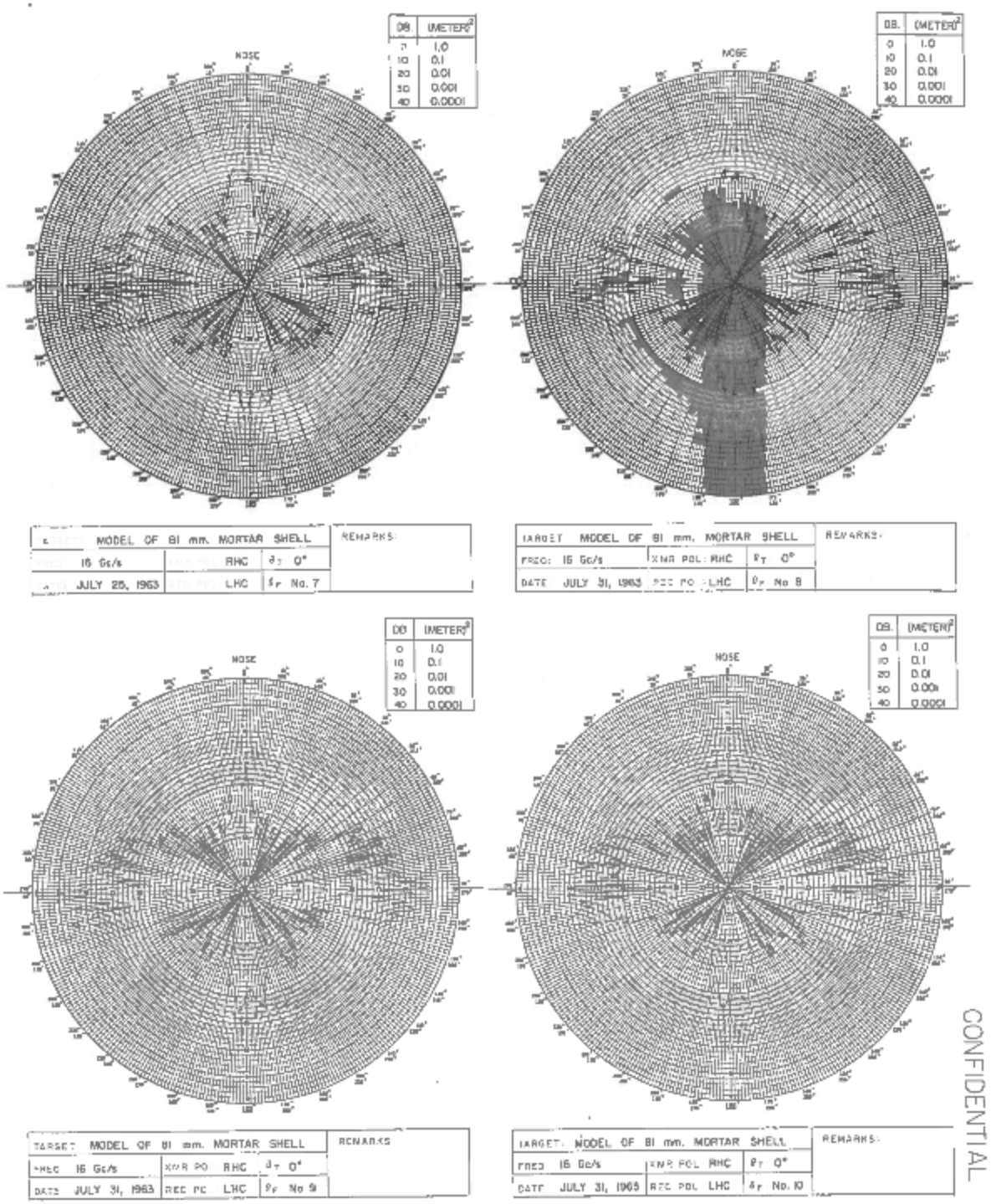

CONFIDENTIAL

Fig. 28 Back-scatter patterns of model of 81-mm mortar shell R-L polarization, 0 db = 1.0 (meter)^2. Fin positions Nos. 7, 8, 9 and 10

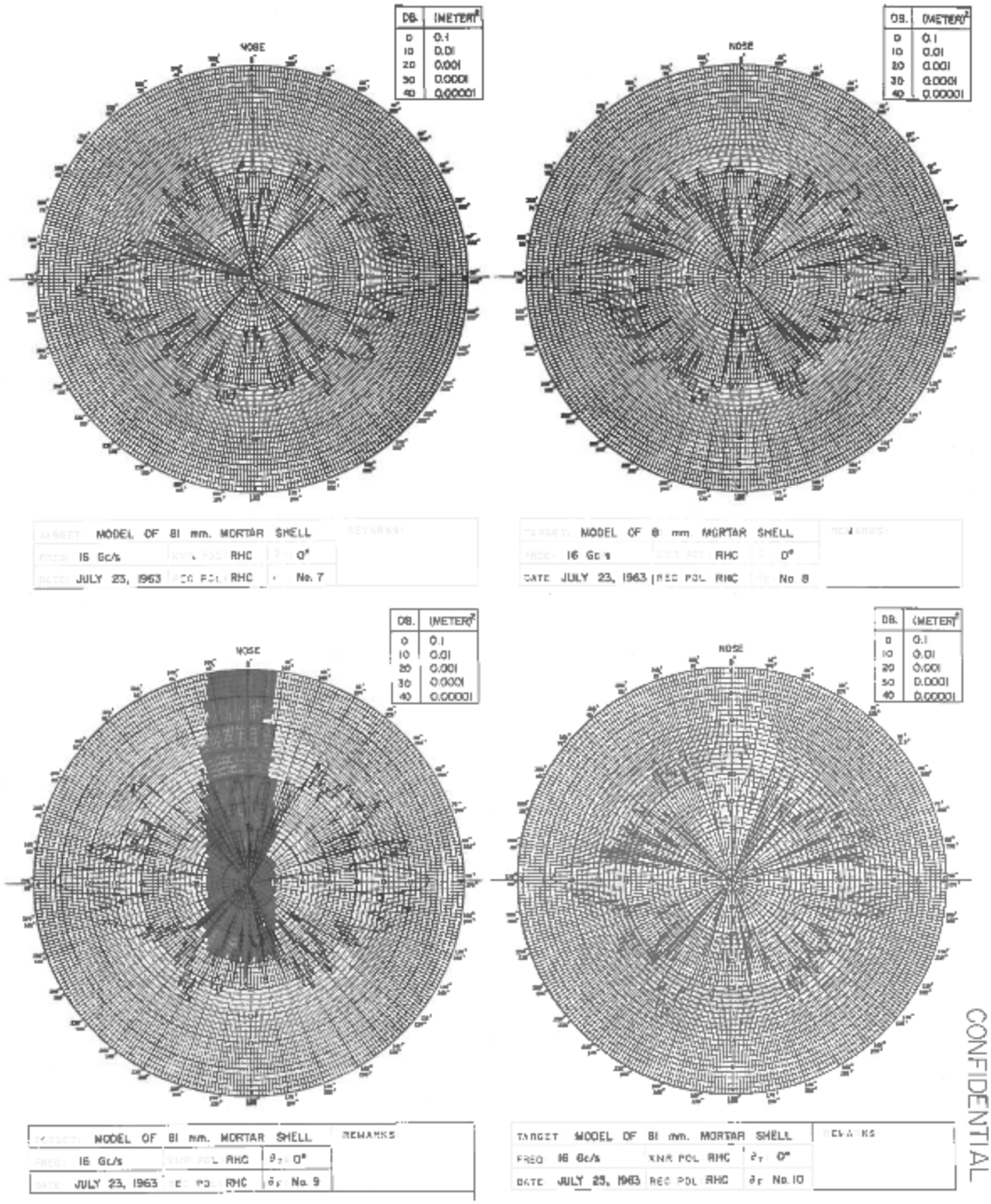

Fig. 29 Back-scatter patterns of model of 81-mm mortar shell R-R polarization, 0 db = 0.1 (meter)². Fin positions Nos. 7, 8, 9 and 10

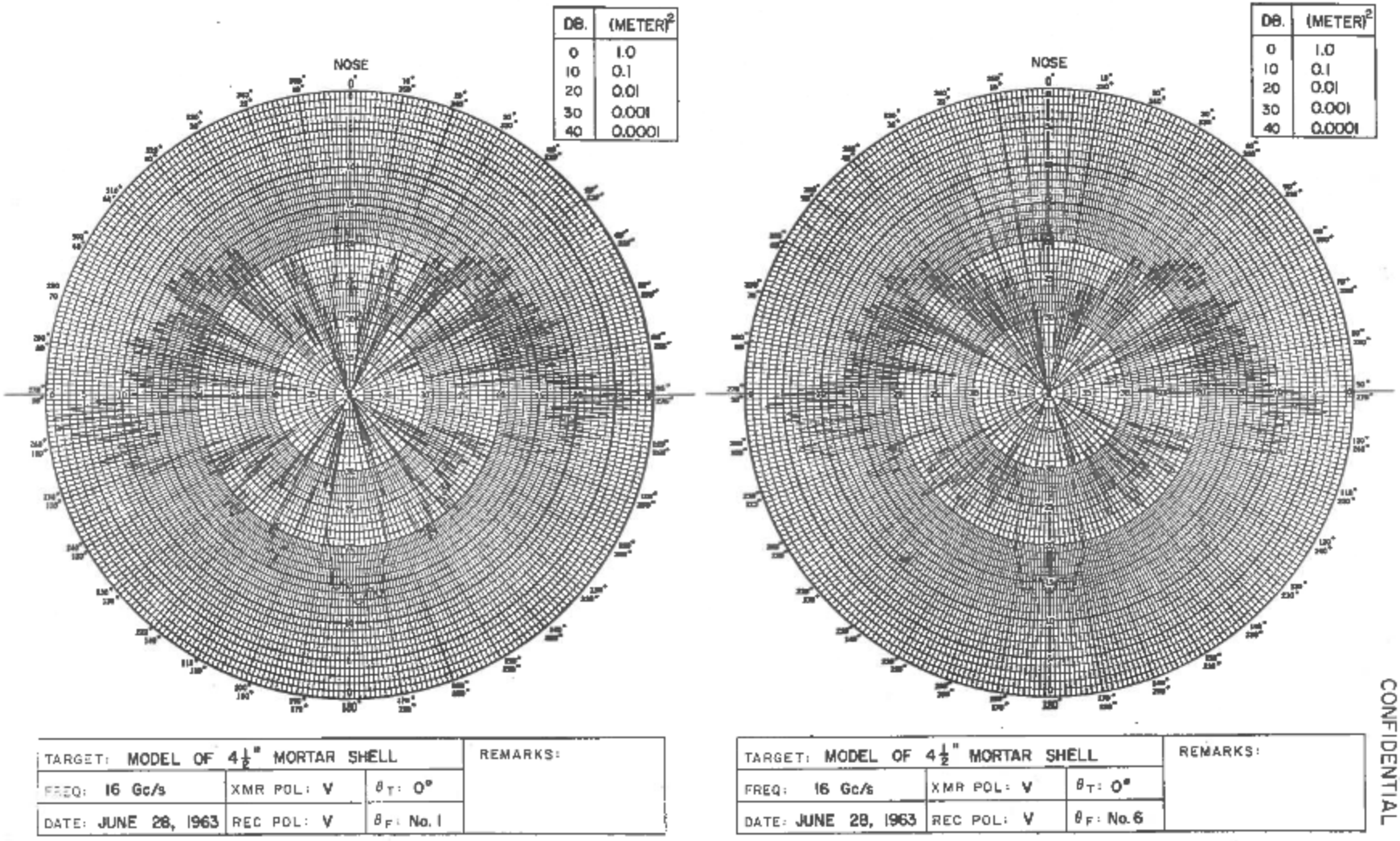

CONFIDENTIAL

Fig. 30 Back-scatter patterns of model of $4\frac{1}{2}$" mortar shell, V-V polarization, 0 db = 1.0 (meter)^2 Fin position vertical (No. 1 and No. 6)

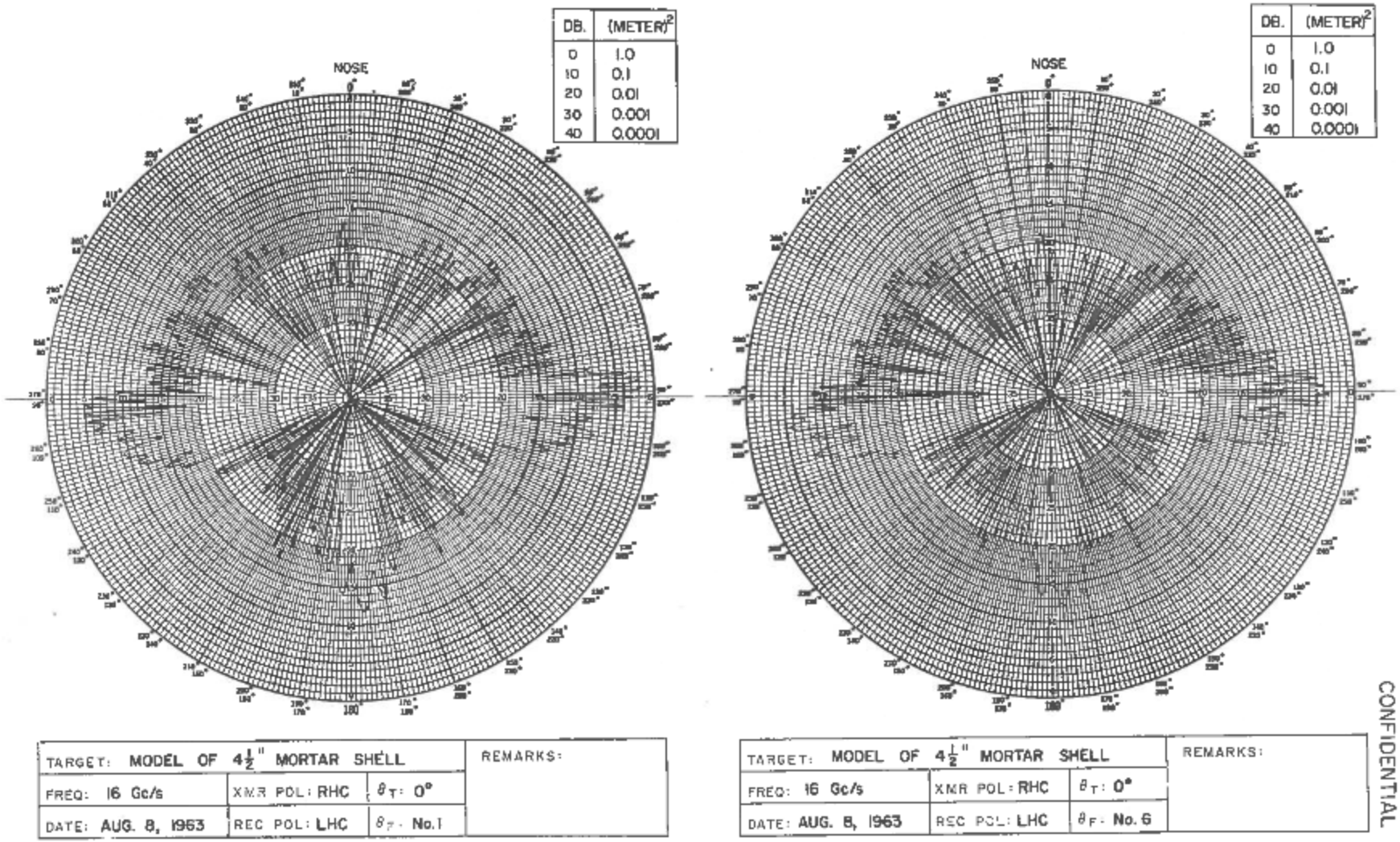

CONFIDENTIAL

Fig. 31 Back-scatter patterns of model of $4\frac{1}{2}$" mortar shell, R-L polarization, 0 db = 1.0 (meter)^2
Fin position vertical (No. 1 and No. 6)

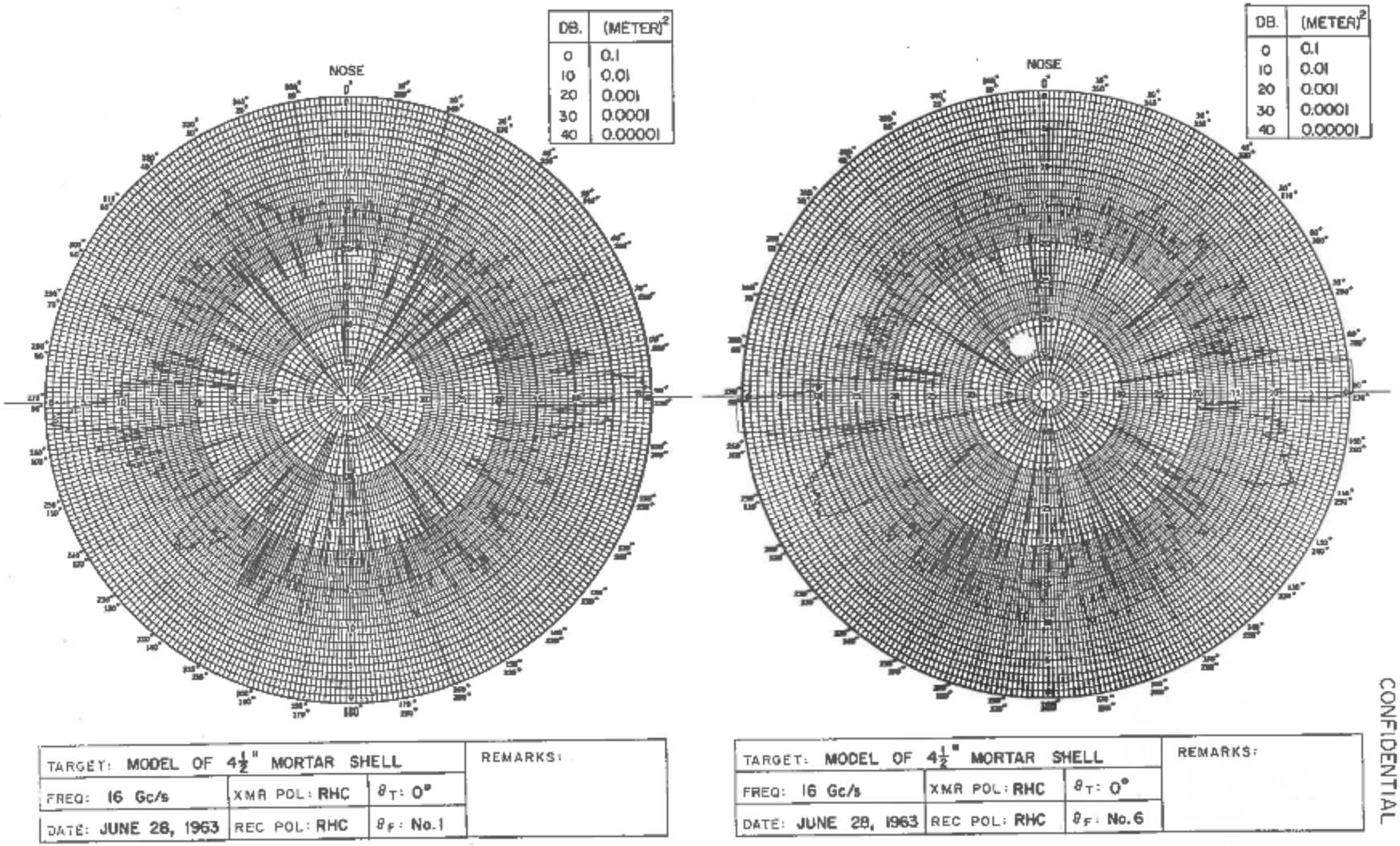

CONFIDENTIAL

Fig. 32 Back-scatter patterns of model of $4\frac{1}{2}$" mortar shell, R-R polarization, 0 db = 0.1 (meter)^2 Fin position vertical (No. 1 and No. 6)

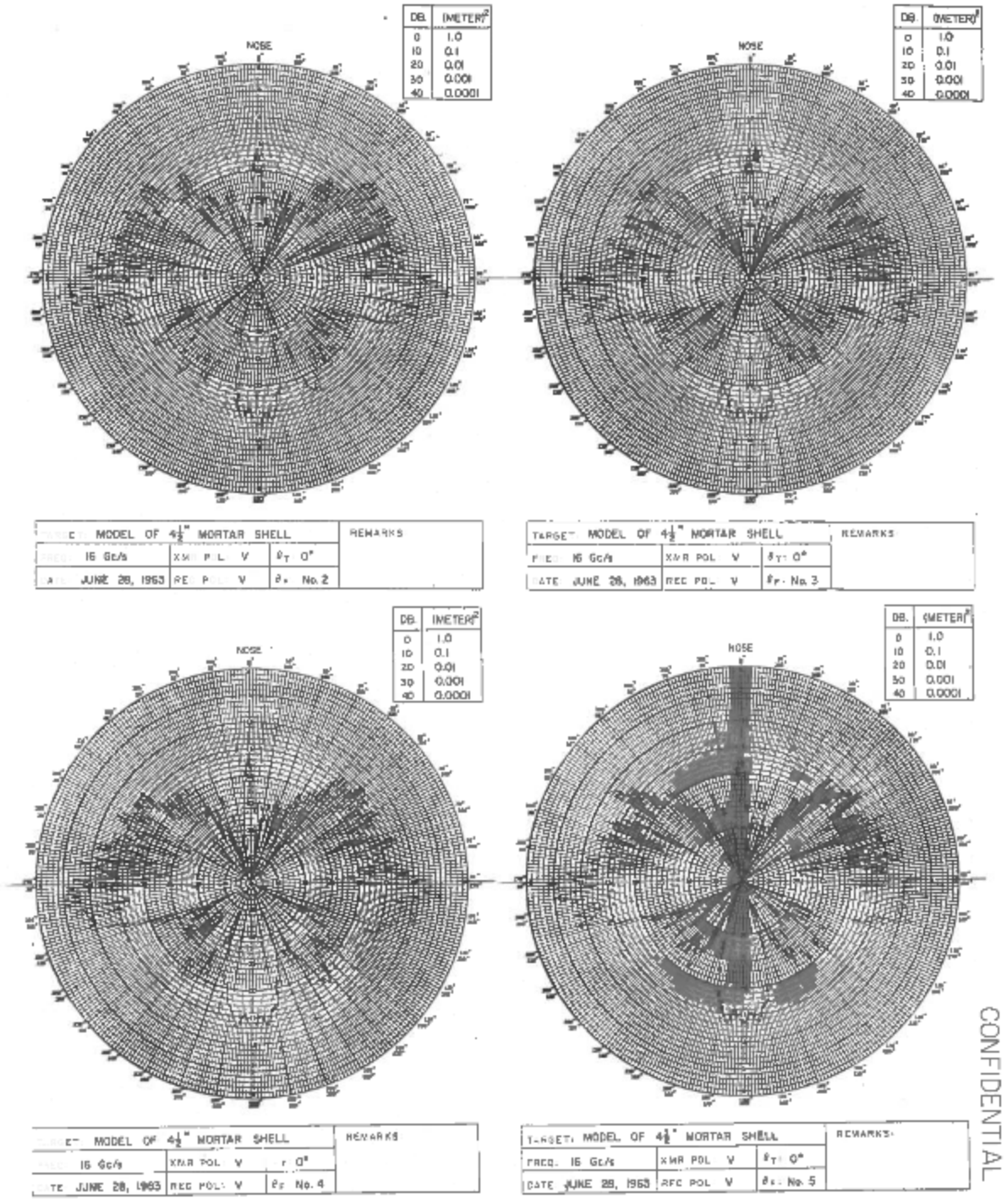

CONFIDENTIAL

Fig. 33 Back-scatter patterns of model of $4\frac{1}{2}$" mortar shell V-V polarization, 0 db = 1.0 (meter)². Fin positions Nos. 2, 3, 4 and 5

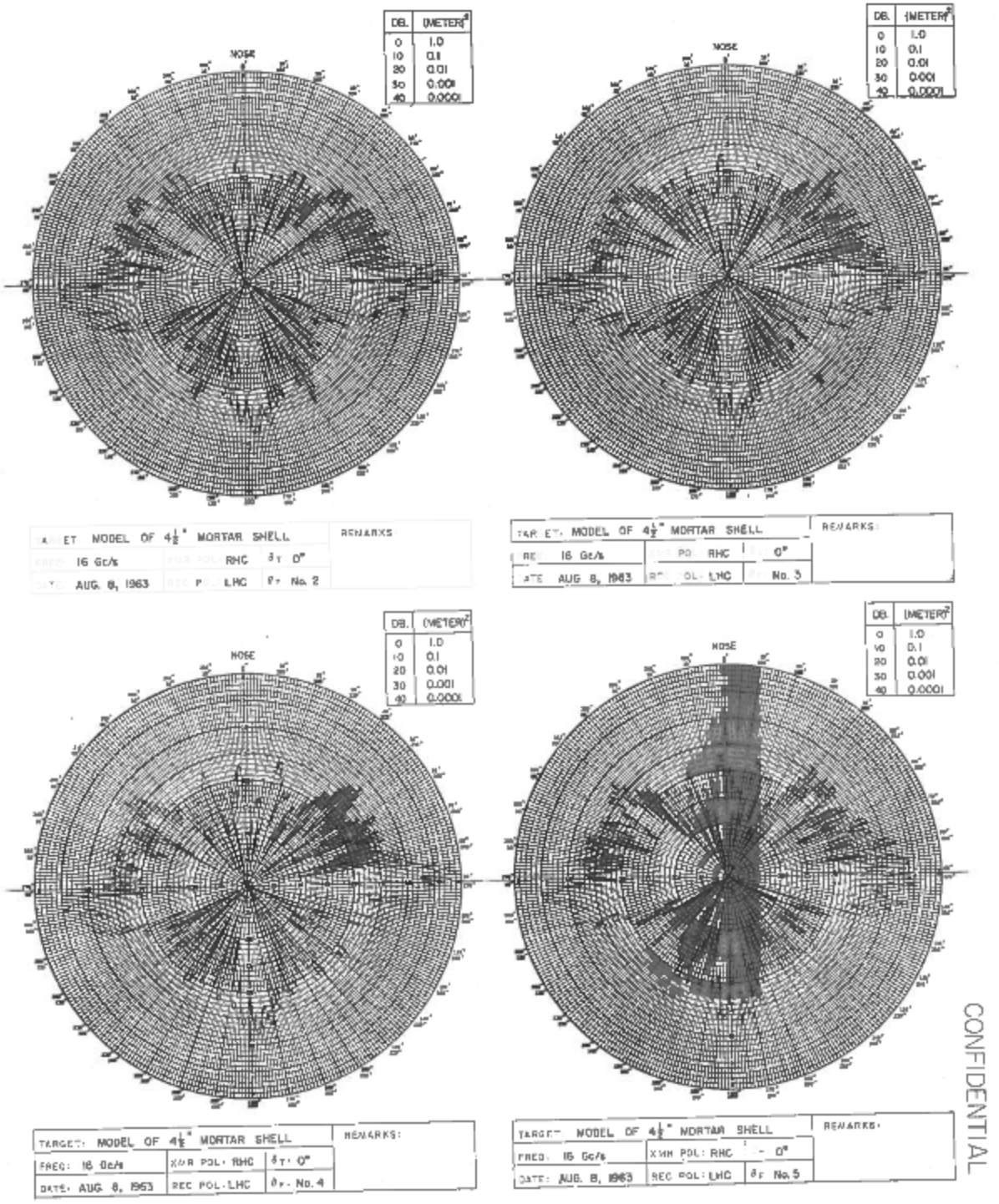

CONFIDENTIAL

Fig. 34 Back-scatter patterns of model of $4\frac{1}{2}$" mortar shell R-L polarization, 0 db = 1.0 (meter)^2. Fin positions Nos. 2, 3, 4 and 5

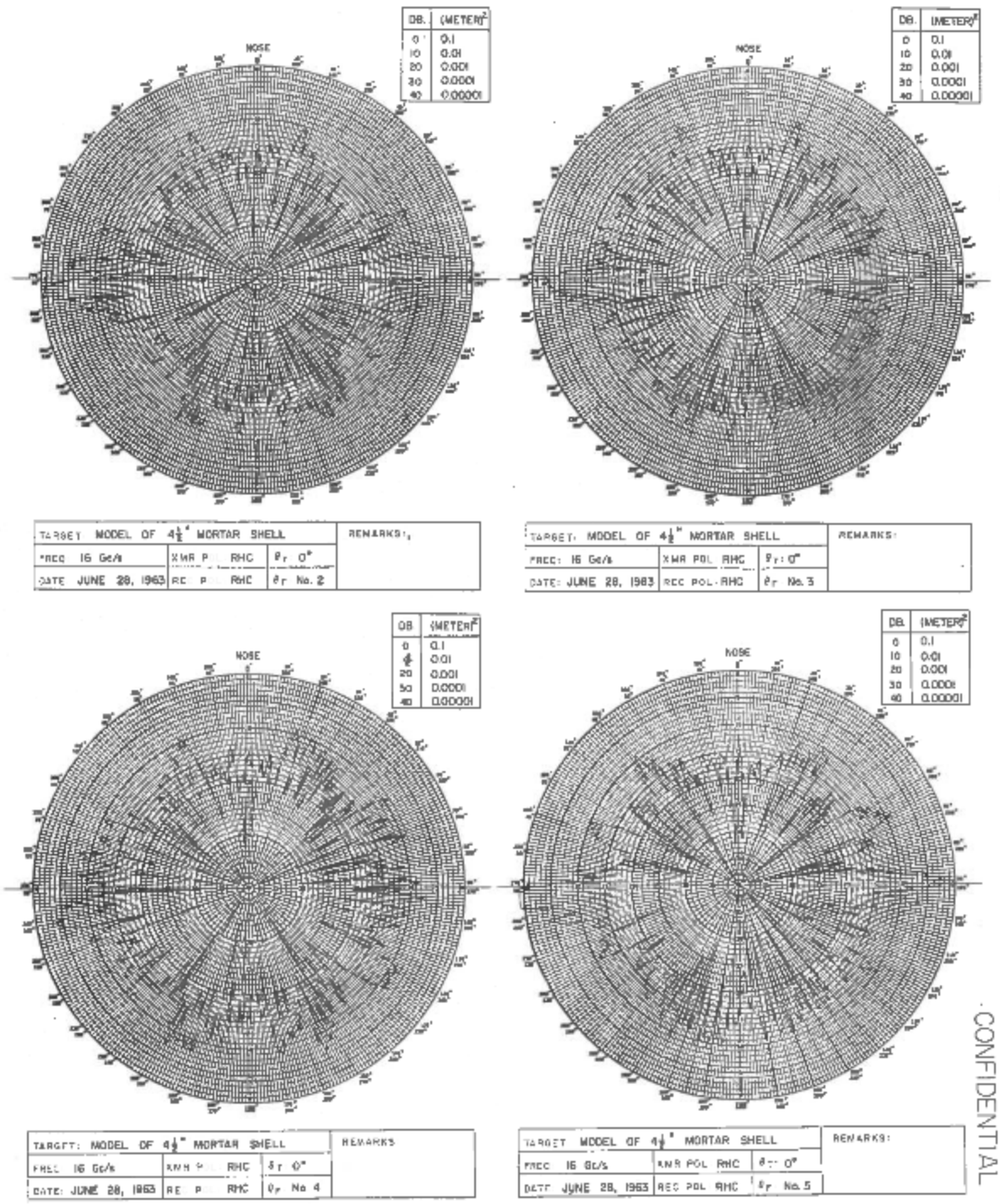

Fig. 35 Back-scatter patterns of model of $4\frac{1}{2}$" mortar shell R-R polarization, 0 db = 0.1 (meter)^2. Fin positions Nos. 2, 3, 4 and 5

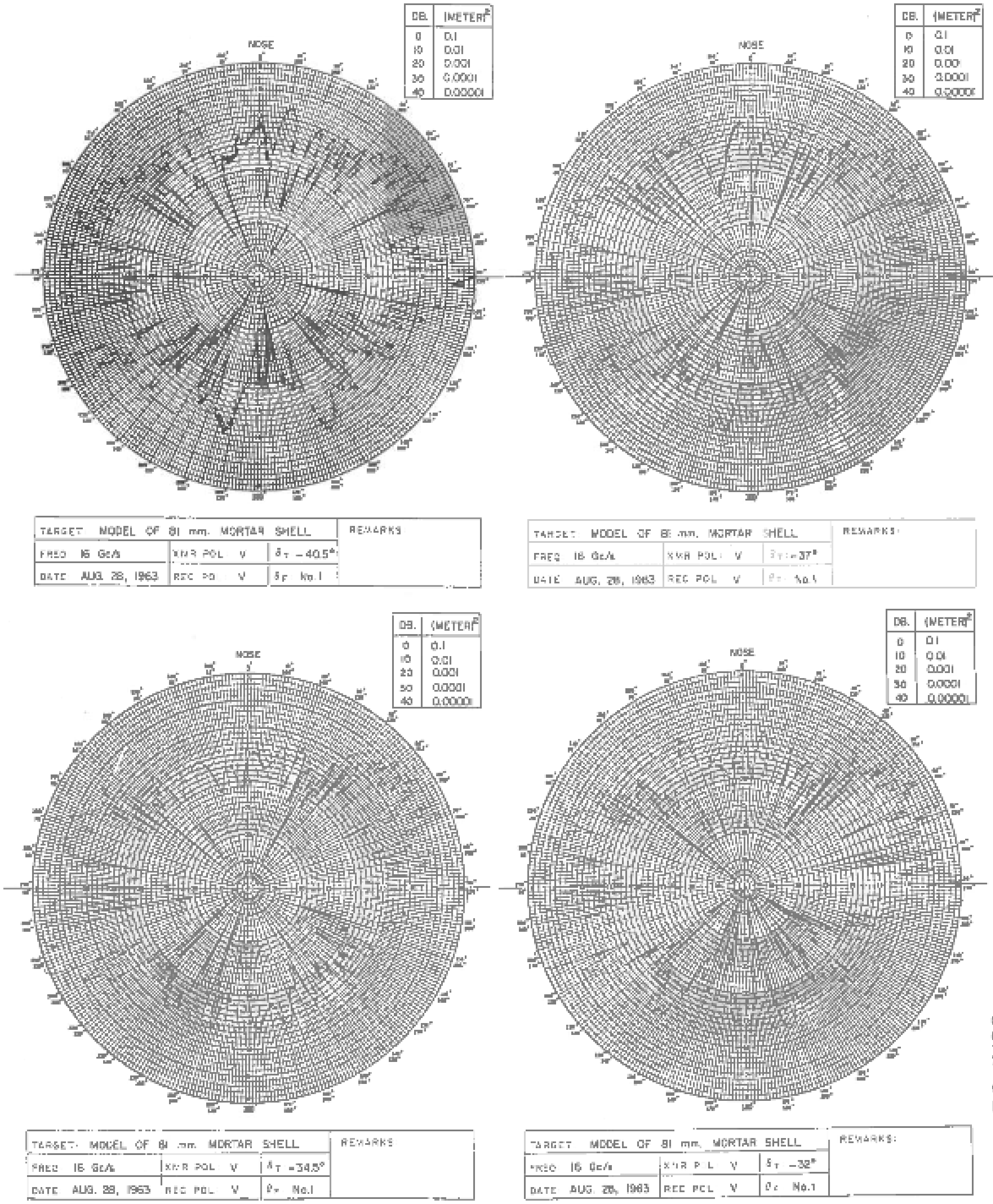

CONFIDENTIAL

Fig. 36 Back-scatter patterns of model of 81-mm mortar shell
Tilt angles, -40.5°, -37°, -34.5° and -32°

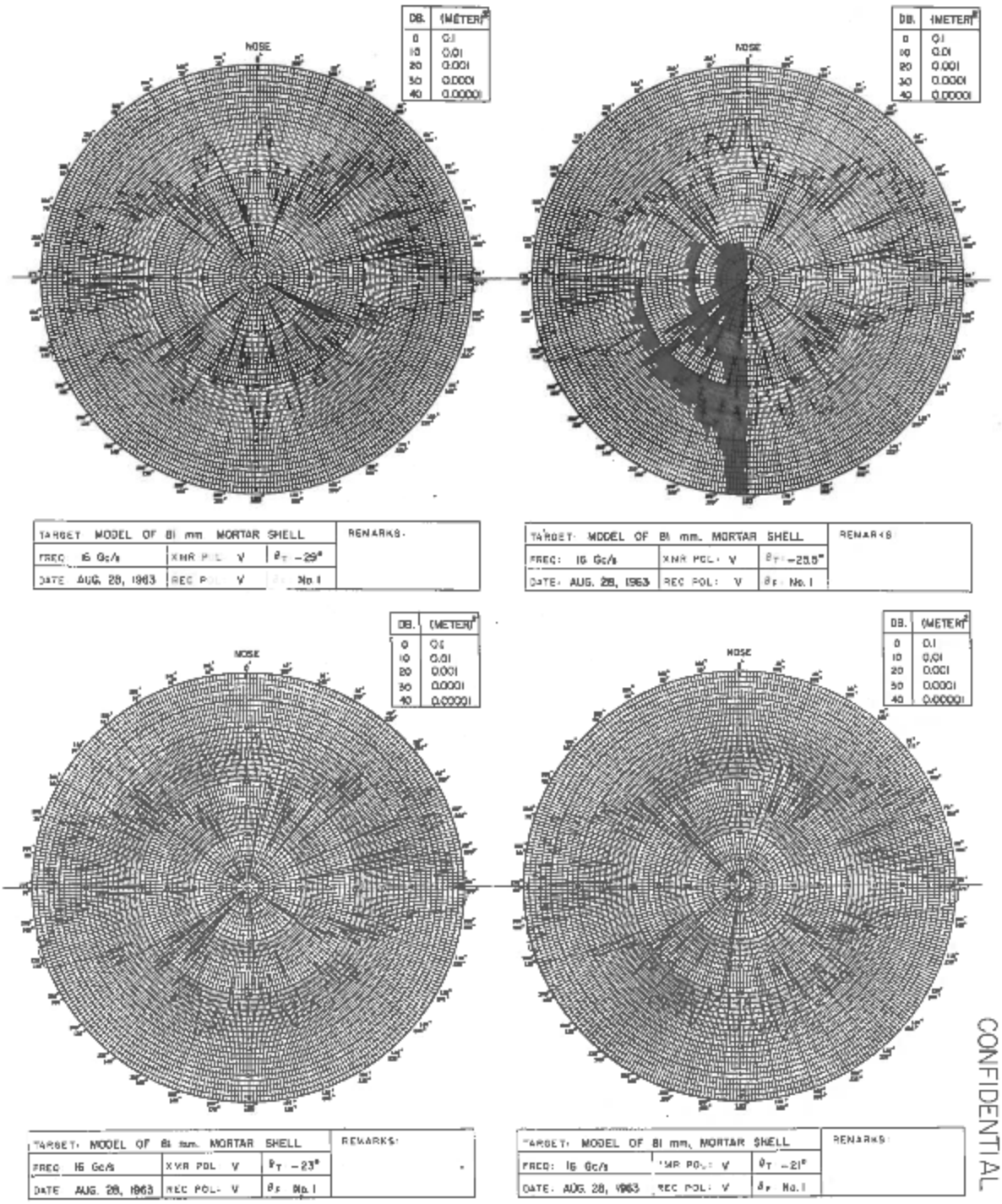

CONFIDENTIAL

Fig. 37 Back-scatter patterns of model of 81-mm mortar shell
Tilt angles, -29°, -25.5°, -23° and -21°

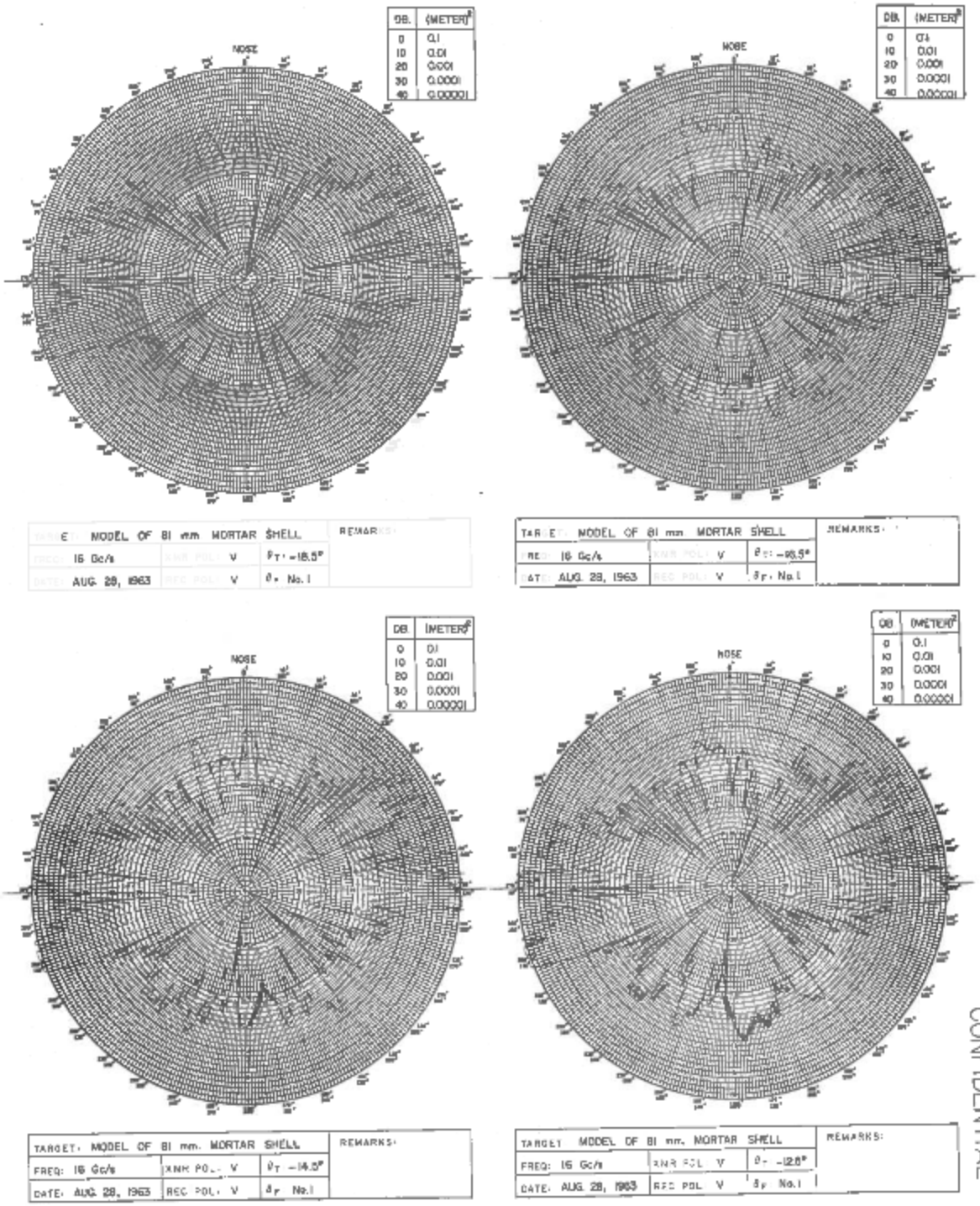

Fig. 38 Back-scatter patterns of model of 81-mm mortar shell
Tilt angles, -18.5°, -16.5°, -14.5°, and -12.5°

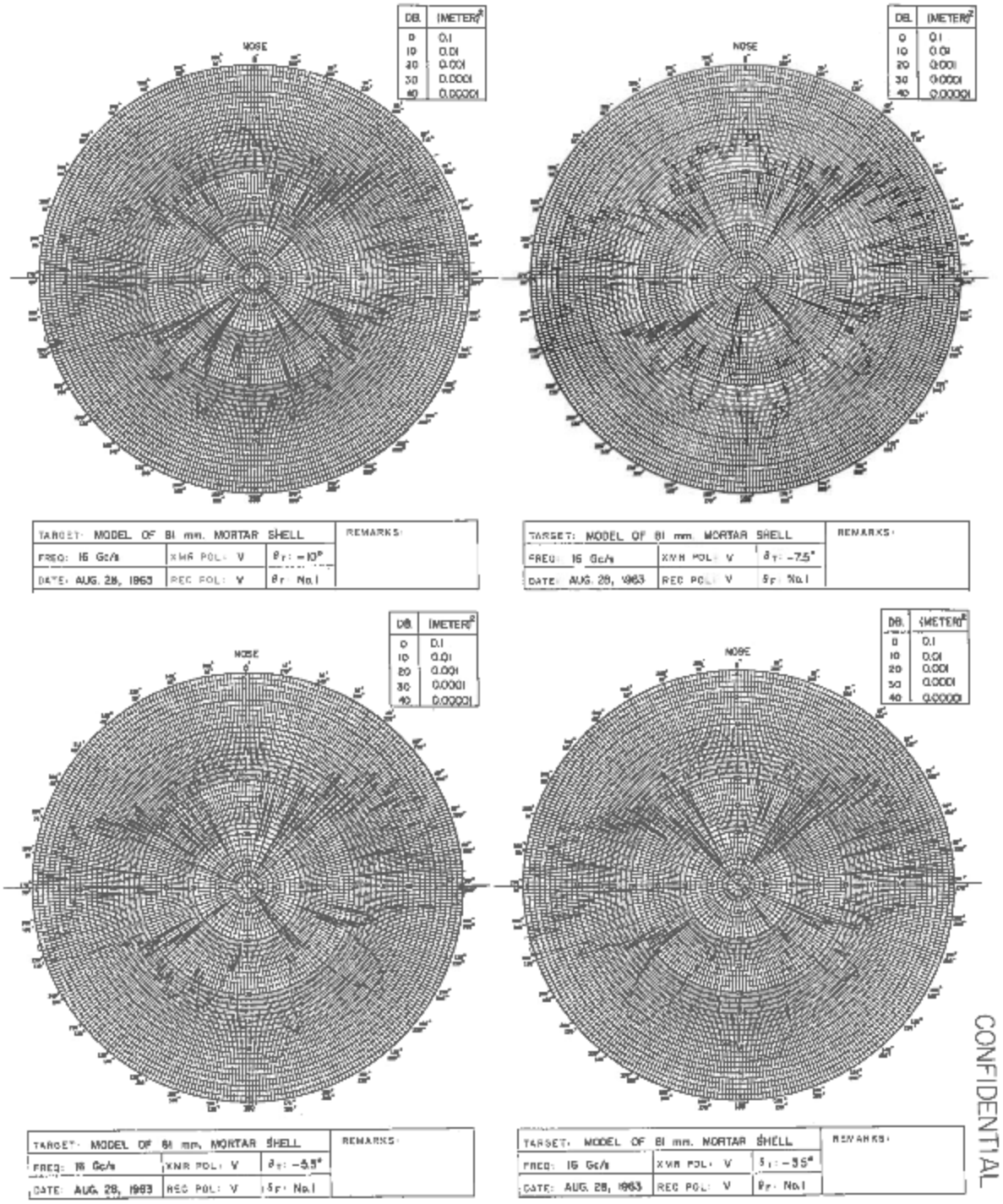

Fig. 39 Back-scatter patterns of model of 81-mm mortar shell
Tilt angles, -10°, -7.5°, -5.3°, and -3.5°

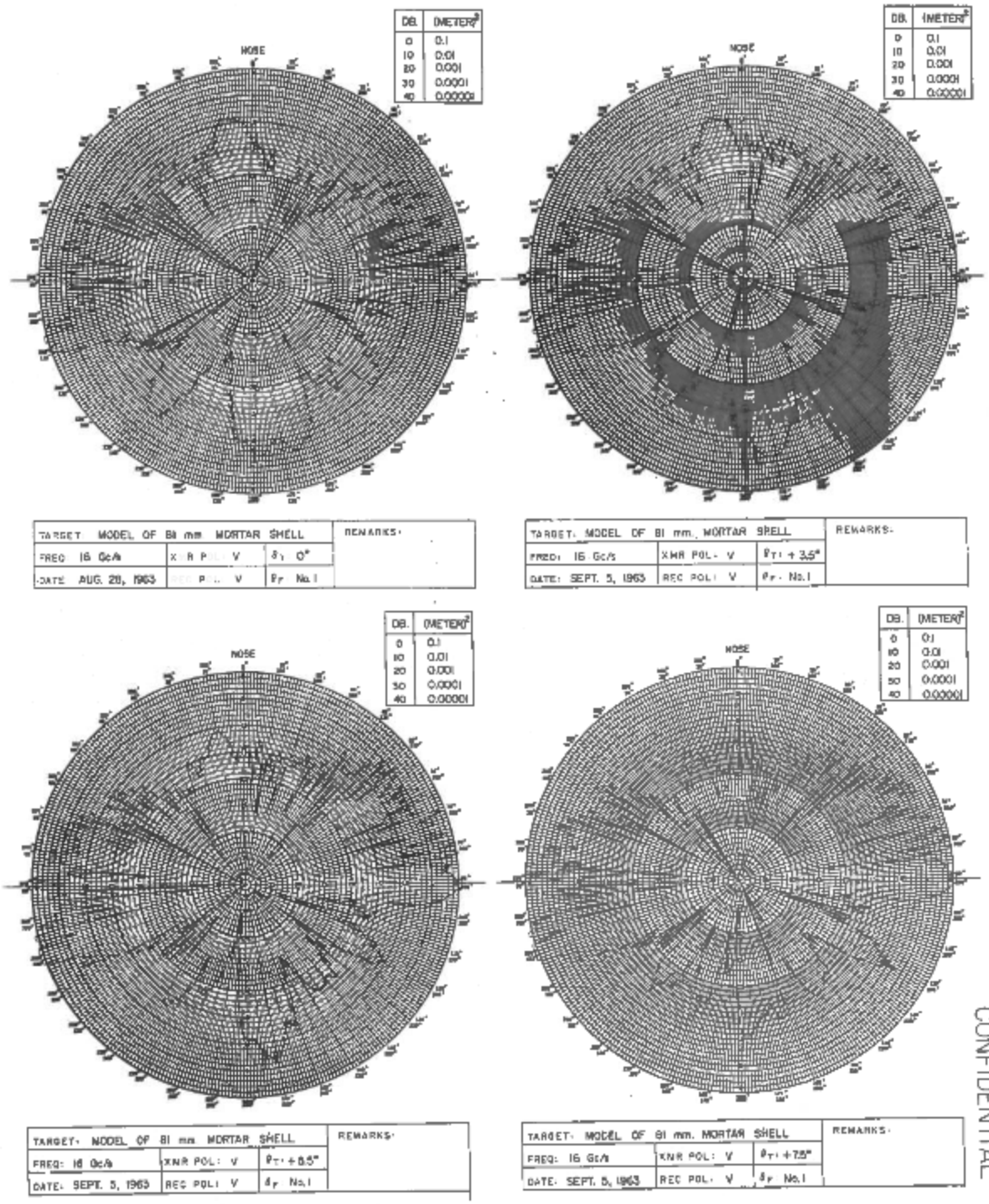

CONFIDENTIAL

Fig. 40 Back-scatter patterns of model of 81-mm mortar shell
Tilt angles, 0°, 3.5°, 5.5°, and 7.5°

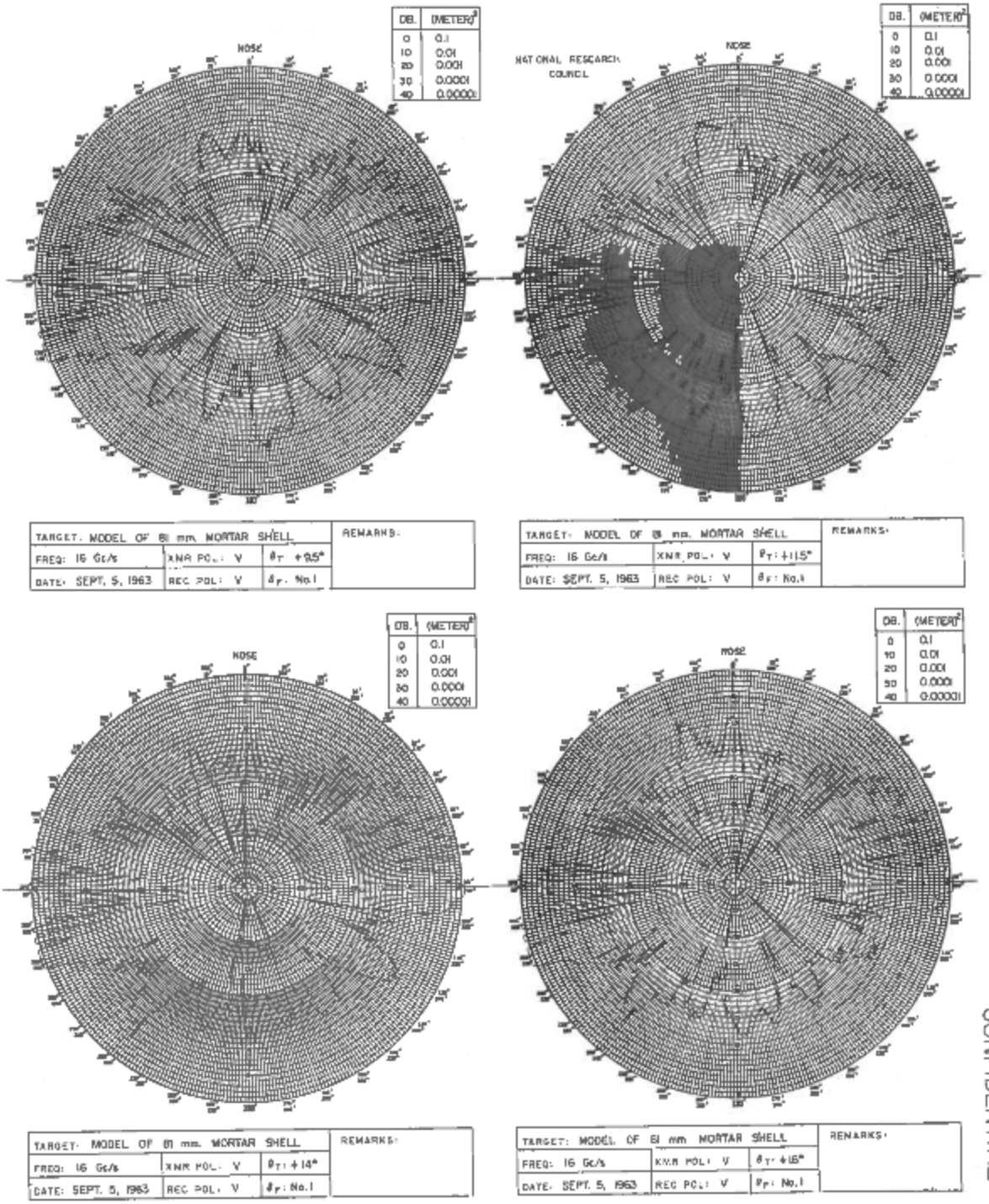

CONFIDENTIAL

Fig. 41 Back-scatter patterns of model of 81-mm mortar shell
Tilt angles, 9.5°, 11.5°, 14°, and 16°

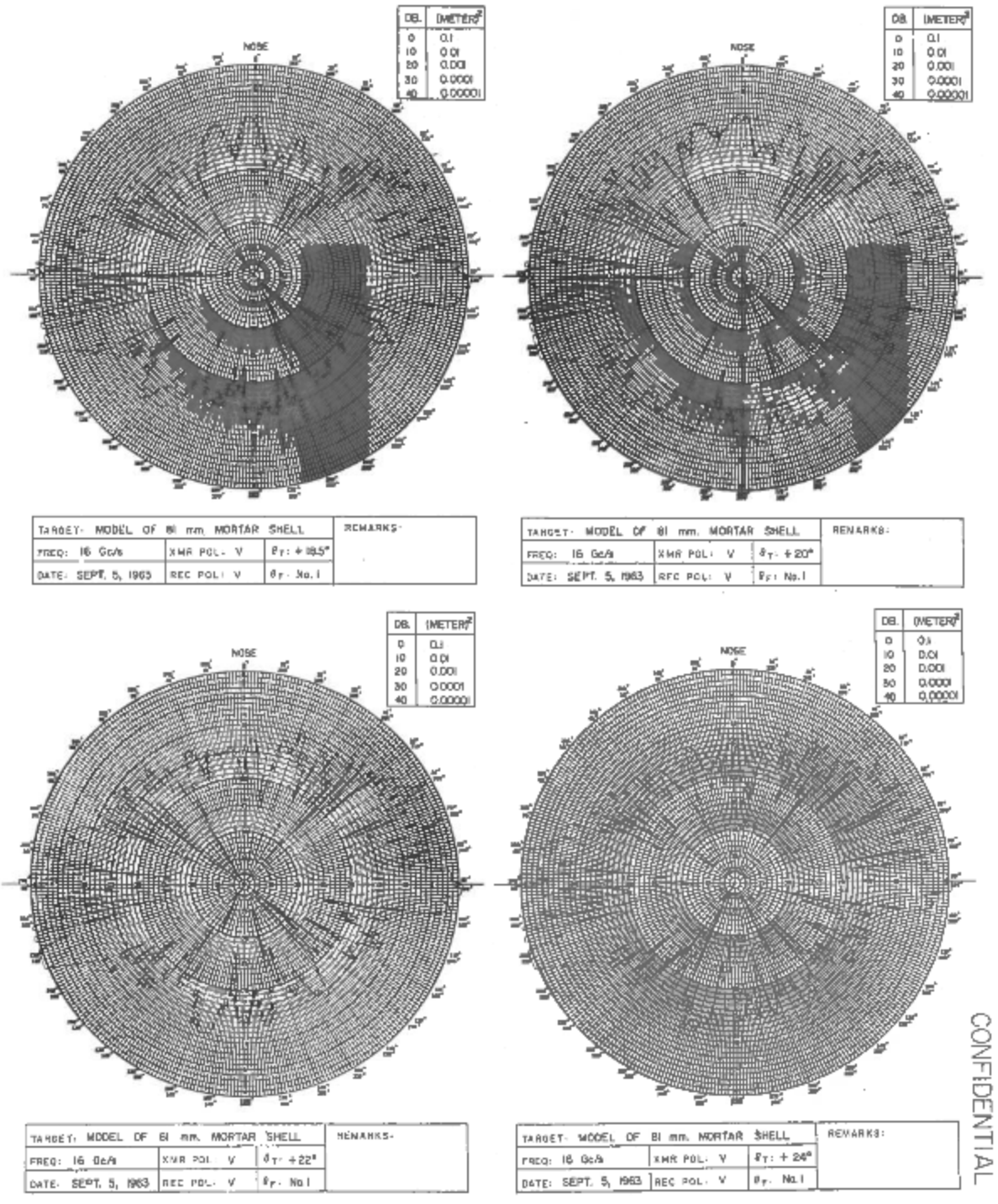

CONFIDENTIAL

Fig. 42 Back-scatter patterns of model of 81-mm mortar shell
Tilt angles, 18.5°, 20°, 22°, and 24°

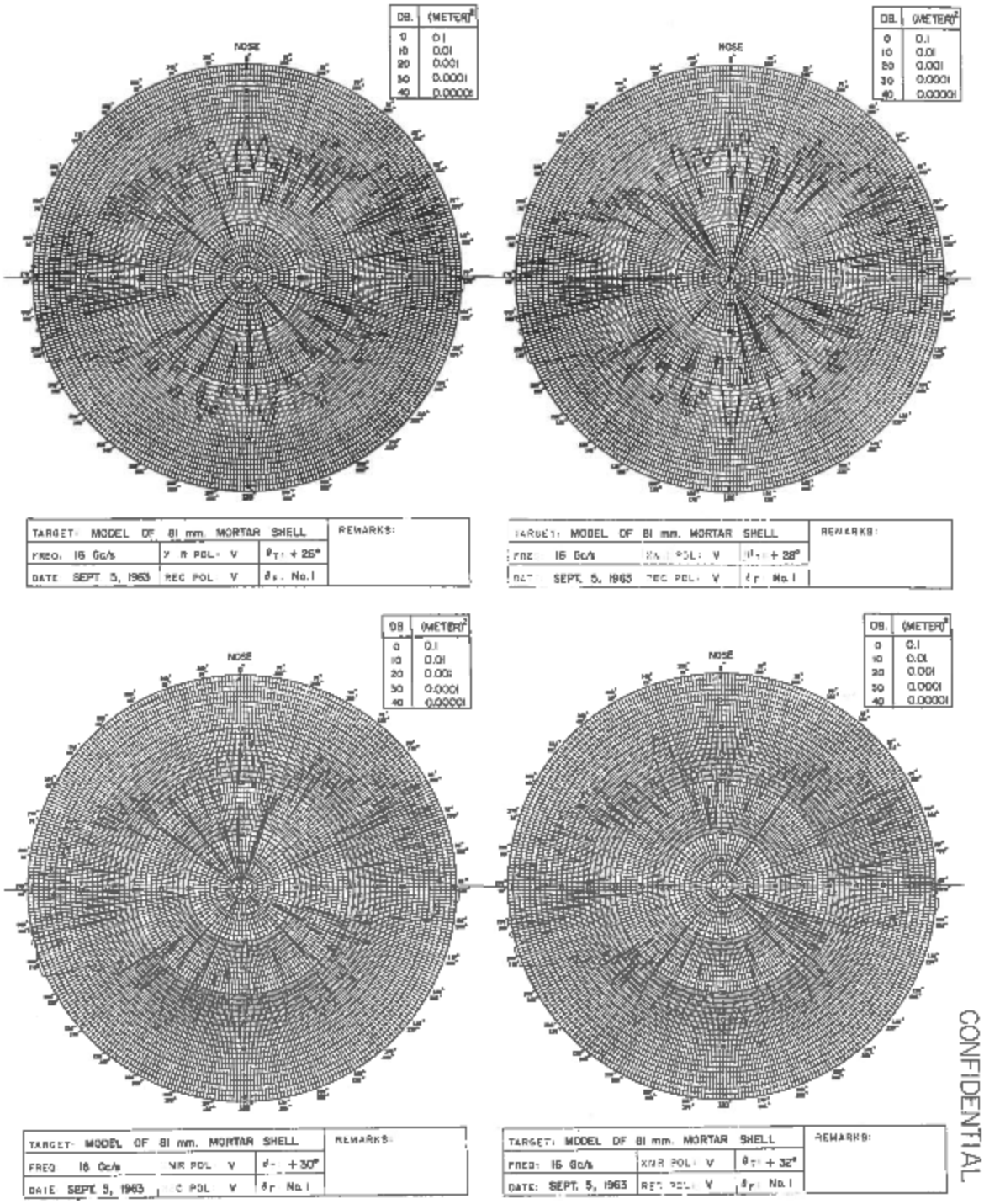

Fig. 43 Back-scatter patterns of model of 81-mm mortar shell
Tilt angles, 26°, 28°, 30°, and 32°

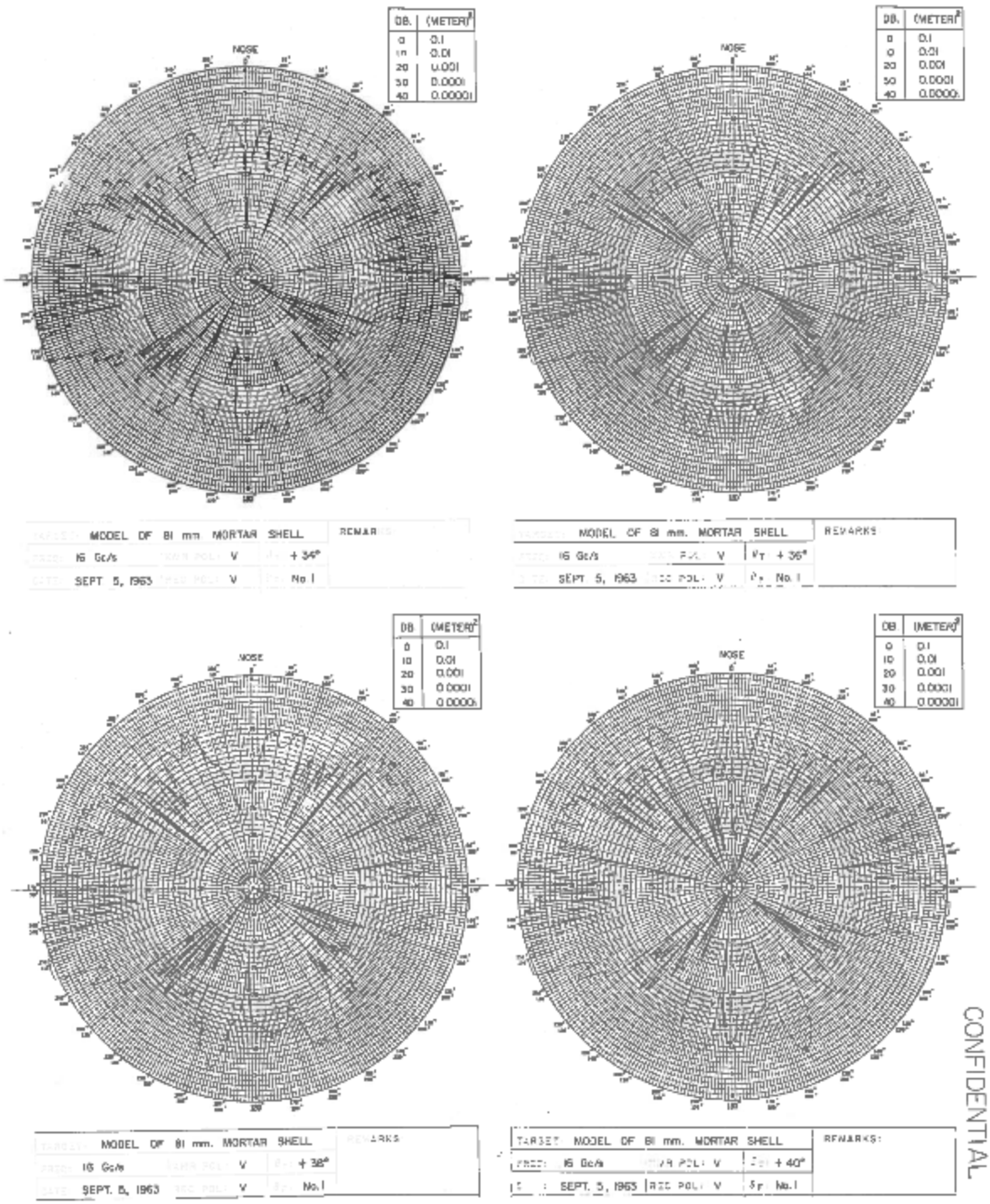

CONFIDENTIAL

Fig. 44 Back-scatter patterns of model of 81-mm mortar shell
Tilt angles, 34°, 36°, 38°, and 40°

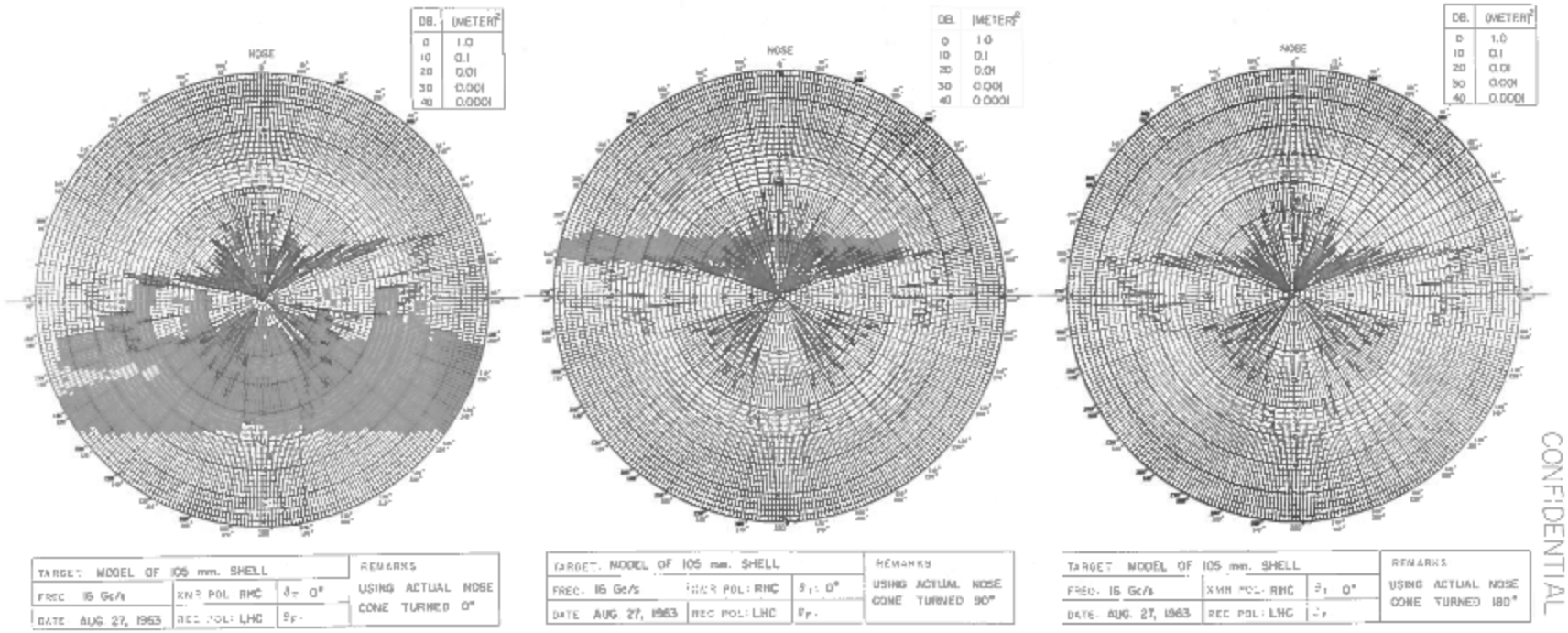

CONFIDENTIAL

Fig. 45 Back-scatter patterns of model of 105-mm artillery shell with model nose cone removed and replaced by actual nose cone. R-L polarization

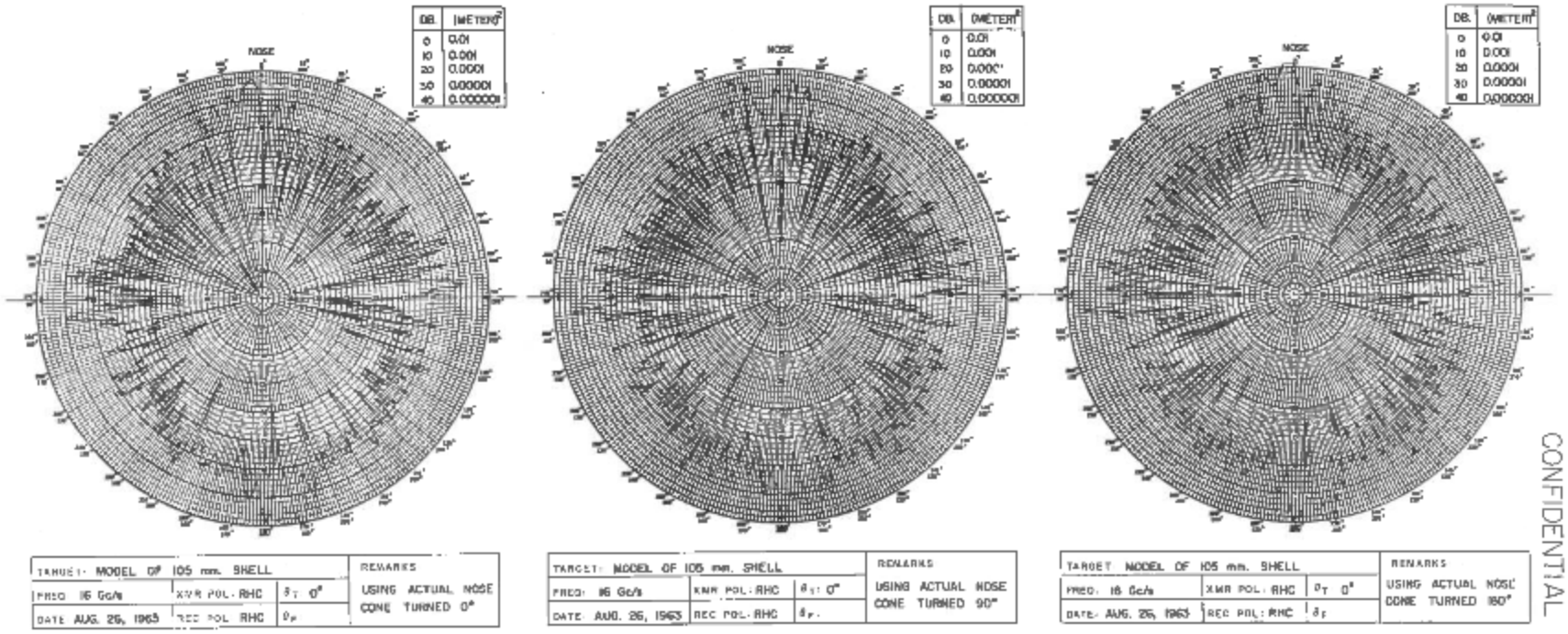

Fig. 46 Back-scatter patterns of model of 105-mm artillery shell with model nose cone removed and replaced by actual nose cone. R-R polarization

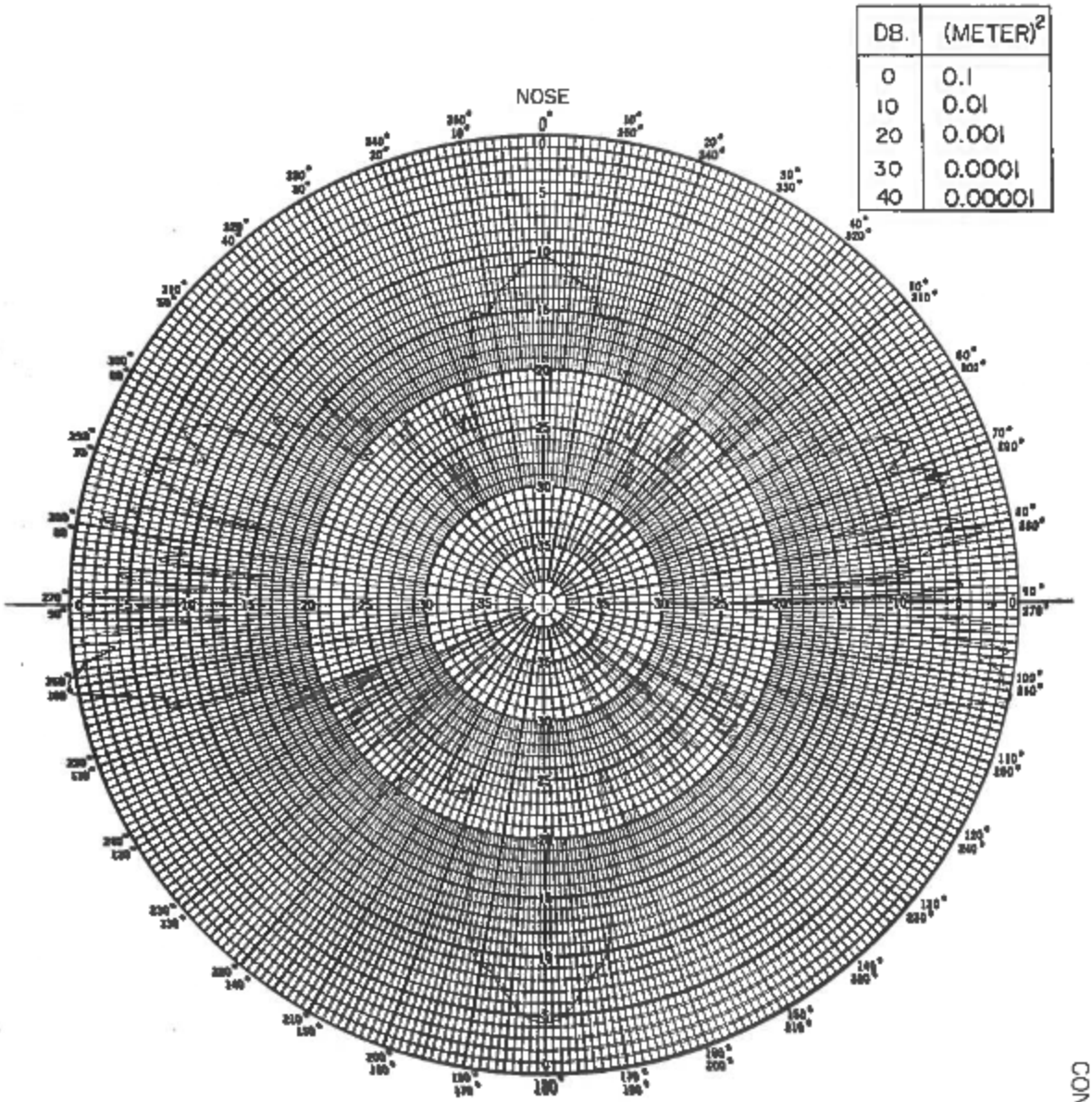

TARGET: TEST MODEL			REMARKS:
FREQ: 15.92 Gc/s	XMR POL: V	θ_T: 0°	
DATE: NOV. 13, 1963	REC POL: V	θ_F:	

CONFIDENTIAL

Fig. 47 Back-scatter pattern of model of 81-mm mortar shell with fins removed. f = 15.92 Gc/s

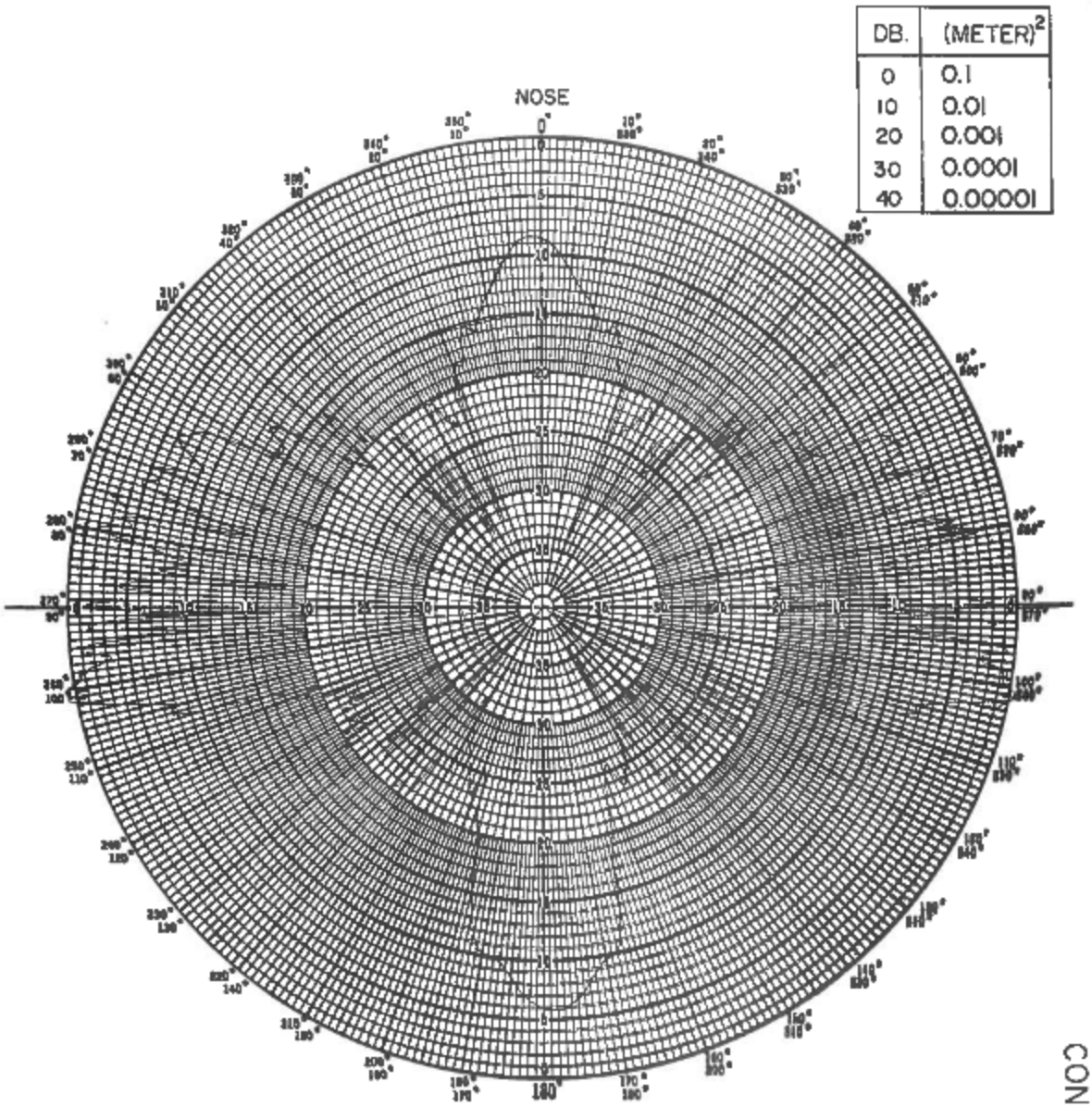

TARGET: TEST MODEL			REMARKS:
FREQ: 16 Gc/s	XMR POL: V	θ_T: 0°	
DATE: NOV. 13, 1963	REC POL: V	θ_F:	

CONFIDENTIAL

Fig. 48 Back-scatter pattern of model of 81-mm mortar shell with fins removed. f = 16.00 Gc/s

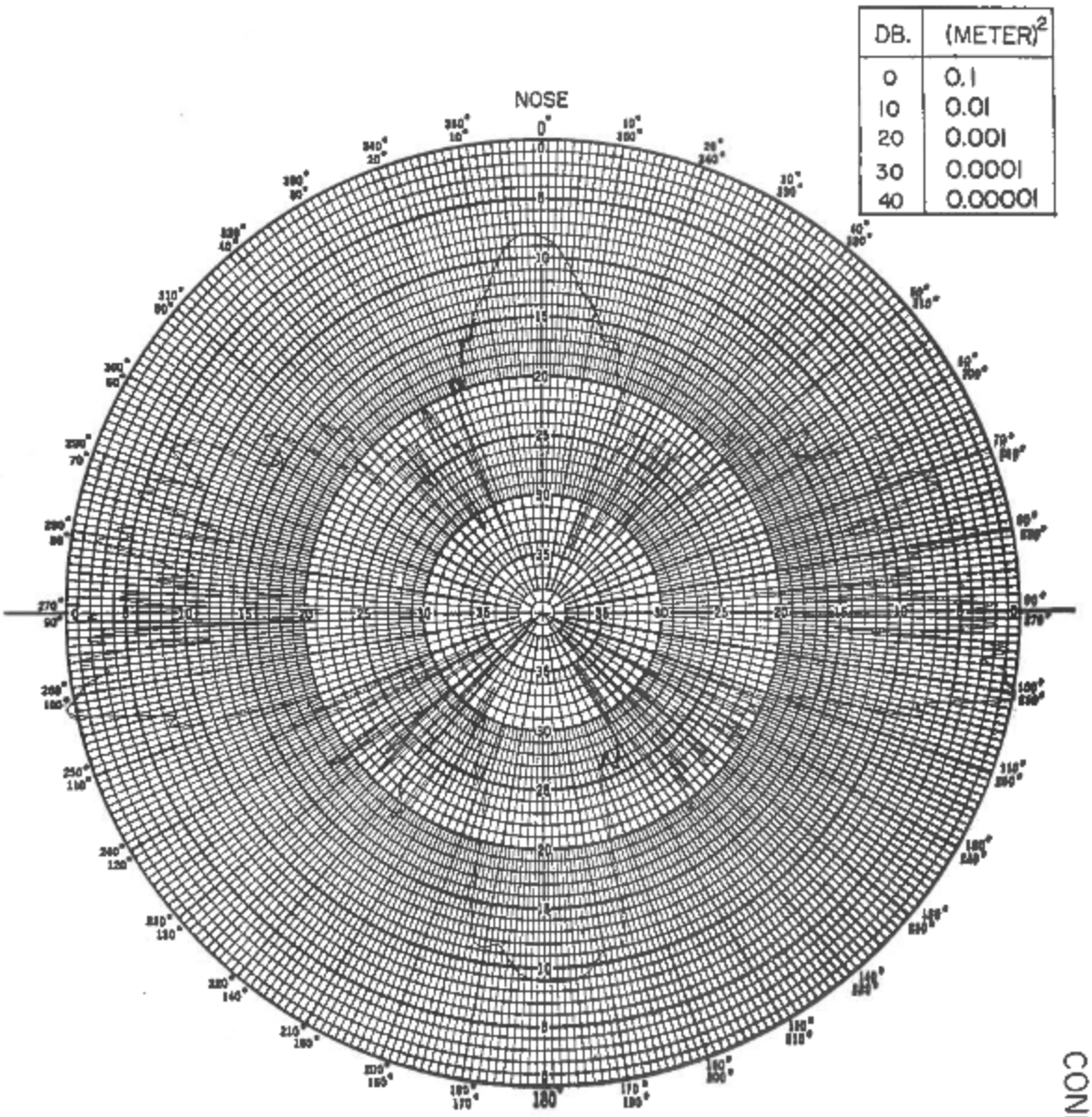

TARGET: TEST MODEL			REMARKS:
FREQ: 16.08 Gc/s	XMR POL: V	θ_T:	
DATE: NOV. 13, 1963	REC POL: V	θ_F:	

CONFIDENTIAL

Fig. 49 Back-scatter pattern of model of 81-mm mortar shell with fins removed. f = 16.08 Gc/s

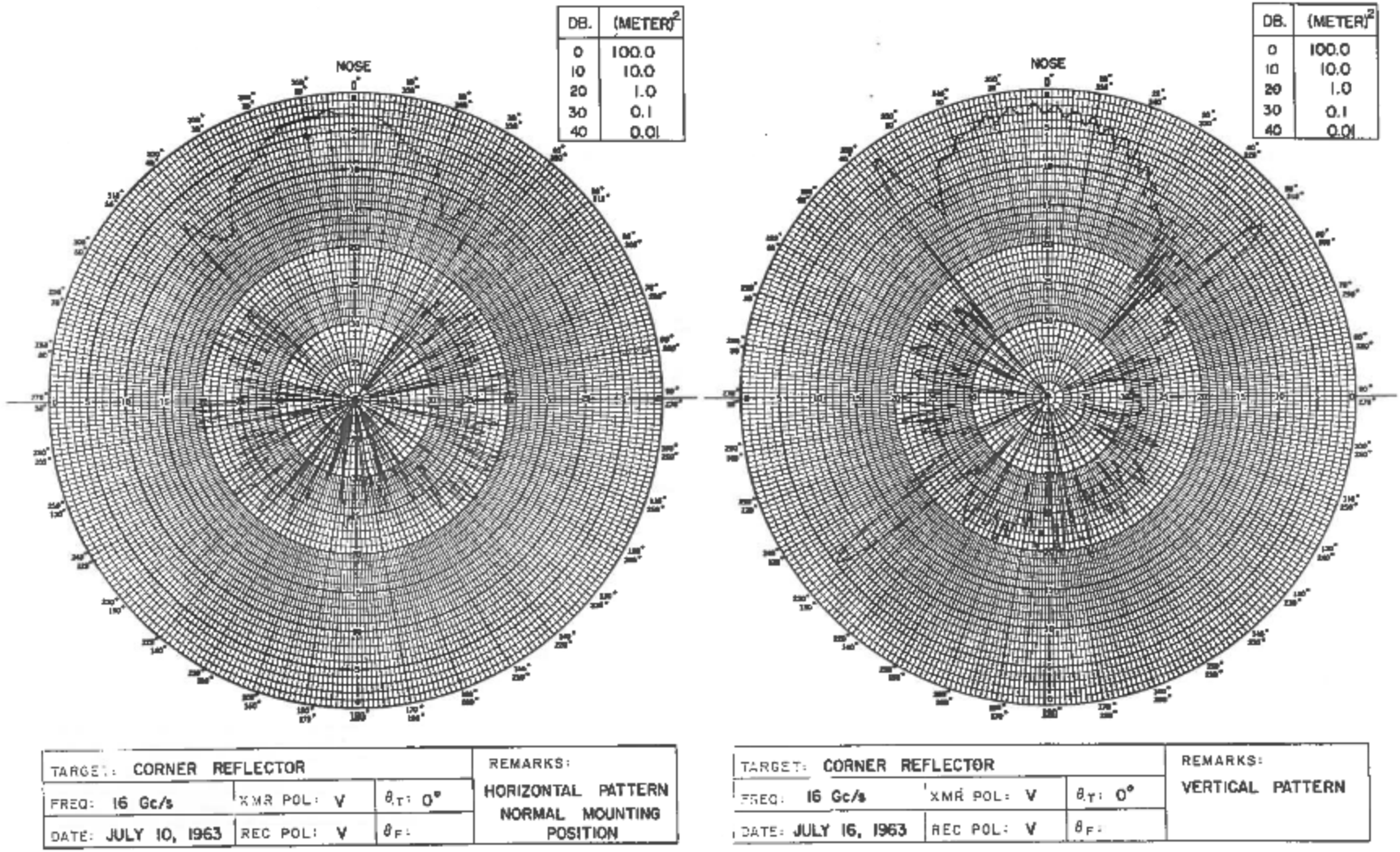

Fig. 50 Back-scatter patterns of corner reflector (left) base of reflector perpendicular to axis of rotation (right) base of reflector parallel to axis of rotation

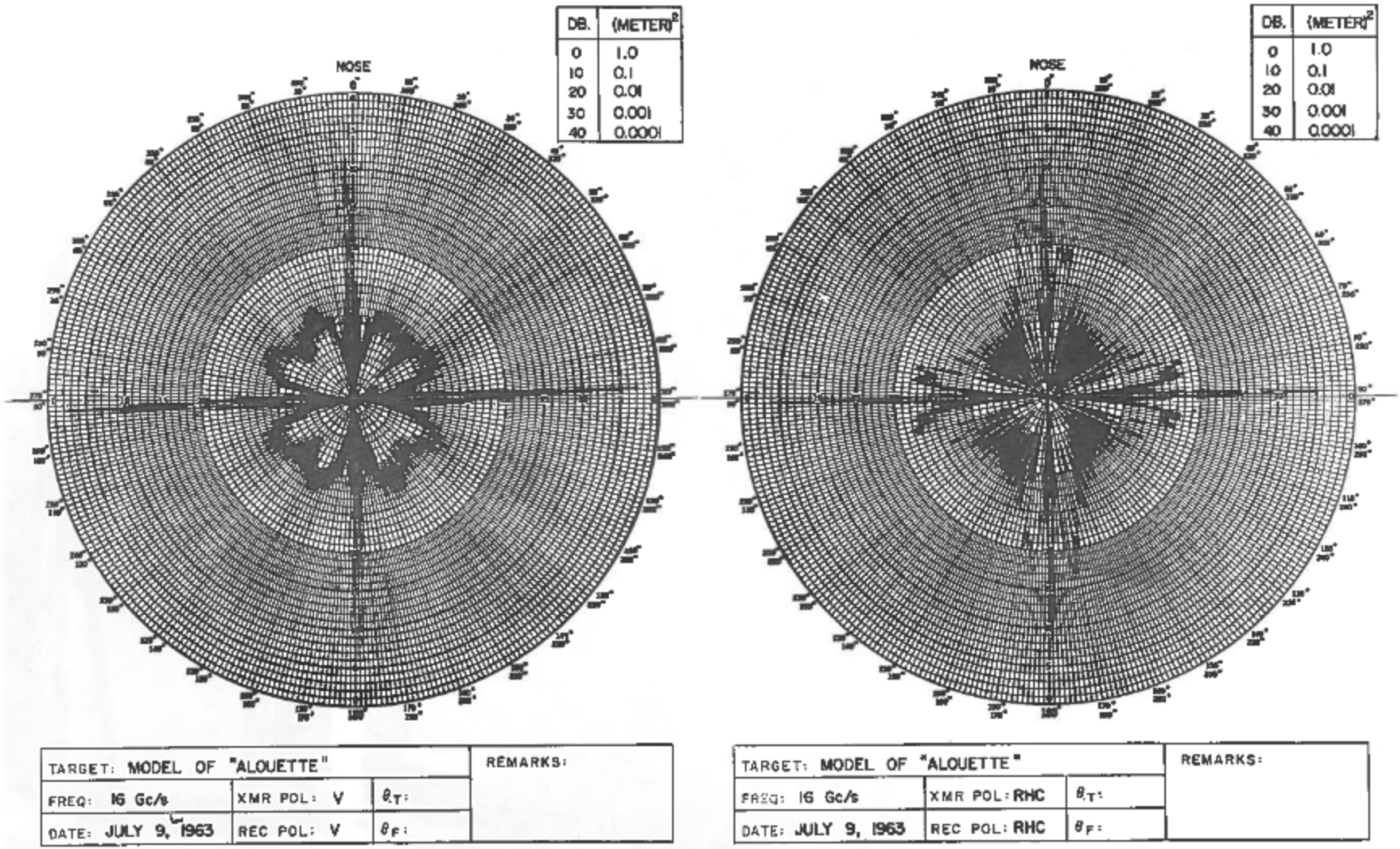

Fig. 51 Back-scatter patterns of 1/36 model of "Alouette" satellite (left) V-V polarization (right) R-R polarization

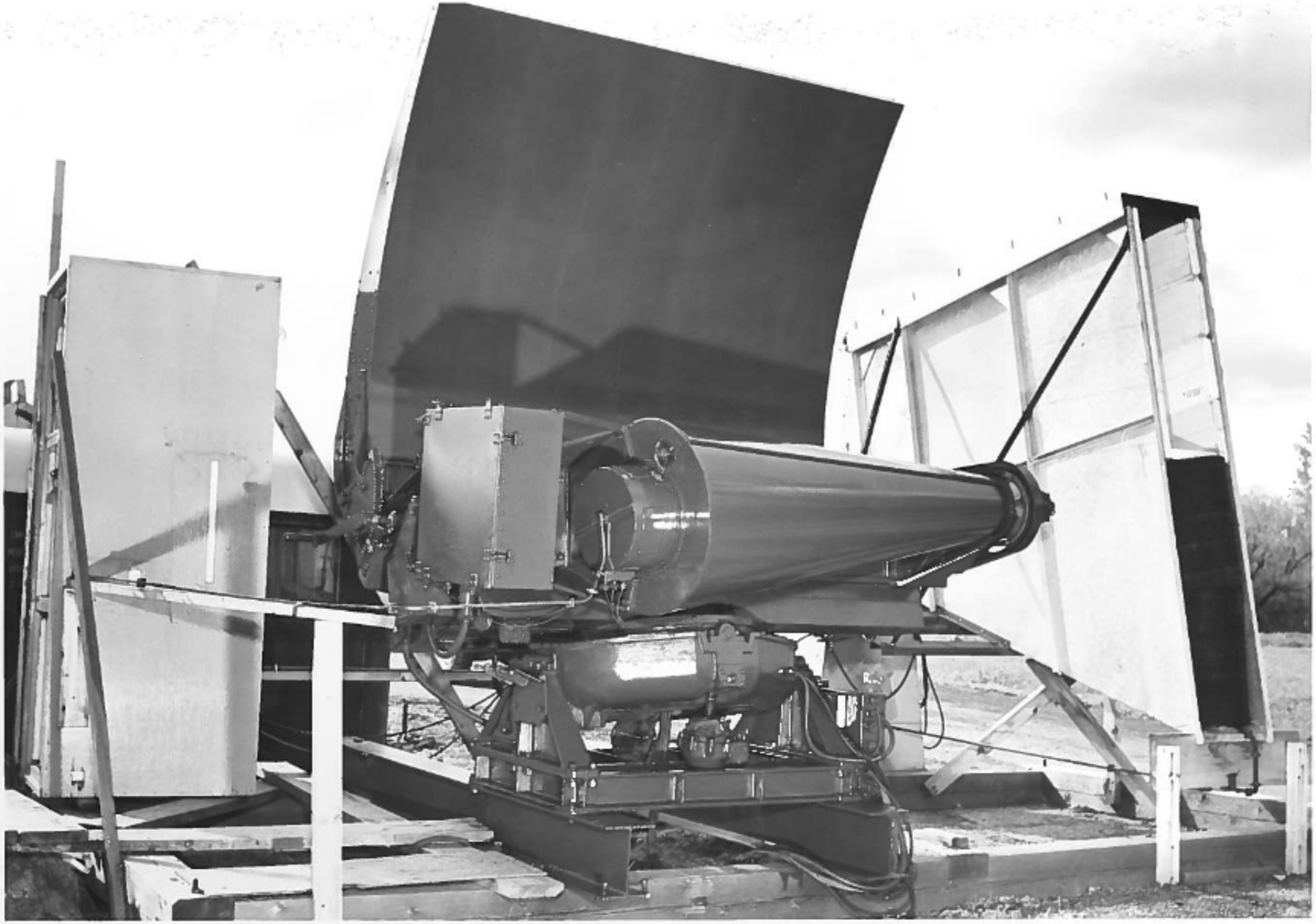

Plate I — Transmitting and receiving antennas

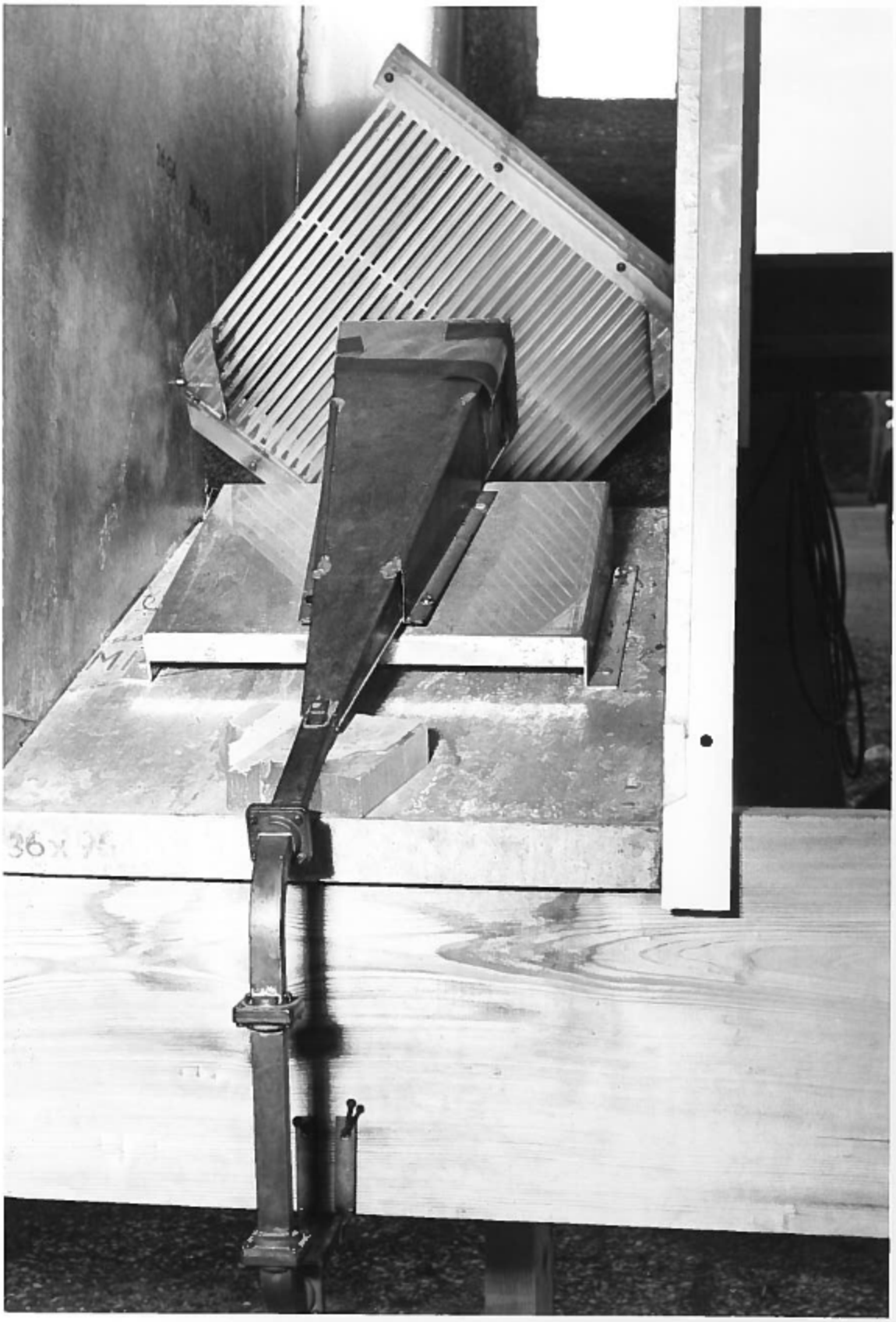

Plate II — Receiving antenna with feed horn and polarizer

Plate III — Mount for targets showing cancellation horn and smaller Styrofoam columns

Plate IV — Target mount showing Styrofoam hemispherical bowl above the larger column

Plate V — Projectile models (left to right) 81-mm mortar shell, $4\frac{1}{2}$-inch mortar shell, 105-mm artillery shell (with actual nose cone), M30 mortar shell, and 155-mm artillery shell